

# **Understanding of the Self- and Co-Assembly Behavior of Recombinant Protein Polymers**

From design to implementation

**Monika Dominika Golińska**

## **Thesis committee**

### **Promotor**

Prof. Dr. M.A. Cohen Stuart  
Professor of Physical Chemistry and Colloid Science,  
Wageningen University

### **Co-promotors**

Dr. R. de Vries  
Associate Professor,  
Laboratory of Physical Chemistry and Colloid Science  
Wageningen University

Dr. F.A. de Wolf  
Senior Scientist at Wageningen UR Food & Biobased Research,  
Wageningen University

### **Other members**

Prof. Dr G. Eggink, Wageningen University  
Prof. Dr W.J.H. van Berkel, Wageningen University  
Dr ir. T. Vermonden, Utrecht University, The Netherlands  
Prof. Dr J. van Hest, Radboud University Nijmegen, The Netherlands

This thesis has been conducted under the auspices of the Graduate School VLAG  
(Advanced studies in Food Technology, Agrobiotechnology, Nutrition and Health Sciences).

# **Understanding of the Self- and Co- Assembly Behavior of Recombinant Protein Polymers**

From design to implementation

Monika Dominika Golińska

## **Thesis**

submitted in fulfillment of the requirements for the degree of doctor

at Wageningen University

by the authority of the Rector Magnificus

Prof. dr. M.J. Kropff,

in the presence of the

Thesis Committee appointed by the Academic Board

to be defended in public

on Tuesday 7 January 2014

at 4 p.m. in the Aula.

Monika Dominika Golińska

Understanding of the Self- and Co-Assembly Behavior of Recombinant Protein Polymers  
From design to implementation,

166 pages

PhD thesis, Wageningen University, Wageningen, NL (2014)

With references, with summaries in English, Dutch and Polish

ISBN: 978-94-6173-813-4

*To my parents*

*Rodzicom*



## **CONTENT**

<b>Chapter 1</b>	General Introduction	1
<b>Chapter 2</b>	Fibril formation by pH and temperature responsive silk-elastin block co-polymers	21
<b>Chapter 3</b>	Dilute self-healing hydrogels of silk-collagen-like block copolypeptides at neutral pH	43
<b>Chapter 4</b>	Modulation of mechanical properties of hydrogels composed of protein-based polymers using cross-linking enzymes	69
<b>Chapter 5</b>	Pearl-necklace complexes of flexible polyanions with neutral-cationic diblock copolymers	95
<b>Chapter 6</b>	General Discussion	115
<b>Summary</b>		139
<b>Samenvatting</b>		143
<b>Streszczenie</b>		147
<b>Acknowledgement</b>		153
<b>About the Author</b>		159
<b>List of publications</b>		163
<b>Overview of completed training activities</b>		165



# Chapter 1

---

## General Introduction

---

In this section we are giving an introduction to the next chapters of this thesis. We describe our motivation and the background of the research goals in order to get the reader familiar with the main concepts and the relevance of this study to other areas of science.



## 1.1 Protein polymers as biomaterials

This thesis is about materials that are designed to be in contact and interact in a specific ways with living tissues and cells. Or, in short, this thesis is about biomaterials. These materials can be natural, synthetic or hybrids. A first key requirement is that these materials do not cause any harm to host cells, tissues or organs, or in a word, that they are biocompatible. The requirements for biocompatibility are complex and depend on the details of the specific application. Another key requirement is that such materials must have mechanical properties that are compatible with the particular application at hand. For example, in tissue engineering, mechanical properties of scaffolds for cell growth must be carefully tuned to the type of tissue for which the scaffold is meant [1]. The field of biomaterials is very broad with applications from sutures and wound dressings to drug delivery systems and tissue engineering. In this thesis we focus mainly on one particular type of material that has many biomedical applications, namely hydrogels. Biomedical applications of hydrogels include for example, scaffolds in tissue engineering [2], drug delivery system [3], contact lenses [4] and biosensors [5].

Hydrogels are cross-linked molecular networks that can hold large amount of water. The cross-links that give rise to the mechanical integrity of the hydrogels can be either covalent (chemical) or non-covalent (physical). Chemical crosslinks can be introduced by a range of crosslinking agents [6, 7] or sometimes by applying radiation [8]. Covalent crosslinks are permanent and prevent flow of the material even at long timescales. However, once ruptured, they are permanently broken. On the other hand, the much weaker bonds in physical gels are often (but not always) reversible such that the gels can heal after fracture, and exhibit flow at large timescales. Both chemical and physical hydrogels can react to changes in environment as pH, temperature and ionic strength.

Many hydrogels for biomedical applications are based on synthetic polymers such as poly(2-hydroxyethyl methacrylate), poly(acrylamide), poly(methacrylamide), poly (N-vinyl-2-pyrrolidone), polyelectrolyte complexes, poly(vinyl alcohol) or copolymerized

poly(ethylene glycol) with biodegradable and biocompatible polyesters [9-11]. The chemistry and architecture of these polymers, and the way they are cross-linked can be controlled to a high degree. However, these synthetic polymers are not bioactive and may give rise to problems such as inflammatory response [12-14], hence they need to be engineered after formation by conjugations with bioactive peptides, proteins, or polysaccharides.

When considering applications such as tissue engineering the role of the hydrogels is essentially to replace or mimic the extracellular matrix that consists of a broad group of self-assembled protein structures such as collagen, fibronectin and laminin, embedded in a matrix of flexible polysaccharides. Therefore, it is not surprising that another approach in developing hydrogels for biomedical applications is to extract proteins and polysaccharides from natural sources and to use these to construct hydrogels. Polymers that are being used in this way include not only polysaccharides such as agarose, chitosan, amylose, and hyaluronic acid, but also protein-based polymers such as collagen in various physical states (native fibrils, denatured). A major issue when using natural materials is the lack of control and poor reproducibility, in view of the variability of the starting material obtained from different donors. As a result of this, a major current effort is to precisely engineer these biopolymers in order to construct well defined, biopolymer-based hydrogels. Whereas engineering and design of defined polysaccharides such as those of the extracellular matrix is still very difficult, engineering and design of self-assembling peptides and proteins is a rapidly developing field. Using the set of 20 naturally occurring amino acids, one can design an almost endless number of proteins structures. Amino-acid sequences that are not too long can be conveniently synthesized using solid-state synthesis. Longer designed amino-acid sequences can be produced via recombinant DNA technology. Sequences are usually (but not always) inspired by natural proteins. In particular, structural polypeptides such as collagen, keratin, elastin, etc., are a rich source of inspiration for materials scientists.

This thesis deals with *de novo* designed polypeptides that are typically called protein-based polymers, or simply protein polymers. These consist of multiple functional blocks, where each of the blocks consist of a highly repetitive sequence that is typically bioinspired (e.g. silk-like, collagen-like, elastin-like, resilin-like etc. [15]). Due to the repetitive primary sequence, these blocks are able to assemble into stable, ordered conformations depending on structure and microenvironment [16] and to form various nanostructures in aqueous solutions that can be exploited in biomedical applications. A further attractive possibility is to incorporate various bioactive groups (e.g. cell binding sites, adhesion molecules, growth factors, enzyme recognition sequence) into the polymer designs [17-19].

A series of protein block copolymers can be synthesized by varying the length, sequence and composition, where two or more blocks of amino acids are covalently linked (by peptide bonds). Protein block copolymers can be used for various applications such as self-healing coatings, tissue engineering, drug delivery, surgical stitches, nanofibrils, and cell-specific surface coatings which are crucial to study the cell-scaffold interactions that regulate cell adhesion, viability, migration, proliferation and differentiation [20]. They can be easily modified by attachment of non-peptide components, such as saccharide chains or lipids, for example in order to make hydrogels that respond to complex stimuli [21-23].

### **1.2 *Pichia pastoris* as a host system for protein polymer production**

*Pichia pastoris* has been an increasingly attractive microorganism used to express heterologous proteins [24]. Nevertheless, in molecular biology research, *Escherichia coli* is the most frequently used organism due to its fast growth rate, reasonable protein production rate and undemanding growth conditions. The major advantage of *P. pastoris* over *E. coli* is capacity of diverse posttranslational modifications (producing disulfide bonds, glycosylations, methylation, acylation, and proteolytic adjustment) in proteins which is a crucial for correct protein folding, additionally it has better capability to produce efficiently larger proteins with higher molecular weight [25]. Moreover, genetic

manipulation is relatively simple as the expression vector of *P. pastoris* can be designed in specific ways to be able to up-take the insertion of a foreign coding sequence, usually carried out in *Escherichia coli*. *P. pastoris* has the methanol-induced alcohol oxidase (AOX1) promoter, that is very efficient and may be used for controlled expression of heterologous genes [26]. The growth rate of *P. pastoris* is relatively fast and can be carried with ease to high cell density in a simple mineral salts medium with good secretion capacity of only a few endogenous proteins, which simplifies the product recovery and purification as no cell harvest is needed. Compared to other systems *P. pastoris* productivity is usually higher, cheaper and easier.

The well-characterized yeast *Saccharomyces cerevisiae* is also used as an expression system with similar advantages over *E. coli*. However it cannot grow to very high cell densities and would not be able to grow in methanol medium (which is cheaper to set up and maintain) as its only carbon source for the growth. *Pichia pastoris* is particularly suitable for the production of heterologous proteins that form inclusion bodies in *E. coli*, and have low expression levels in mammalian cell lines. *Pichia pastoris* has been already used for the production of vaccines, coagulation inhibitors, allergens, antibodies, protease inhibitors, hormones, cytokines, receptors, and ligands.

In this thesis, we use *Pichia pastoris* to produce a range of protein-polymer designs, that are tested with respect to their self-assembly properties, emphasizing especially hydrogel formation at physiological conditions. The protein polymers are based on bio-inspired blocks which will be introduced in the following section.

### 1.3 Elastin-like protein polymers (ELPs)

Elastin is a self-assembling extracellular matrix protein that provides elasticity and strength to vertebrate arterial vessels, connective tissues, lungs and skin. The monomeric precursor of elastin, tropoelastin, is highly hydrophobic with high content of proline and glycine residues. Tropoelastin stays disordered and flexible in the solution [27-29] even when assembled and cross-linked into elastin polymers [30-33]. The repeat sequence, found in hydrophobic region of tropoelastin was used to create elastin-like polymers (ELPs). The most commonly used is the pentapeptide repeat sequence – (VPGXG)<sub>n</sub>, where at the X position can be any amino acid except proline. ELPs and tropoelastin are stimuli responsive and follow inverse temperature transition behavior in solution. This means that below transition temperature ( $T_t$ ), the proteins are highly soluble in aqueous solution, but when the solution is heated above  $T_t$ , protein contracts, dehydrates and aggregates [34-36]. This process is reversible; therefore, cooling the solution below  $T_t$ , results in resolubilizing of elastin. The value of the transition temperature can be controlled through amino acid sequence, chain length or by modulation of environmental condition e.g. ionic strength, addition of co-solutes [37, 38].

The unique properties of ELPs include high elasticity, self-assembly properties, and long fatigue lifetime. Elastin-like protein can be easily, fast and inexpensively purified by ITC (inverse temperature transition) cycle (see Fig 1.1) which is promising alternative to chromatography and requires no particular reagents or equipment [39]. ITC can be easily scalable and is a very efficient purification method even at low concentrations.

ELPs are attractive materials for many different applications from nanotechnology to medicine and pharmacology. They are used for tissue engineering, implantation [40] and gene delivery [41, 42]. In the other non-medical applications, ELPs were used as a fusion-tag that helps to purify other proteins by ITC [43].

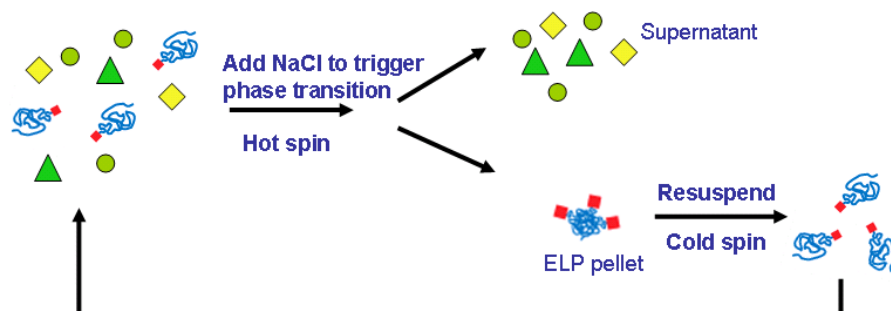


**Figure 1.1** Schematic illustration of inverse transition cycling (ITC) purification. The phase transition is induced by adding NaCl to the soluble cell lysate. The aggregated protein is separated by centrifugation in temperature above the  $T_t$  (hot spin). After discarding supernatant, the pellet is resuspended in cold buffer. Because some denatured protein contaminants will spin down with the ELP pellet, the additional centrifugation step (cold spin) is done below its  $T_t$ . The fusion protein will stay in solution and contaminants will precipitate. Hot and cold spins are carried out 3-5 times to obtain pure fusion protein [38].

#### 1.4 Silk-like protein polymers (SLPs)

Silks are protein polymers that are produced by specialized glands of insects and spiders. They exhibit excellent mechanical strength, high elasticity, toughness, biological compatibility, and biodegradability that is especially important in biomedical application (e.g. sutures, scaffold for tissue engineering) [44-47]. Silks differ widely in composition, structure, properties and function, depending on the producing species. Nevertheless, they have some common characteristics as they tend to have highly repetitive primary structure consisting of multiple repeats of specific motifs of the amino acids mainly alanine, alanine-glycine (GAGA sequence of *Bombyx mori*) or alanine-glycine-serine that leads to significant homogeneity in secondary structure and formation of  $\beta$ -sheets.  $\beta$ -forming peptides have ability to form fibrils and fibers as well as protein aggregates. Fibrils formation came from a hydrogen bond network between the amide groups of one  $\beta$ -sheet strands with the carbonyl groups of the neighboring strand [16]. The  $\beta$ -sheets structure is associated with significant crystallinity that exhibit low biodegradability [2].

The design of silk-like protein used in this study is based on the (GA)<sub>3</sub>GX sequence [48], where the edges of the  $\beta$ -sheet were functionalized by the charged amino acids, that impart pH-responsive properties. The two variants were construct one positively charged with histidine residue on X position and negative one with glutamic acid [49, 50]. It has been found that, upon increasing the pH, the positively charged block self-assembles into semi-flexible fibrils, whereas the negatively charge block behave in similar matter upon lowering the pH [50-52].

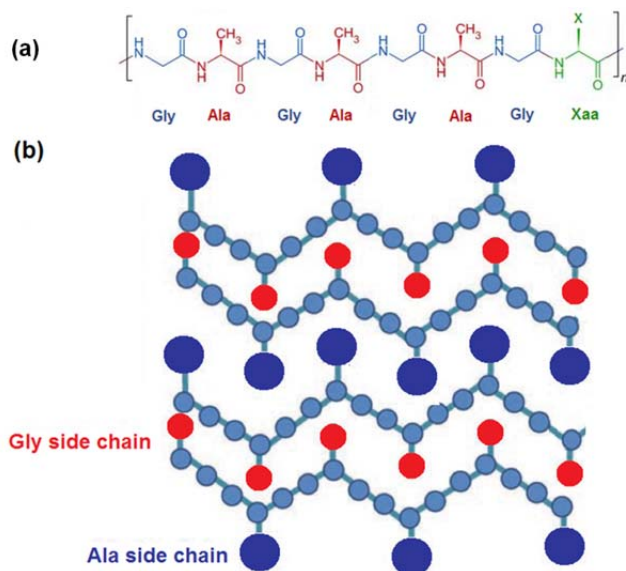


**Figure 1.2.** (a) Primary structure, (b) Secondary structure of silk-like protein polymers with interdigitation of the alanine and glycine side chains, a property which contributes to tensile strength and the  $\beta$ -sheet sheets structure.

Currently silk-based materials are already being used as a suture biomaterial, but due to its unique mechanical properties, the number of biomedical applications of silk-based materials is expected to increase. Silk-like proteins have already been considered for many biomedical applications, such as tissue engineering [46], in biosensors [53] and as a drug-delivery system [54].

## 1.5 Collagen and gelatin-like proteins

Collagen is the most abundant protein in mammals. Collagen fibrils have great tensile strength and are the main component of connective tissue (e.g. ligaments, tendons, cartilages, bones and skin) in the extracellular matrix. It not only provides the tissue structure, but can also mediate intracellular communication. The interactions between collagen and cell play an important role in cell attachment and migration [55], collagen degradation [56], tissue repair and the adhesion of platelet membrane glycoprotein [57]. At least 28 collagen types have been described in vertebrates [58]. All collagen proteins have at least one domain with a specific triple-helical structure, composed of three polypeptide  $\alpha$  chains, containing a repetitive (Gly-Xaa-Yaa)<sub>n</sub> sequence (where Xaa and Yaa are frequently occupied by the imino acids, proline and hydroxyproline respectively) [59-62]. The presence of glycine residues (Gly) at every third position and the high content of the stabilizing amino acids (proline and hydroxyproline) impose the triple helix conformation (see Figure 1.2) [63, 64].

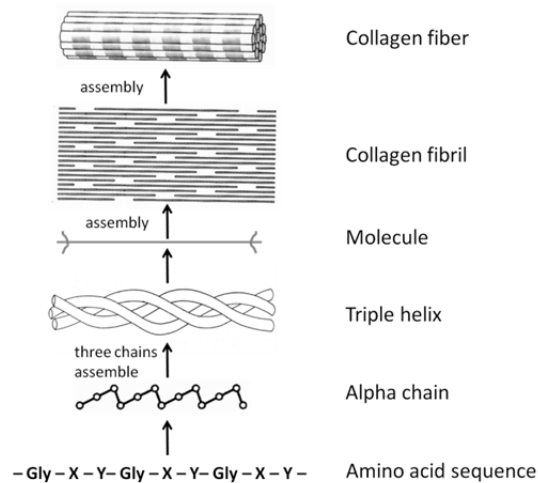


**Figure 1.3** Schematic illustration of collagen self-assembly into fibrils. Collagen is composed of three chains that contain a helical domain with a repeating triplet of Gly-X-Y sequence.

Gelatine is a heterogeneous product derived from denatured and partially degraded (usually after hydrolysis) collagen [65]. Its composition and properties depends on the age, type and source of collagen [66]. In this thesis, we use a collagen-inspired sequence first reported by Wertén *et al.* [49], as an important block in the protein polymer designs. It is a highly hydrophilic collagenous based structure that does not form triple-helices even at 4°C, as it lacks the presence of hydroxyproline. In this structure the Gly-Xaa-Yaa repeat contains (besides 33.7 mol % of glycine) 22.4 mol % of proline and several other amino acids [49].

Collagen and gelatin are currently mainly obtained from animals. However the extraction from their natural sources is often difficult, expensive and carries a high risk of contamination or allergic reactions. Thus, recombinant technology brings a big potential as it produces animal component-free collagen [67, 68]. Recombinant expression in *Pichia pastoris* is very promising as collagen requires specific folding and post-translational modifications which are achieved in yeast. The exceptional biocompatibility as well as biodegradability and weak antigenicity, make collagen and gelatin (denatured and partially degraded collagen) one of the most popular biomaterials in drug delivery system and tissue engineering [69].

### **1.6 Protein self –assembly**

Molecular self-assembly is the spontaneous association of components into structures without guidance from an outside source, through non-covalent interactions, weak covalent interactions (e.g. hydrogen bonding, metal coordination, hydrophobic forces, van der Waals forces,  $\pi$ - $\pi$  interactions, electrostatic) or electromagnetic interactions [70]. Ultimately it relies on a subtle balance between the enthalpic and entropic contributions to the free energies of both, the dissolved molecules and the solvent [71]. Many biological structures spontaneously self-assemble from protein components, even *in vitro*. Hence it is not surprising that mimicking or exploiting protein and peptide self-assembly is a key theme in current studies of protein-based biomaterials.

Proteins can assemble into various structural motifs including particles, micelles, fibers, ribbons and sheets. Some proteins and peptides can self-assemble into fibrillar structures by hydrogen bonding interaction forming amyloid-like fibrils. These fibrils can vary in amino acid composition, shape and size, reaching from nanometers to micrometers. Formation of amyloid fibrils is often related to the several diseases [72] (e.g. Parkinson's disease [73], Alzheimer's disease [74], diabetes [75], atherosclerosis [76], Creutzfeldt-Jakob disease [77, 78] and rheumatoid arthritis [79, 80]). For this reason correct self-assembly and controlled aggregation are particularly important as they might be a source of pathogenesis. In contrast, amyloid fibrils are present in many living organisms (mammals, fungi, insects or some bacteria like *E. coli*) where they play an important biological function [81].

Self-assembly is crucial for many technological applications, including nanoscale materials, biosensors for the recognition of rare cancer cells, biomaterials for scaffolds or biological signals [82-84]. Their function is essential for selective transport, structural scaffolding and propagation of, or defense against pathogenesis. Most of the applications of self-assemble systems have been directed towards regenerative medicine as they are able to heal damaged cells in the body and provide a favorable environment for externally transplanted elements (e.g. stem cells) [85]. Additionally, many studies are focused on bio-inspired materials that can self-assemble upon specific stimuli (pH, temperature, UV), as an understanding of supramolecular assembly that can lead to the design of new biomaterials [86, 87]. A range of macromolecular complexes or structural materials including silk, collagen and elastin display self-assembly and have been study in recent years [88-91].

## 1.7 Aim and thesis outline

The aim of this thesis is to construct, synthesize and characterize new self-assembling systems of protein polymers, with an emphasis on protein polymers that self-assemble into responsive hydrogels that could have eventual biomedical applications.

All the proteins used for this study were obtained by molecular engineering, starting by design and cloning of various genes that encoded block copolymers, followed by expression in yeast *Pichia pastoris* as a promising host for production of repetitive proteins polymers.

In **Chapter 2** we study the self-assembly properties of di- and triblock protein polymers with silk-, elastin- and collagen-like blocks. These proteins were designed to respond to both pH and temperature changes. We show that the design was successful and that we can use pH to direct self-assembly of the proteins into fibers and temperature to regulate interactions between fibers.

In **Chapter 3** we investigate the self-assembly behavior of collagen-silk-like triblock protein polymers that self-assemble into fibers under physiological conditions. At higher concentrations the fibers form hydrogels for which we characterize the rheological properties. These pH-responsive gels are self-healing and are expected to be an excellent scaffold structure that can be adapted for a range of biomedical hydrogel applications.

In **Chapter 4** we investigate whether enzymatic cross-linking can be used to create completely biosynthesized hydrogels with both chemical and physical cross-links. First we characterize the suitability of our collagen-like hydrophilic blocks as a substrate for microbial transglutaminase (mTGase). Next, we explore the impact of introducing additional chemical cross-links on the mechanical properties of two types of self-assembled protein-polymer hydrogels.

In **Chapter 5** we study electrostatically driven self-assembly of collagen-like blocks with short cationic tails with oppositely charged, long and flexible polyelectrolytes. Surprisingly,

this gives rise to a "pearl-necklace" structure consisting of a string of so-called complex coacervate core micelles.

Finally, in the general discussion on **Chapter 6**, we put the current thesis work in perspective, we review current work on *de novo* designed proteins that form hydrogels, discuss constraint of hydrogels if they are going to be used in biomedical applications, and finally, we discuss challenges that need to be addressed before these materials can be used in real biomedical applications.

---

## References

1. Chen, Q., S. Liang, and G.A. Thouas, *Elastomeric biomaterials for tissue engineering*. Progress in Polymer Science, 2013. **38**(3-4): p. 584-671.
2. Zhao, W., et al., *Degradable natural polymer hydrogels for articular cartilage tissue engineering*. Journal of Chemical Technology & Biotechnology, 2012. **88**(3): p. 327-339.
3. Cappello, J., et al., *In-situ self-assembling protein polymer gel systems for administration, delivery, and release of drugs*. Journal of Controlled Release, 1998. **53**(1-3): p. 105-117.
4. Ottenbrite, R.M., et al., *Hydrogels Contact Lenses*, in *Biomedical Applications of Hydrogels Handbook*. 2010, Springer New York: Prague. p. 303-315.
5. Meiring, J.E., et al., *Hydrogel Biosensor Array Platform Indexed by Shape*. Chemistry of Materials, 2004. **16**(26): p. 5574-5580.
6. Chen, T., et al., *In vitro protein-polysaccharide conjugation: Tyrosinase-catalyzed conjugation of gelatin and chitosan*. Biopolymers, 2002. **64**(6): p. 292-302.
7. Skrzyszewska, P.J., et al., *Shape-Memory Effects in Biopolymer Networks with Collagen-Like Transient Nodes*. Biomacromolecules, 2011. **12**(6): p. 2285-2292.
8. Wang, M., et al., *Enhanced radiation crosslinking of carboxymethylated chitosan in the presence of acids or polyfunctional monomers*. Polymer Degradation and Stability, 2008. **93**(10): p. 1807-1813.
9. Ratner, B.D. and A.S. Hoffman. *Synthetic hydrogels for biomedical applications*. in *Hydrogels for Medical and Related Applications, ACS symposium series*. 1976: ACS Publications.
10. Klouda, L. and A.G. Mikos, *Thermoresponsive hydrogels in biomedical applications*. European Journal of Pharmaceutics and Biopharmaceutics, 2008. **68**(1): p. 34-45.
11. Hoffman, A.S., *Hydrogels for biomedical applications*. Advanced drug delivery reviews, 2012. **64**: p. 18-23.
12. Anderson, J.M., *Inflammatory response to implants*. ASAIO Journal, 1988. **34**(2): p. 101-107.
13. Bostman, O., et al., *Foreign-body reactions to fracture fixation implants of biodegradable synthetic polymers*. Journal of Bone & Joint Surgery, British Volume, 1990. **72**(4): p. 592-596.
14. Tang, L. and J.W. Eaton, *Fibrin (ogen) mediates acute inflammatory responses to biomaterials*. The Journal of experimental medicine, 1993. **178**(6): p. 2147-2156.
15. Bracalello, A., et al., *Design and Production of a Chimeric Resilin-, Elastin-, and Collagen-Like Engineered Polypeptide*. Biomacromolecules, 2011. **12**(8): p. 2957-2965.
16. Voet, D. and J.G. Voet, *Biochemistry* 3rd ed. Inc., Somerset. 2005, New York: Wiley and Sons.
17. Bini, E., et al., *RGD-Functionalized Bioengineered Spider Dragline Silk Biomaterial*. Biomacromolecules, 2006. **7**(11): p. 3139-3145.

18. Yamaguchi, N., et al., *Growth Factor Mediated Assembly of Cell Receptor-Responsive Hydrogels*. Journal of the American Chemical Society, 2007. **129**(11): p. 3040-3041.
19. George, P.A., et al., *Nanoscale presentation of cell adhesive molecules via block copolymer self-assembly*. Biomaterials, 2009. **30**(27): p. 4732-4737.
20. Fischer, S.E., et al., *Controlling cell adhesion to surfaces via associating bioactive triblock proteins*. Biomaterials, 2007. **28**(22): p. 3325-3337.
21. Lindahl, U. and M. Hook, *Glycosaminoglycans and their binding to biological macromolecules*. Annual review of biochemistry, 1978. **47**(1): p. 385-417.
22. Yannas, I.V., et al., *Crosslinked collagen-mucopolysaccharide composite materials*. 1981, Google Patents.
23. Wang, X.H., et al., *Crosslinked collagen/chitosan matrix for artificial livers*. Biomaterials, 2003. **24**(19): p. 3213-3220.
24. Cregg, J.M., T.S. Vedvick, and W.C. Raschke, *Recent advances in the expression of foreign genes in Pichia pastoris*. Bio/technology (Nature Publishing Company), 1993. **11**(8): p. 905-910.
25. Fahnstock, S.R. and S.L. Irwin, *Synthetic spider dragline silk proteins and their production in Escherichia coli*. Applied microbiology and biotechnology, 1997. **47**(1): p. 23-32.
26. Sreekrishna, K., et al., *High level expression of heterologous proteins in methylotrophic yeast Pichia pastoris*. Journal of Basic Microbiology, 1988. **28**(4): p. 265-278.
27. Toonkool, P., et al., *Thermodynamic and Hydrodynamic Properties of Human Tropoelastin Analytical Ultracentrifuge and Pulsed Field-Gradient Spin-Echo NMR Studies*. Journal of Biological Chemistry, 2001. **276**(30): p. 28042-28050.
28. Tamburro, A.M., B. Bochicchio, and A. Pepe, *Dissection of Human Tropoelastin: Exon-By-Exon Chemical Synthesis and Related Conformational Studies†*. Biochemistry, 2003. **42**(45): p. 13347-13362.
29. Muiznieks, L.D. and A.S. Weiss, *Flexibility in the Solution Structure of Human Tropoelastin†*. Biochemistry, 2007. **46**(27): p. 8196-8205.
30. Lyerla, J.R. and D.A. Torchia, *Molecular mobility and structure of elastin deduced from the solvent and temperature dependence of carbon-13 magnetic resonance relaxation data*. Biochemistry, 1975. **14**(23): p. 5175-5183.
31. Kumashiro, K.K., et al., *<sup>13</sup>C cross-polarization/magic angle spinning NMR studies of  $\alpha$ -elastin preparations show retention of overall structure and reduction of mobility with a decreased number of cross-links*. Biopolymers, 2001. **59**(4): p. 266-275.
32. Perry, A., et al., *Solid-State <sup>13</sup>C NMR Reveals Effects of Temperature and Hydration on Elastin*. Biophysical Journal, 2002. **82**(2): p. 1086-1095.
33. Pometun, M.S., E.Y. Chekmenev, and R.J. Wittebort, *Quantitative Observation of Backbone Disorder in Native Elastin*. Journal of Biological Chemistry, 2004. **279**(9): p. 7982-7987.

34. Cox, B., B. Starcher, and D. Urry, *Coacervation of tropoelastin results in fiber formation*. J Biol Chem, 1974. **249**(3): p. 997-998.
35. Urry, D.W., *On the molecular mechanisms of elastin coacervation and coacervate calcification*. Faraday Discuss. Chem. Soc., 1976. **61**: p. 205-212.
36. Urry, D.W., et al., *Temperature of polypeptide inverse temperature transition depends on mean residue hydrophobicity*. J Am Chem Soc, 1991. **113**(11): p. 4346-4348.
37. Ribeiro, A., et al., *Influence of the Amino-Acid Sequence on the Inverse Temperature Transition of Elastin-Like Polymers*. Biophysical Journal, 2009. **97**(1): p. 312-320.
38. Golemis, E., *Protein Purification by Inverse Transition Cycling*, in *Protein-Protein Interactions: A Molecular Cloning Manual*, D.E. Meyer and A. Chilkoti, Editors. 2002, Cold Spring Harbor Laboratory Press. p. 329-343.
39. Lim, D.W., et al., *Improved Non-chromatographic Purification of a Recombinant Protein by Cationic Elastin-like Polypeptides*. Biomacromolecules, 2007. **8**(5): p. 1417-1424.
40. Lim, D.W., et al., *In Situ Cross-Linking of Elastin-like Polypeptide Block Copolymers for Tissue Repair*. Biomacromolecules, 2008. **9**(1): p. 222-230.
41. Haider, M., et al., *Molecular Engineering of Silk-Elastinlike Polymers for Matrix-Mediated Gene Delivery: Biosynthesis and Characterization*. Molecular Pharmaceutics, 2005. **2**(2): p. 139-150.
42. Chen, T.-H.H., Y. Bae, and D. Furgeson, *Intelligent Biosynthetic Nanobiomaterials (IBNs) for Hyperthermic Gene Delivery*. Pharmaceutical Research, 2008. **25**(3): p. 683-691.
43. Trabbic-Carlson, K., et al., *Expression and purification of recombinant proteins from Escherichia coli: Comparison of an elastin-like polypeptide fusion with an oligohistidine fusion*. Protein Science, 2004. **13**(12): p. 3274-3284.
44. Hinman, M.B., J.A. Jones, and R.V. Lewis, *Synthetic spider silk: a modular fiber*. Trends in Biotechnology, 2000. **18**(9): p. 374-379.
45. Vollrath, F. and D.P. Knight, *Liquid crystalline spinning of spider silk*. 2001. **410**(6828): p. 541-548.
46. Altman, G.H., et al., *Silk-based biomaterials*. Biomaterials, 2003. **24**(3): p. 401-416.
47. Schacht, K. and T. Scheibel, *Controlled Hydrogel Formation of a Recombinant Spider Silk Protein*. Biomacromolecules, 2011. **12**(7): p. 2488-2495.
48. Krejchi, M.T., et al., *Chemical sequence control of beta-sheet assembly in macromolecular crystals of periodic polypeptides*. Science, 1994. **265**(5177): p. 1427-1432.
49. Werten, M.W.T., et al., *Secreted production of a custom-designed, highly hydrophilic gelatin in Pichia pastoris*. Protein Engineering, 2001. **14**(6): p. 447-454.
50. Martens, A.A., et al., *Triblock Protein Copolymers Forming Supramolecular Nanotapes and pH-Responsive Gels*. Macromolecules, 2009. **42**(4): p. 1002-1009.

51. Cantor, E.J., et al., *Effects of Amino Acid Side-Chain Volume on Chain Packing in Genetically Engineered Periodic Polypeptides*. *Journal of Biochemistry*, 1997. **122**(1): p. 217-225.
52. Schor, M., et al., *Prediction of solvent dependent [small beta]-roll formation of a self-assembling silk-like protein domain*. *Soft Matter*, 2009. **5**(13): p. 2658-2665.
53. Demura, M. and T. Asakura, *Immobilization of glucose oxidase with Bombyx mori silk fibroin by only stretching treatment and its application to glucose sensor*. *Biotechnology and Bioengineering*, 1989. **33**(5): p. 598-603.
54. Tsukada, M., et al., *Preparation and application of porous silk fibroin materials*. *Journal of Applied Polymer Science*, 1994. **54**(4): p. 507-514.
55. Perris, R., et al., *Molecular mechanisms of neural crest cell attachment and migration on types I and IV collagen*. *Journal of Cell Science*, 1993. **106**(4): p. 1357-1368.
56. van der Zee, E., et al., *Cytokines modulate phagocytosis and intracellular digestion of collagen fibrils by fibroblasts in rabbit periosteal explants. Inverse effects on procollagenase production and collagen phagocytosis*. *Journal of Cell Science*, 1995. **108**(10): p. 3307-3315.
57. Staatz, W.D., et al., *The alpha 2 beta 1 integrin cell surface collagen receptor binds to the alpha 1 (I)-CB3 peptide of collagen*. *Journal of Biological Chemistry*, 1990. **265**(9): p. 4778-4781.
58. Kadler, K.E., et al., *Collagens at a glance*. *Journal of Cell Science*, 2007. **120**(12): p. 1955-1958.
59. Ramachandran, G.N. and G. Kartha, *Structure of Collagen*. 1955. **176**(4482): p. 593-595.
60. Rich, A. and F.H.C. Crick, *The molecular structure of collagen*. *Journal of Molecular Biology*, 1961. **3**(5): p. 483-IN4.
61. Bella, J., et al., *Crystal and molecular structure of a collagen-like peptide at 1.9 Å resolution*. *Science (New York, N.Y.)*, 1994. **266**(5182): p. 75-81.
62. Brodsky, B., et al., *Molecular Structure of the Collagen Triple Helix*, in *Advances in Protein Chemistry*. 2005, Academic Press. p. 301-339.
63. Mechling, D.E. and H.P. Bächinger, *The Collagen-like Peptide (GER)15GPCCG Forms pH-dependent Covalently Linked Triple Helical Trimers*. *Journal of Biological Chemistry*, 2000. **275**(19): p. 14532-14536.
64. Saito, M., et al., *Complete primary structure of rainbow trout type I collagen consisting of  $\alpha 1(I)\alpha 2(I)\alpha 3(I)$  heterotrimers*. *European Journal of Biochemistry*, 2001. **268**(10): p. 2817-2827.
65. Johnston-Banks, F.A., *Gelatin in Food Gels*, P. Harris, Editor. 1990, Elsevier Applied Science Publ: London. p. 233-289.
66. Simon, A., et al., *A comparative study of the rheological and structural properties of gelatin gels of mammalian and fish origins*. *Macromolecular Symposia*, 2003. **203**(1): p. 331-338.
67. Yao, C.-H., et al., *Preparation of networks of gelatin and genipin as degradable biomaterials*. *Materials Chemistry and Physics*, 2004. **83**(2-3): p. 204-208.

- 
68. Báez, J., D. Olsen, and J.W. Polarek, *Recombinant microbial systems for the production of human collagen and gelatin*. Applied microbiology and biotechnology, 2005. **69**(3): p. 245-252.
  69. Lee, C.H., A. Singla, and Y. Lee, *Biomedical applications of collagen*. International Journal of Pharmaceutics, 2001. **221**(1–2): p. 1-22.
  70. Zhang, S., *Emerging biological materials through molecular self-assembly*. Biotechnology Advances, 2002. **20**(5-6): p. 321-339.
  71. Stephanopoulos, N., J.H. Ortony, and S.I. Stupp, *Self-assembly for the synthesis of functional biomaterials*. Acta Materialia, 2013. **61**(3): p. 912-930.
  72. Koo, E.H., P.T. Lansbury, and J.W. Kelly, *Amyloid diseases: abnormal protein aggregation in neurodegeneration*. Proceedings of the National Academy of Sciences, 1999. **96**(18): p. 9989-9990.
  73. Conway, K.A., J.D. Harper, and P.T. Lansbury, *Fibrils formed in vitro from  $\alpha$ -synuclein and two mutant forms linked to Parkinson's disease are typical amyloid*. Biochemistry, 2000. **39**(10): p. 2552-2563.
  74. Hardy, J. and D.J. Selkoe, *The amyloid hypothesis of Alzheimer's disease: progress and problems on the road to therapeutics*. Science, 2002. **297**(5580): p. 353-356.
  75. Lorenzo, A. and B. Yankner, *Amyloid Fibril Toxicity in Alzheimer's Disease and Diabetes*. Annals of the New York Academy of Sciences, 1996. **777**(1): p. 89-95.
  76. Howlett, G.J. and K.J. Moore, *Untangling the role of amyloid in atherosclerosis*. Current opinion in lipidology, 2006. **17**(5): p. 541-547.
  77. Goldfarb, L.G., et al., *Synthetic peptides corresponding to different mutated regions of the amyloid gene in familial Creutzfeldt-Jakob disease show enhanced in vitro formation of morphologically different amyloid fibrils*. Proceedings of the National Academy of Sciences, 1993. **90**(10): p. 4451-4454.
  78. Namba, Y., et al., *Apolipoprotein E immunoreactivity in cerebral amyloid deposits and neurofibrillary tangles in Alzheimer's disease and kuru plaque amyloid in Creutzfeldt-Jakob disease*. Brain research, 1991. **541**(1): p. 163-166.
  79. Cunnane, G. and A.S. Whitehead, *Amyloid precursors and amyloidosis in rheumatoid arthritis*. Best Practice & Research Clinical Rheumatology, 1999. **13**(4): p. 615-628.
  80. Husby, G., *Amyloidosis and rheumatoid arthritis*. Clinical and experimental rheumatology, 1985. **3**(2): p. 173.
  81. Fowler, D.M., et al., *Functional amyloid-from bacteria to humans*. Trends in biochemical sciences, 2007. **32**(5): p. 217-224.
  82. Huebsch, N. and D.J. Mooney, *Inspiration and application in the evolution of biomaterials*. Nature, 2009. **462**(7272): p. 426-432.
  83. Williams, D.F., *On the nature of biomaterials*. Biomaterials, 2009. **30**(30): p. 5897-5909.
  84. Yun, Y.-H., et al., *Tiny medicine: nanomaterial-based biosensors*. Sensors, 2009. **9**(11): p. 9275-9299.
  85. Matson, J.B. and S.I. Stupp, *Self-assembling peptide scaffolds for regenerative medicine*. Chemical Communications, 2012. **48**(1): p. 26-33.

86. Collier, J.H., et al., *Thermally and photochemically triggered self-assembly of peptide hydrogels*. Journal of the American Chemical Society, 2001. **123**(38): p. 9463-9464.
87. Rajagopal, K. and J.P. Schneider, *Self-assembling peptides and proteins for nanotechnological applications*. Current opinion in structural biology, 2004. **14**(4): p. 480-486.
88. Kyle, S., et al., *Production of self-assembling biomaterials for tissue engineering*. Trends in Biotechnology, 2009. **27**(7): p. 423-433.
89. Scheibel, T., *Protein fibers as performance proteins: new technologies and applications*. Current opinion in biotechnology, 2005. **16**(4): p. 427-433.
90. Termonia, Y., *Nanoscale Self-Assembly of Multiblock Copolymer Chains into Rods*. Biomacromolecules, 2004. **5**(6): p. 2404-2407.
91. Xia, X.-X., et al., *Tunable self-assembly of genetically engineered silk–elastin-like protein polymers*. Biomacromolecules, 2011. **12**(11): p. 3844-3850.

## Chapter 2

---

# Fibril formation by pH and temperature responsive silk-elastin block co-polymers

---

In this chapter we study the self-assembly of two silk-elastin like proteins: one is a diblock  $S_{24}E_{40}$  composed of 24 silk-like ( $S$ ) repeats and 40 elastin-like ( $E$ ) repeats; the other is a triblock  $S_{12}C_4E_{40}$ , in which the  $S$  and  $E$  blocks are separated by a random coil block ( $C_4$ ). Upon lowering the pH, the acidic silk-like blocks fold and self-assemble into fibrils by a nucleation-and-growth process. While silk-like polymers without elastin-like blocks form fibrils by heterogeneous nucleation, leading to monodisperse populations, the elastin-like blocks allow for homogeneous nucleation, which gives rise to polydisperse length distributions, as well as a concentration-dependent fibril length. Moreover, the elastin-like blocks introduce temperature-sensitivity: at high temperature, the fibrils become sticky and tend to bundle and aggregate in an irreversible manner. Concentrated solutions of  $S_{12}C_4E_{40}$  form weak gels at low pH that irreversibly lose elasticity in temperature cycling; this is also attributed to fibril aggregation.

Publish as: M.D. Golinska, T.T.H. Pham, M.W.T. Werten, F.A. de Wolf, M.A. Cohen Stuart, J. van der Gucht; Fibril formation by pH and temperature responsive silk-elastin block co-polymers, *Biomacromolecules*, **2013**, 14 (1), 48-55.



## 2.1 Introduction

Stimuli-responsive protein polymers are a very promising group of materials that have significant potential in many different applications, e.g., for regenerative medicine, tissue engineering, bioseparation, self-healing coatings, gene therapy or drug delivery [1-6]. Because of their interesting physicochemical properties and applicability these proteins are gaining more attention. Useful stimuli to which they reversibly respond can be pH, temperature or ionic strength. Genetic engineering provides the tool to design such protein-based polymers with precisely defined monomer sequences and molecular weights, thereby controlling physicochemical properties and biological fate, as needed for biomedical applications.

In this chapter, we focus on the production and characterisation of two novel silk-elastin like protein polymers with pH- and temperature-responsive blocks where stimuli can be separately addressed. We compare two proteins: 1) a 'diblock' polymer, labelled  $S_{24}E_{40}$  which is composed of 24 silk-like ( $S$ ) and 40 elastin-like ( $E$ ) repeats, and 2) a 'triblock' polymer  $S_{12}C_4E_{40}$  where 12 silk-like and 40 elastin-like sequences are connected by a random coil ( $C_4$ ) block, that serves as an inert 'spacer' between silk-like and elastin-like blocks. The combination of sequences was designed to achieve distinct physical behaviours in one single hybrid molecule, in order to: 1) assess how they influence each other and 2) see whether qualitatively new behaviour would emerge. The presence of the  $C_4$  spacer may 'decouple' the silk-like and elastin-like blocks, so that only self-interactions of these blocks occur. Moreover, the  $C_4$  block will probably affect the kinetics of self-assembly.

The random coil block ( $C_4$ ) is composed of four identical, 99 amino acid long units that carry many uncharged and hydrophilic amino acids such as glutamine, asparagine and serine. These amino acids are inert to almost all stimuli, and therefore the  $C_4$  block maintains a random coiled structure in a broad range of pH values and temperatures [7, 8]. The silk-like block ( $S$ ) has been inspired by poly (GA) sequences found in natural silk as

produced by the silkworm (*Bombyx mori*). It consists of repeats of the octapeptide GAGAGAGE [9], where glutamic acid imparts pH responsive properties [10]. It has been found that, upon lowering the pH, this block self-assembles into semi-flexible fibrils which feature a rather special secondary structure in water, related to (but somewhat different from) the familiar  $\beta$ -sheet [8, 11, 12]. The elastin-like block (*E*) is composed of a pentapeptide repeat motif (VPGXG) where the X position is occupied by either valine, alanine, or glycine in a 5:3:2 ratio, respectively [13, 14]. Elastins with this kind of sequence are known to undergo a temperature-induced phase transition: above the transition temperature (lower critical solution temperature, LCST) the random-coiled structure changes into a so-called  $\beta$ -spiral, thereby forming aggregates [15-17]. The transition temperature of these elastins depends on the hydrophobicity of the amino acid at the X position, the length of the block, the polymer concentration, and the nature and concentration of added salt [13].

Some silk-elastin like protein polymers have been described previously in literature and were reported to spun into fibers [18], self-assembly into micelle-like structure [19] or physically cross-linked networks [20]. They were used to develop protein-based tissue scaffolds [21] or systems for drug delivery and release [22]. Our group previously reported block copolymers, consisting of  $S_{24}$  and  $C_2$  blocks, which spontaneously organize into stable nanofibers. The present work is the first report in which doubly responsive behaviour (pH and temperature) is considered. We will compare the behaviours with singly-responsive counterparts such as the silk-random coil (*S-C*) combinations that have been described earlier [8, 23].

For the production of the heterologous proteins considered here we prefer the methylotrophic yeast *Pichia pastoris* because of its ability to excrete the product from the cell and to give very high yields of recombinant proteins. The purification of both proteins, which involves a precipitation with ammonium sulphate or a temperature cycle directly applied to the cell-free fermentation supernatant, is simple and very effective.

The physical properties and self-assembly into fibrils of  $S_{24}E_{40}$  and  $S_{12}C_4E_{40}$  were characterized by atomic force microscopy (AFM), light scattering and rheology. The properties were compared while changes of temperature and pH were applied either separately or simultaneously.

## 2.2 Materials and Methods

### 2.2.1. Construction of vectors and strains

The gene encoding the  $S_{12}C_4E_{40}$  triblock was prepared as follows. DNA encoding the silk-like  $S_{12}$ -block was created as illustrated before [10], with a modification in the number of DNA monomer repeats in such a way that the  $S_{12}$ -block encodes 12 repeats of the GAGAGAGE octapeptide. DNA encoding the hydrophilic random-coiled  $C_4$ -block was obtained by digesting the adapter-modified version of vector pMTL23-P2 [8] with *Dralll/Van91I* and inserting the released  $\sim 0.6$  kb fragment into the same vector via *Van91I*. The  $C_4$  fragment was then released from the resulting vector by digestion with *Bsal/BanI*. The gene encoding the elastin-like block  $E_{40}$  was constructed by multimerization of an  $E_{10}$  DNA monomer in vector pMTL23-aIII as described previously [14], with the exception that only four monomers were concatenated. The  $E_{10}$  monomer encodes 10 repeats of the pentapeptide VPGXG, where the X positions are occupied by five valines, three alanines, and two glycines in quasi-random order. The vector pMTL23-aIII- $E_{40}$  so obtained was linearized with *BsmBI* and dephosphorylated, after which the *Bsal/BanI*-digested  $C_4$ -block was inserted. The resulting vector was again linearized with *BsmBI* and dephosphorylated, and the *Bsal/BanI*-digested  $S_{12}$ -block was then inserted to yield vector pMTL23-aIII- $S_{12}C_4E_{40}$ . The encoded triblock copolymer consists of  $\sim 700$  amino acids with three distinct sequence types:  $(\text{GAGAGAGE})_{12}$ -spacer- $(\text{VPGXG})_{40}$ , where the spacer ( $C_4$ ) is  $(\text{GEPGNPSPGNQGGPQGNKGSPGNPGQPGNEGQPGQPGQNGQPGEPSNGPQGSQGNPGKNGQPGSPGSQGSQGNQGSQGNPGQPGNPGQPGEQGKPGNQGPA})_4$  (cloning-derived residues not indicated).

Construction of the diblock-bearing vector pMTL23-aIII- $S_{24}E_{40}$  was analogous to the above, except that no  $C_4$ -block was inserted, and that an  $S_{24}$ -block (encoding 24 repeats of the GAGAGAGE octapeptide) was used instead of the  $S_{12}$ -block. The encoded diblock copolymer consists of  $\sim 400$  amino acids with two distinct sequence types:  $(GAGAGAGE)_{24}$ - $(VPGXG)_{40}$  (cloning-derived residues not indicated).

Finally, the  $S_{12}C_4E_{40}$  and  $S_{24}E_{40}$  fragments were cloned into expression vector pPIC9 (Invitrogen) via *XhoI/EcoRI*. This created a fusion with the *Saccharomyces cerevisiae*  $\alpha$ -mating factor secretion signal present in the vector. The plasmids were linearized with *Sall* to promote homologous integration at the *his4* locus upon transformation of *Pichia pastoris* GS115 by electroporation [24].

### 2.2.2. Fermentation of *Pichia pastoris*

The biopolymers were produced by methanol fed-batch fermentation of *P. pastoris* in 2.5 L Bioflo 3000 bioreactors (New Brunswick Scientific) as described previously [25]. The pH was maintained at 5.5 for  $S_{12}C_4E_{40}$  and at 6.0 for  $S_{24}E_{40}$ , and the growth temperature was 30 °C. The methanol level in the broth during the induction phase was kept constant at  $\sim 0.2$  % (w/v) by means of a gas sensor-controller.

### 2.2.3. Biopolymer purification

The purification of the  $S_{12}C_4E_{40}$  triblock from the cell-free broth was similar to the procedure we described previously for related elastin-free  $S_{24}C_4S_{24}$  triblocks [8], with the exception that 40 % of ammonium sulfate saturation was used for protein precipitation and that dH<sub>2</sub>O was used instead of 10 mM ammonia in all steps.

The diblock  $S_{24}E_{40}$  was purified from the cell-free broth by twice-repeated Inverse Transition Cycling (ITC) [14] in the presence of 2 M NaCl. In this procedure, the elastin-like protein is precipitated by centrifugation after heating to 65 °C ("hot spin"). After resuspending the pellet and cooling to 4 °C the elastin-like protein redissolves, whereas

heat-denatured host-derived proteins remain insoluble and precipitate upon centrifugation (“cold spin”).

Both proteins were dialyzed using Spectra/Por 7 tubing (Spectrum Labs) with a 1 kDa molecular weight cut-off. The desalted proteins were freeze-dried for storage until use.

#### **2.2.4. Product characterization**

Electrophoresis (SDS-PAGE) was performed using the NuPAGE Novex system (Invitrogen) with 10% Bis-Tris gels (Invitrogen), MES-SDS running buffer (Invitrogen) and SeeBlue Plus2 (Invitrogen) prestained molecular mass markers. Gels were stained with Coomassie SimplyBlue SafeStain (Invitrogen). N-terminal sequencing was done by Midwest Analytical (St. Louis, MO), either on the main band in SDS-PAGE after blotting onto PVDF membrane ( $S_{24}E_{40}$ ), or on the purified protein in solution ( $S_{12}C_4E_{40}$ ).

The molecular mass distribution of the product was analysed by matrix-assisted laser desorption/ionization time-of-flight mass spectroscopy (MALDI-TOF MS). The analyses were performed using an Ultraflex mass spectrometer (Bruker), on a 600  $\mu\text{m}$  AnchorChip target (Bruker) and with 2,5-dihydroxyacetophenone (Sigma-Aldrich) as matrix. Samples were prepared and measured as described previously [25].

#### **2.2.5. Atomic Force Microscopy (AFM)**

Stock solutions of  $S_{12}C_4E_{40}$  and  $S_{24}E_{40}$  were prepared by dissolving pure, lyophilized products to a concentration of approximately 10 g/L in 10 mM NaOH (Merk, Germany). They were kept at 4 °C for 20 min, occasionally vortexed to allow complete dissolution of the protein. Then products were acidified with 10 mM HCl (Merk, Germany) and diluted with sodium phosphate buffer pH 2 (10 mM) to a final concentration of 5 g/L for  $S_{24}E_{40}$ . For  $S_{12}C_4E_{40}$ , final protein solutions made by diluting the stock solutions with dH<sub>2</sub>O to concentration of 5 g/L were titrated to pH 2 with 1M HCl. The samples were incubated at five different temperatures (4 °C, 25 °C, 35 °C, 45 °C and 55 °C) to allow supramolecular assembly to occur. To prevent biological contamination, all tubes were sterilized with

ethanol and all solutions were filtered before experiments. At each time point samples were taken and diluted with dH<sub>2</sub>O to a final product concentration of 0.1 g/L for AFM imaging. A drop (50 µl) of each sample was deposited onto a clean hydrophilic silica wafer (Siltronic Corp.) and left for 2 min. The wafer was then washed with 500 µl of dH<sub>2</sub>O to remove salts, and dried under a stream of nitrogen. The dry samples were analysed using a Nanoscope V in Scan Asyst™ imaging mode, using non-conductive silicon nitride probes (Veeco, NY, USA) with a spring constant of 0.32 N/m. Images were recorded between 0.200 - 0.990 Hz and further processed with NanoScope Analysis 1.20 software (Veeco Instruments Inc. 2010, USA).

### **2.2.6. Dynamic Light Scattering (DLS)**

A 5 g/L stock solution was prepared by dissolving pure, lyophilized proteins in 10 mM NaOH. To analyse the kinetics of fibril growth, samples were prepared by diluting the stocks with sodium phosphate buffer pH 2 (10 mM) to a final concentration of 0.2 g/L for the diblock. For the triblock, the working solutions with concentration of 1 g/L made by diluting the stock solution with dH<sub>2</sub>O were titrated to pH 2 to study the growth kinetics. All solutions were sterilized using 0.2 µm filters (Milipore) to prevent contamination and remove dust before measurement. Light scattering was performed using an ALV dynamic light scattering instrument with a Cobolt Samba- 300 DPSS laser (300 mW) operating at a wavelength of 532 nm and an ALV-5000/60X0 multiple  $\tau$  digital correlator. A refractive index matching bath of filtered cis-decalin surrounded the cylindrical scattering cell. All measurements were undertaken at a fixed angle  $\vartheta$  of 90 °, corresponding to a scattering vector  $q = \frac{4\pi n}{\lambda} \sin \frac{\vartheta}{2}$ , where  $n = 1.333$  is the refractive index of the solvent (water). The temperature was varied between 15 °C and 60 °C using a Haake F3-K thermostat.

### **2.2.7. Rheometry**

Experiments were carried out on an Anton Paar MCR501 Rheometer equipped with a C10/TI Couette geometry, with bob and cup diameter of 9.991 and 10.840 mm, respectively. Freeze-dried protein was first dissolved in water at pH 10 and then 1 M HCl

was added until the pH was 1.5 and the final protein concentration was 50 g/L. The solutions were loaded immediately into the rheometer. A thin layer of oil was used to minimize evaporation. Gel formation was monitored by applying a 1 Hz sinusoidal deformation of 1 % to the system. The storage modulus ( $G'$ ) and loss modulus ( $G''$ ) were obtained while different temperature ramps were introduced during gel formation. The temperature was controlled by a Peltier system which allows fast heating and cooling. The temperature-cycles were applied as 5 °C - 15 °C - 25 °C - 35 °C - 25 °C - 15 °C - 5 °C.

## 2.3 Results and Discussion

### 2.3.1 Polymer biosynthesis and product characterization

The two protein polymers,  $S_{12}C_4E_{40}$  and  $S_{24}E_{40}$ , were biosynthesized in *P.pastoris*. The recovery of purified dry product per litre of cell-free broth was above 500 mg. The purified proteins were characterized by SDS-PAGE, MALDI-TOF and N-terminal sequencing. The SDS-PAGE of  $S_{12}C_4E_{40}$  (Appendix, Figure 2.8a) and  $S_{24}E_{40}$  (Appendix, Figure 2.8b) showed that both proteins appear to be pure and intact. Both proteins migrated at an apparent molecular weight much higher than their true molecular weight. Whereas the standard protein markers in SDS-PAGE are always relatively hydrophobic, our products are composed of atypical and relatively polar amino acids. As a consequence, they bind less SDS [7, 10]. This strongly reduces their migration velocity, and leads to a high apparent molecular mass [14, 26, 27]. N-terminal sequencing of the two protein polymers confirmed their identity. For both proteins, roughly one-fourth of the molecules appeared N-terminally extended with a single Glu-Ala repeat, which commonly occurs because of partial processing of the  $\alpha$ -factor prepro secretory signal by the *P. pastoris* dipeptidylaminopeptidase [7]. The molecular mass of  $S_{12}C_4E_{40}$  and  $S_{24}E_{40}$  was verified by MALDI-TOF, which shows monodisperse products with a mass close to the theoretical values of 60134 Da and 30008 Da, respectively (Appendix, Figure 2.9).

### 2.3.2. Fibril formation

Fibril formation was first studied in dilute solutions with concentration of 5 g/L. The preparation of the sample plays an important role, as the proteins need to be well dissolved. After the solutions were acidified to pH 2, they were incubated at different temperatures and sampled at different times for AFM analysis. The super-molecular structures formed were adsorbed, from the solution, onto a clean piece of oxidized silicon wafer. The high pH conditions were also studied by AFM, however no fibrils were observed.

Figure 2.1 (for  $S_{12}C_4E_{40}$ ) and Figure 2.2 (for  $S_{24}E_{40}$ ) provide clear evidence that both proteins form thin fibrils which grow longer in the course of time. At high magnification, the fibrils of the triblock seem to have periodic morphology, whereas those of the diblock are smoother (Appendix, Figure 2.11.). Periodicity, if any, can be only faintly noticed. Such periodicity may result from a twist in a ribbon-like structure; several natural proteins form fibrils which have this feature. The ribbon-like fibrils were previously found in a polymer with only *S* and *C* blocks [8, 12].

The length of the fibrils was calculated by averaging the length of at least 50 well-defined individual fibrils in AFM images, and plotted as a function of incubation time. The filaments of both proteins appeared to be rather polydisperse (Appendix, Figure 2.10). If the growth rate is homogeneous in the sample, new nuclei are formed in the course of experiment, from which fibrils grow: in other words, the concentration of nuclei is not constant in time, but increases. This contrasts with our findings for elastin-free  $S_{24}C_4S_{24}$ , which does not form new nuclei in the course of the experiment and thus forms monodisperse fibrils [23]. Clearly, in the present case of  $S_{12}C_4E_{40}$  and  $S_{24}E_{40}$ , homogeneous nucleation is possible, causing poly-dispersity. The growth rate of both polymers is temperature dependent,  $S_{12}C_4E_{40}$  growing faster than  $S_{24}E_{40}$ . The temperature dependence is probably caused by the elastin blocks.  $S_{12}C_4E_{40}$  fibrils grew equally fast at different temperatures until 8 hours (when a length of about 300 nm was reached), but after that time, the growth rate increased with increasing temperatures up to 35 °C. After 24 hours,

the fibril length often exceeded the maximum AFM frame size (10  $\mu\text{m}$ ). The filaments of the diblock, which grew much more slowly, did not display such multiphasic growth and their length did not exceed 1  $\mu\text{m}$ , even after one week.

The elastin-free triblock  $S_{24}C_4S_{24}$  [8, 10, 23, 28] grows much faster than both  $S_{12}C_4E_{40}$  and  $S_{24}E_{40}$ : after 1 hour at room temperature, filaments can grow up to 1.5  $\mu\text{m}$ . However, as the elastin-free triblock has more silk-like octapeptides, it is at this stage not possible to discern whether this difference in growth speed is caused by the presence of the elastin-like block in  $S_{12}C_4E_{40}$  and  $S_{24}E_{40}$ .

After 48 hours at 35  $^{\circ}\text{C}$ , the length of  $S_{24}E_{40}$  fibrils, as measured by AFM, seems to decrease. The same was observed for  $S_{12}C_4E_{40}$  but after 24 hours at 45  $^{\circ}\text{C}$  and 55  $^{\circ}\text{C}$  (Figure 2.3). There may be several explanations for this observation. First, fibrils might become weaker at high temperature and then be susceptible to breaking. Thermally activated breaking implies very weak bonds ( $\sim 10$  kT) which are very unlikely since this would also imply fast breaking under mechanical shear, which is not observed. Secondly, the change in length may be apparent due to some other effects. For example, if longer fibrils are unstable with respect to aggregation, and aggregates are not captured by the sampling method adopted here, one expects that long fibrils would become progressively underrepresented in the AFM sample. Hence, this observation may also be a first indication that the fibrils have a tendency to aggregate. Below we discuss evidence for aggregation, so this may indeed explain the apparent decrease in length, as well as the clusters observed in AFM images.

The morphology of  $S_{24}E_{40}$  fibrils (after 6 hours of incubation) does not seem to significantly depend on temperature (Figure 2.2 A, B, C). After a long incubation time (7 days, Figure 2.2 D, E, F), the fibrils of  $S_{24}E_{40}$  had a less well-defined structure; we mainly visualized many short rod-shaped particles. In contrast, the fibrils from  $S_{12}C_4E_{40}$  (Figure 2.1) were longer and more homogenous.

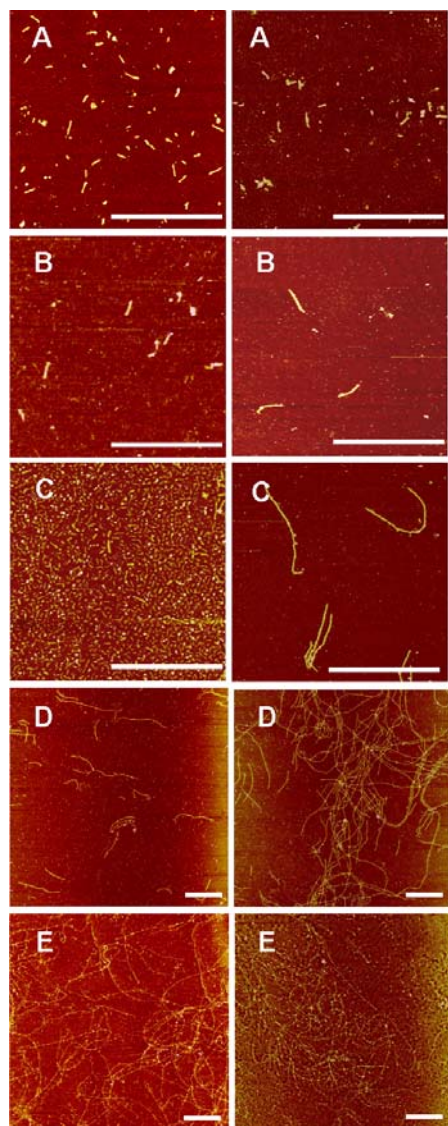


**Figure 2.1.** Representative AFM images of fibrils by low-pH induction of  $S_{12}C_4E_{40}$  at 4 °C (left column) and 35 °C (right column) after (A) 1 hour, (B) 3 hours, (C) 7 hours, (D) 24 hours and (E) 48 hours, respectively. All the scale bars correspond to 1.5  $\mu\text{m}$ .

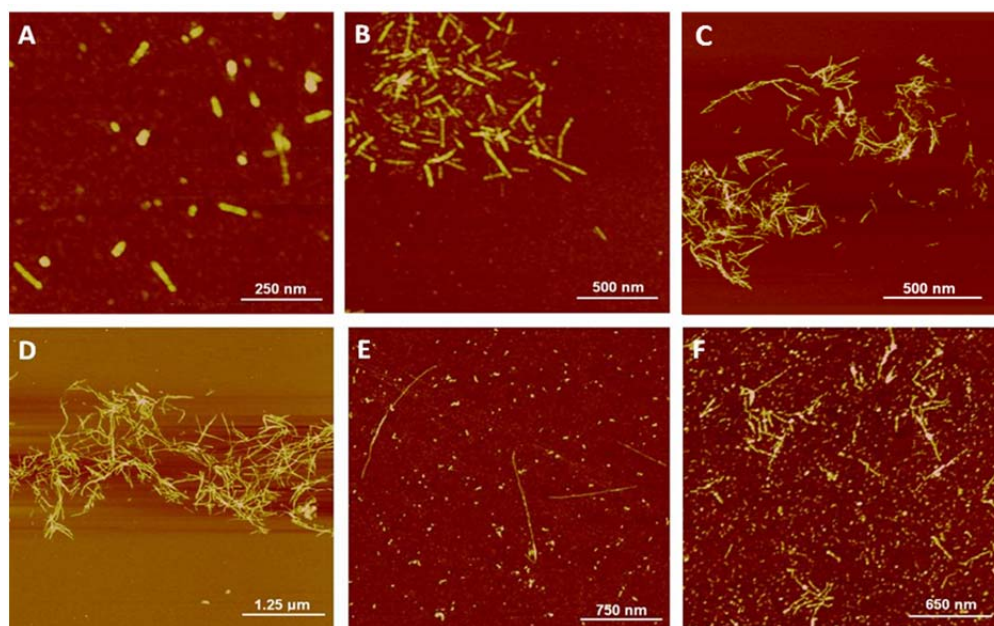


**Figure 2.2.** Representative AFM images of fibrils by low-pH induction of  $S_{24}E_{40}$  (A) at 4 °C after 6 hours; (B) at 25 °C after 6 hours; (C) at 35 °C after 6 hours; (D) at 4 °C after 7 days; (E) at 25 °C after 7 days; (F) at 35 °C after 7 days.

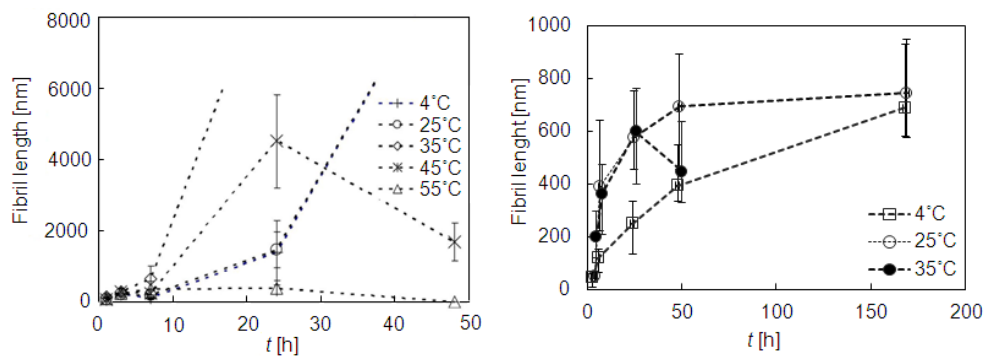


**Figure 2.3.** Fibril growth as a function of time  $t$  elapsed after the onset of growth of  $S_{12}C_4E_{40}$  (left) and  $S_{24}E_{40}$  (right), as induced by pH. Fibril length was determined as the average of 50 individual fibrils imaged by AFM at different times and temperatures.

### 2.3.3. Light scattering: growth followed by sedimentation

Figure 2.4 shows light scattering intensity data as a function of time after acidification for dilute samples at various temperatures. In Figure 2.4a ( $S_{12}C_4E_{40}$ ), we observe a fast initial increase, followed by a slower increase for 15 °C and 20 °C, and a slow decrease for 35 °C. In Figure 2.4b ( $S_{24}E_{40}$ ), in all three cases (25 °C, 35 °C and 45 °C), there is an initial increase, followed by a decrease to very low intensity; this happens on time scales from 1 hour to 4 hours, being faster at higher temperatures. The intensity in 2.4b fluctuates considerably between individual readings. All the features in figure 2.4b indicate that fibril growth is followed by sedimentation during the experiment, most likely caused by aggregation of the fibrils into larger objects. In the earlier study on elastin-free  $S_{24}C_4S_{24}$  polymers [23] where non-aggregated fibrils were found, no such intensity decays were seen implying absence of any sedimentation. The driving force for aggregation is probably temperature-enhanced hydrophobic attraction between the elastin-like units. This also explains the increasing rate of sedimentation with temperature in Figure 2.4b. The highly hydrophilic  $C_4$  block [7] in  $S_{12}C_4E_{40}$  has a stabilizing influence, so that only at 35 °C the triblock aggregates sufficiently to show clear sedimentation. At 15 °C and 20 °C, there is a trade-off between growth and sedimentation but the overall trend is still an increase in scattering. Fused proteins were reported to have an effect on the transition temperature of a responsive elastin-like polypeptide, in which surface hydrophobicity in molecular proximity to the elastin-like polypeptide depresses the transition temperature [29].

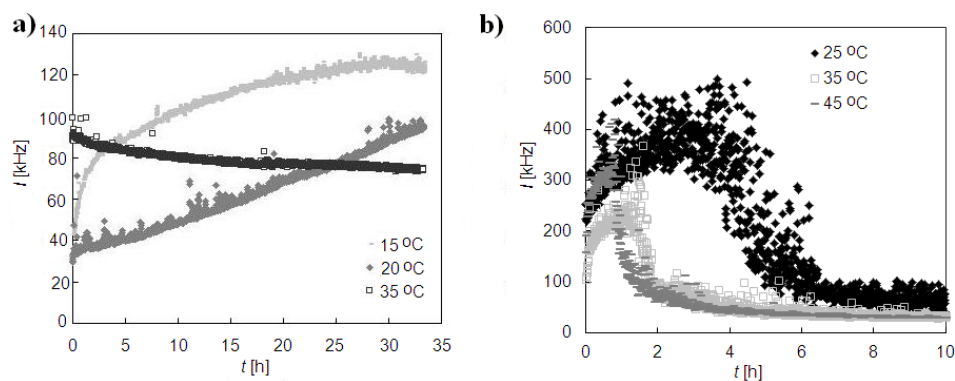


**Figure 2.4.** Growth kinetics as a function of time  $t$  followed by measuring the intensity of scattered light  $I$  of a)  $1 \text{ g/L } S_{12}C_4E_{40}$ ; b)  $0.2 \text{ g/L } S_{24}E_{40}$  at different temperatures

### 2.3.4. Fibril bundling at high temperature

The indication from Figure 2.4 that aggregation may occur, particularly at higher temperatures, is further supported by an AFM image of filaments prepared at  $55 \text{ }^\circ\text{C}$ , 24 hours (Figure 2.5B). Indeed, a comparison between fibrils grown during one month at  $4 \text{ }^\circ\text{C}$  (Figure 2.5A) and at  $55 \text{ }^\circ\text{C}$  (Figure 2.5C) clearly shows that bundling is induced by temperature likely higher than transition temperature, i.e. when individual fibrils become ‘sticky’.

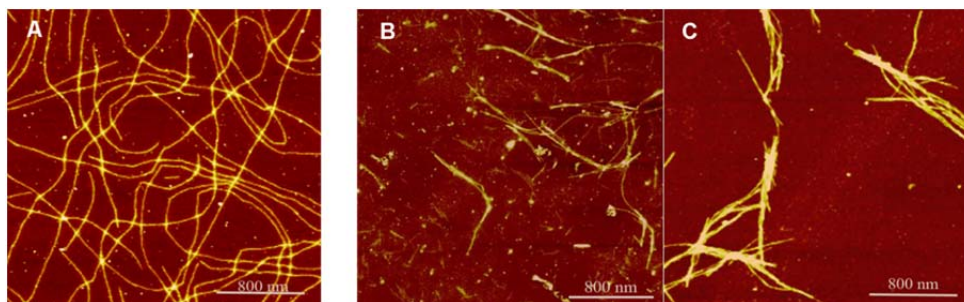


**Figure 2.5.** AFM images of  $S_{12}C_4E_{40}$  fibril bundles formed at low pH and high temperature: (A)  $4 \text{ }^\circ\text{C}$  after one month, (B)  $55 \text{ }^\circ\text{C}$  after 24 hours, (C)  $55 \text{ }^\circ\text{C}$  after one month.

### 2.3.5 The effect of concentration and temperature on filament length

When fibrils are formed at a higher polymer concentration, their length is much smaller. An example is given for  $S_{12}C_4E_{40}$  (Figure 2.6B). Since the length is determined by the ratio between the concentration of protein and the concentration of nuclei, this implies that the concentration of nuclei increases relatively more than the total polymer concentration. This supports our earlier conclusion that homogeneous nucleation occurs in these polymers, in contrast to elastin-free silk-like polymers [23]. Apparently, the elastin-like block enhances not only aggregation and sedimentation but also nucleation. Probably, the hydrophobic attraction brings protein molecules together in dense clusters, thereby facilitating folding and nucleation of a fibril. If this is indeed the case, then it is to be expected that the rate of nucleation should increase with increasing temperature, as the elastin-like block has a stronger tendency to cluster at higher temperature. To test this, we heated a sample for 15 minutes at 45 °C before quenching to low pH. The resulting fibrils were indeed much shorter than fibrils in samples that had not been pre-heated (Figures 2.6C and A, respectively). This indicates that heating indeed increases the number of nuclei.

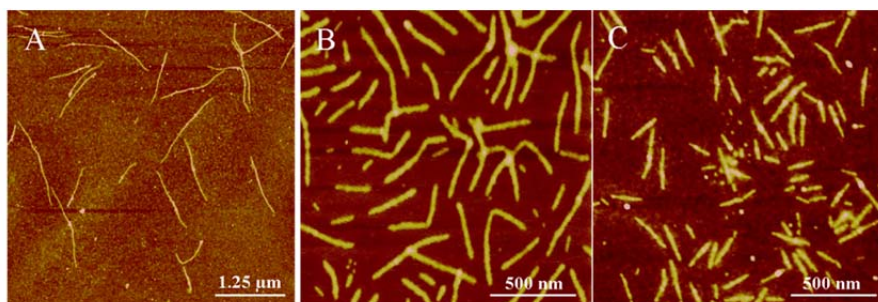


**Figure 2.6.** AMF images of fibrils made at (A) low concentration, no pre-heating, (B) high concentration and no-preheating, (C) low concentration (same as in A) but with pre-heating.

### 2.3.6. Gel formation

At concentrations of 35 g/L and higher, gels are formed by  $S_{12}C_4E_{40}$  at pH 2. For example, with protein concentration of 50 g/L, gelation occurred after 6 hours of incubation at 4 °C. Figure 2.7 shows the storage moduli of gels made at 50 g/L and 90 g/L, respectively, as a function of time, when cycling the temperature between 5 °C and 35 °C. The fresh gels at 5 °C are rather weak, having moduli of 39 Pa and 420 Pa, respectively. In contrast, gels formed by the elastin-free  $S_{24}C_4S_{24}$  prominently display a high modulus ( $\sim 10000$  Pa) at protein concentrations as low as 1 g/L [8, 28]. The difference may be well explained by the much smaller length of  $S_{12}C_4E_{40}$  fibrils at higher concentrations, as discussed in the previous section (Figure 2.6).

To investigate the temperature response of the  $S_{12}C_4E_{40}$  gels, the modulus was measured over two temperature cycles, where heating and cooling between 5 °C and 35 °C was performed discontinuously in steps of 10 °C. Figure 2.7 shows that the modulus decreases upon heating from 5 °C to 35 °C, but the gel is not capable of full recovery upon cooling from 35 °C to 5 °C. This suggests that irreversible aggregation of fibrils occurs over the heating cycle, which very likely hampers the recovery of the initially formed network. The irreversible character of the triblock is probably due to the silk-like block as the gel formation was triggered by pH. The elastin-like block makes the system temperature-sensitive, but the thermo-responsive reversibility may be lost because elastin-like block is connected to the silk-like fibrils rather than free in solution. As a result, bundled fibrils may not be able to separate upon cooling. Possibly, we are observing the combined effects of interaction between elastin-like and silk-like blocks. Literature reports of comparable tandem silk-elastin like copolymers [30, 31] also describe hydrogels at concentrations of the order of 100 g/L, but these did not display significant environmental post-gelation temperature sensitivity [30] due to irreversible crystallization of the silk-like blocks which prevent the elastin-like block from reversible folding.

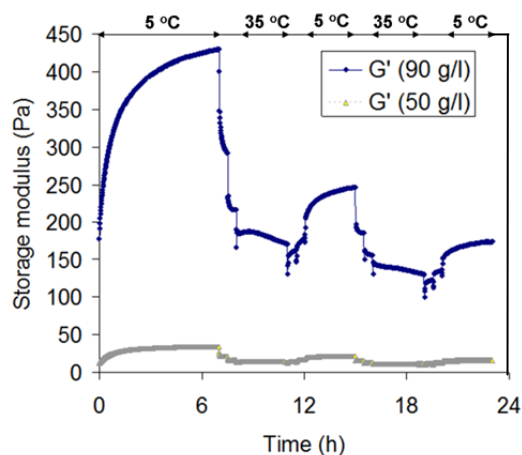


**Figure 2.7.** Storage modulus as a function of time during gelation of  $S_{12}C_4E_{40}$  when the solutions are quenched to low pH at 5 °C with concentrations of 90 g/L and 50 g/L. After forming the gel, the temperature was cycled between 5 °C and 35 °C as indicated.

## 2.4 Conclusions

We have produced two biosynthetic protein block copolymers (a diblock and a triblock) which both contain silk-like (*S*) and elastin-like (*E*) sequences; one of the two also contains a hydrophilic random coil sequence (*C*). Both the diblock ( $S_{24}E_{40}$ ) and the triblock ( $S_{12}C_4E_{40}$ ) are capable of pH-triggered, slow self-assembly into fibrils. This behavior, which is also known for elastin-free silk-like block copolymers, must clearly be attributed to the silk-like block. The elastin-like block introduces temperature sensitivity, due to its nature as an LCST polymer. This has two consequences: (a) it allows homogeneous fibril nucleation to occur, which introduces fibril poly-dispersity and a concentration dependence of fibril length; (b) it leads to ‘sticky’ fibrils, which undergo temperature-dependent bundling, aggregation and sedimentation. The latter effects are most prominent for  $S_{24}E_{40}$  which lacks the hydrophilic *C* block in  $S_{12}C_4E_{40}$ . Weak gels are formed in  $S_{12}C_4E_{40}$  solutions when they are quenched to low pH at concentrations higher than about 40 g/L. These gels respond to temperature in an irreversible manner, which we also ascribe to fibril aggregation.

---

**References**

1. Tirrell, D.A., M.J. Fournier, and T.L. Mason, *Protein engineering for materials applications*. Curr. Opin. Struct. Biol., 1991. **1**(4): p. 638-641.
2. Meyer, D.E., K. Trabbic-Carlson, and A. Chilkoti, *Protein Purification by Fusion with an Environmentally Responsive Elastin-Like Polypeptide: Effect of Polypeptide Length on the Purification of Thioredoxin*. Biotechnol. Prog., 2001. **17**(4): p. 720-728.
3. Zhang, S., *Fabrication of novel biomaterials through molecular self-assembly*. Nat. Biotechnol., 2003. **21**(10): p. 1171-1178.
4. Huang, J., C. Wong Po Foo, and D.L. Kaplan, *Biosynthesis and Applications of Silk-like and Collagen-like Proteins*. Polym. Rev. (Philadelphia, PA, U. S.), 2007. **47**(1): p. 29-62.
5. Dandu, R., H. Ghandehari, and J. Cappello, *Characterization of Structurally Related Adenovirus-laden Silk-elastinlike Hydrogels*. J. Bioact. Compat. Polym., 2008. **23**(1): p. 5-19.
6. Nettles, D.L., A. Chilkoti, and L.A. Setton, *Applications of elastin-like polypeptides in tissue engineering*. Adv. Drug Delivery Rev., 2010. **62**(15): p. 1479-1485.
7. Werten, M.W.T., et al., *Secreted production of a custom-designed, highly hydrophilic gelatin in Pichia pastoris*. Protein Eng., 2001. **14**(6): p. 447-454.
8. Martens, A.A., et al., *Triblock Protein Copolymers Forming Supramolecular Nanotapes and pH-Responsive Gels*. Macromolecules, 2009. **42**(4): p. 1002-1009.
9. Krejchi, M., et al., *Chemical sequence control of beta-sheet assembly in macromolecular crystals of periodic polypeptides*. Science, 1994. **265**(5177): p. 1427-1432.
10. Werten, M.W.T., et al., *Biosynthesis of an Amphiphilic Silk-Like Polymer*. Biomacromolecules, 2008. **9**(7): p. 1705-1711.
11. Cantor, E.J., et al., *Effects of Amino Acid Side-Chain Volume on Chain Packing in Genetically Engineered Periodic Polypeptides*. J. Biochem., 1997. **122**(1): p. 217-225.
12. Schor, M., et al., *Prediction of solvent dependent  $\beta$ -roll formation of a self-assembling silk-like protein domain*. Soft Matter, 2009. **5**(13): p. 2658-2665.
13. Meyer, D.E. and A. Chilkoti, *Quantification of the Effects of Chain Length and Concentration on the Thermal Behavior of Elastin-like Polypeptides*. Biomacromolecules, 2004. **5**(3): p. 846-851.
14. Schipperus, R., et al., *Secreted production of an elastin-like polypeptide by Pichia pastoris*. Appl. Microbiol. Biotechnol., 2009. **85**(2): p. 293-301.
15. Langer, R., et al., *Future directions in biomaterials*. Biomaterials, 1990. **11**(9): p. 738-745.
16. Urry, D.W., *Molecular Machines: How Motion and Other Functions of Living Organisms Can Result from Reversible Chemical Changes*. Angew. Chem., Int. Ed. Engl., 1993. **32**(6): p. 819-841.

17. Urry, D.W., *Physical Chemistry of Biological Free Energy Transduction As Demonstrated by Elastic Protein-Based Polymers*. J. Phys. Chem. B, 1997. **101**(51): p. 11007-11028.
18. Qiu, W., et al., *Wet-Spinning of Recombinant Silk-Elastin-Like Protein Polymer Fibers with High Tensile Strength and High Deformability*. Biomacromolecules, 2009. **10**(3): p. 602.
19. Xia, X.-X., et al., *Tunable Self-Assembly of Genetically Engineered Silk–Elastin-like Protein Polymers*. Biomacromolecules, 2011. **12**(11): p. 3844-3850.
20. Dinerman, A.A., et al., *Solute diffusion in genetically engineered silk–elastinlike protein polymer hydrogels*. J. Controlled Release, 2002. **82**(2–3): p. 277-287.
21. Qiu, W., et al., *Complete Recombinant Silk-Elastinlike Protein-Based Tissue Scaffold*. Biomacromolecules, 2010. **11**(12): p. 3219-3227.
22. Cappello, J., et al., *In-situ self-assembling protein polymer gel systems for administration, delivery, and release of drugs*. J. Controlled Release, 1998. **53**(1–3): p. 105-117.
23. Beun, L.H., et al., *Self-Assembly of Silk-Collagen-like Triblock Copolymers Resembles a Supramolecular Living Polymerization*. ACS Nano, 2011. **6**(1): p. 133-140.
24. Wertén, M.W.T., et al., *High-yield secretion of recombinant gelatins by Pichia pastoris*. Yeast, 1999. **15**(11): p. 1087-1096.
25. Wertén, M.W.T., et al., *Precision Gels from Collagen-Inspired Triblock Copolymers*. Biomacromolecules, 2009. **10**(5): p. 1106-1113.
26. McPherson, D.T., J. Xu, and D.W. Urry, *Product Purification by Reversible Phase Transition Following Escherichia coli Expression of Genes Encoding up to 251 Repeats of the Elastomeric Pentapeptide GVGVP*. Protein Expression Purif., 1996. **7**(1): p. 51-57.
27. Meyer, D.E. and A. Chilkoti, *Genetically Encoded Synthesis of Protein-Based Polymers with Precisely Specified Molecular Weight and Sequence by Recursive Directional Ligation: Examples from the Elastin-like Polypeptide System*. Biomacromolecules, 2002. **3**(2): p. 357-367.
28. Martens, A.A., et al., *Dilute gels with exceptional rigidity from self-assembling silk-collagen-like block copolymers*. Soft Matter, 2009. **5**(21): p. 4191-4197.
29. Trabbic-Carlson, K., et al., *Effect of protein fusion on the transition temperature of an environmentally responsive elastin-like polypeptide: a role for surface hydrophobicity?* Protein Eng., Des. Sel., 2004. **17**(1): p. 57-66.
30. Dinerman, A.A., et al., *Swelling behavior of a genetically engineered silk-elastinlike protein polymer hydrogel*. Biomaterials, 2002. **23**(21): p. 4203-4210.
31. Haider, M., et al., *Molecular Engineering of Silk-Elastinlike Polymers for Matrix-Mediated Gene Delivery: Biosynthesis and Characterization*. Mol. Pharmaceutics, 2005. **2**(2): p. 139-150.

## Appendix

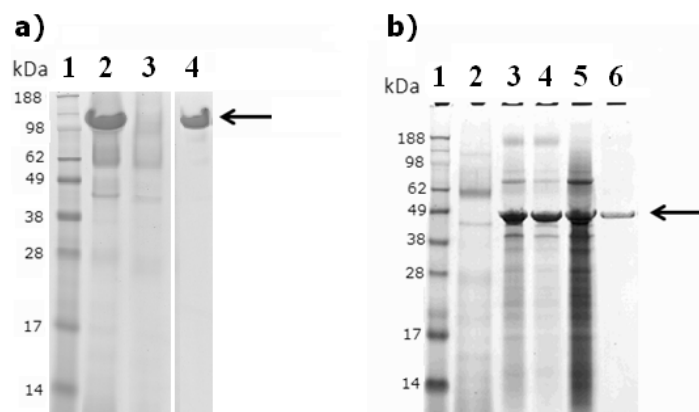


**Figure 2.8.** SDS PAGE of **a)**  $S_{12}C_4E_{40}$  purified by ammonium sulfate precipitation: **Lane 1:** molecular mass marker, **Lane 2:** fermentation supernatant, **Lane 3:** supernatant after precipitation with ammonium sulfate at 40% saturation (host-derived proteins), **Lane 4:** pellet after precipitation with ammonium sulfate at 40% saturation (product); **b)**  $S_{24}E_{40}$  purified by ITC method with 2M NaCl; **Lane 1:** molecular mass marker; **Lane 2:** supernatant after hot spin; **Lane 3:** pellet with protein after hot spin; **Lane 4:** supernatant with protein after cold spin; **Lane 5:** pellet after second hot spin; **Lane 6:** supernatant after second cold spin (purified protein). The arrows point to the product bands.

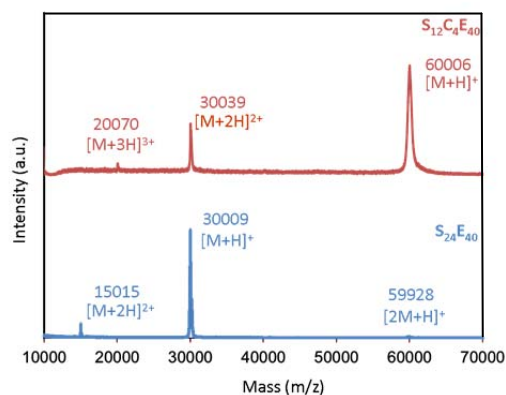


**Figure 2.9** MALDI-TOF of purified  $S_{12}C_4E_{40}$  and  $S_{24}E_{40}$ . The various charged- molecular ions are indicated.

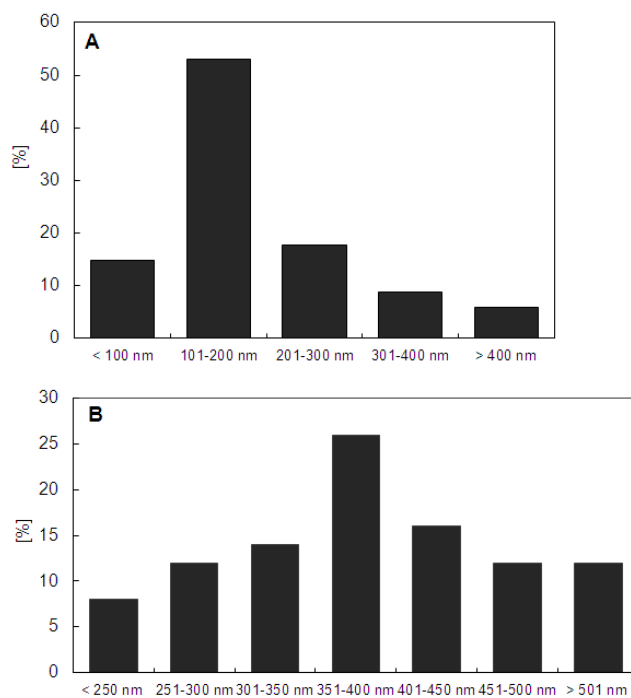


**Figure 2.10.** Fibril length distribution of A)  $S_{12}C_4E_{40}$  and B)  $S_{24}E_{40}$  at 25 °C after 6 hours.

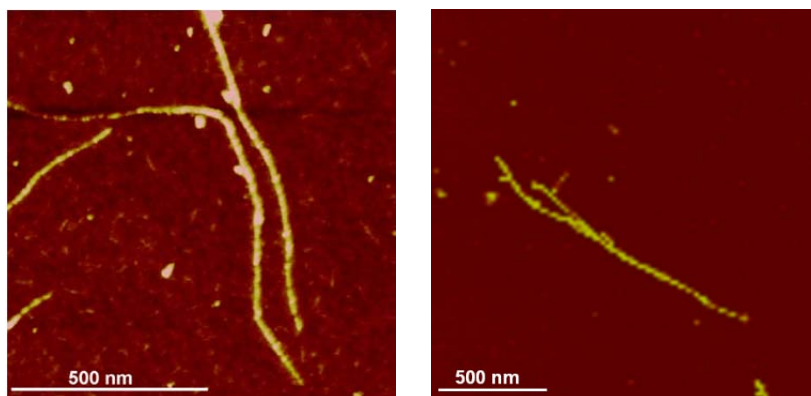


**Figure 2.11.** Fibril morphology obtained by AFM of single fibril formed by pH-triggered self-assembly of (Left)  $S_{12}C_4E_{40}$  in 20 hours at 4 °C; (Right) for  $S_{24}E_{40}$  in 24 hours at 4 °C.

## Chapter 3

---

# Dilute self-healing hydrogels of silk-collagen-like block co-polypeptides at neutral pH

---

We report on self-healing, pH-responsive hydrogels that are entirely protein-based. The protein is a *de novo* designed recombinant triblock polypeptide of 66 kDa/mol consisting of a silk-like middle block (GAGAGAGH)<sub>48</sub>, flanked by two long collagen-inspired hydrophilic random coil side blocks. The pH-dependent charge on the histidines in the silk block controls folding and stacking of the silk block. At low pH the protein exists as monomers, but above pH 5.6 it self-assembles into long fibers. At higher concentrations the fibers form self-healing physical gels. Optimal gel-strength and self-healing are found at a pH of around 7. The modulus of a 2 wt % gel at pH 7 is  $G' = 1700$  Pa. Being protein-based, and amenable to further sequence engineering, we expect that these proteins are promising scaffold materials to be developed for a broad range of biomedical applications.

Accepted as: M.D. Golinska, M.K. Włodarczyk-Biegun, M.W.T. Werten, M.A. Cohen Stuart, F.A. de Wolf, and R. de Vries; Dilute self-healing hydrogels of silk-collagen-like block co-polypeptides at neutral pH, *Biomacromolecules*



### 3.1 Introduction

Hydrogels are being used in a steadily increasing number of biomedical applications, such as for oxygen-permeable contact lenses [1, 2], as cell carriers [3], in wound management [4], as biodegradable delivery systems for drugs [5-7], as scaffolds for regenerative medicine and tissue engineering [8-11], and more [12]. All of these applications impose a large number of constraints on the type of hydrogel that can be used, both in terms of the chemistry and physics of the gels, and in terms of their interaction with cells and tissues. To start with constraints on the physics and chemistry, many applications require that gelation can be induced by simple stimuli such as a change in temperature, pH, by mixing etc., and that the kinetics of gelation falls within a certain time window. Other constraints include, for example, limits on the erosion of the gel that can be tolerated, as it is exposed to the application environment. In addition to the purely physical-chemical constraints, there are obviously many constraints related to their interaction with cells and tissue, such as low toxicity, non-immunogenicity, biodegradability, favourable attachment and growth of some types of cells, etc.

Many, but certainly not all hydrogels that are being explored for biomedical applications consist of polymers, both synthetic and natural. Synthetic polymers that are used extensively include poly (glycolic acid) (PGA) [13], poly(lactic acid) (PLA) [14], poly(ethylene oxide) (PEO) [15], poly(vinyl alcohol) (PVA) [16], and poly(acrylic acid) (PAA) [17]. Besides synthetic polymers, thermo- or pH-responsive gels are also formed by many naturally occurring polymers such as gelatine, agarose, carrageenans, amylose, amylopectin, chitosan, etc. These naturally derived materials [18] are thought to be more appropriate for applications such as tissue engineering applications than the synthetic ones [19, 20], since their chemistry and structure more closely resembles that of the components of the natural extracellular matrix (ECM) [21, 22].

A downside of the use of naturally occurring polymers can be poor reproducibility of gel properties, due to variations related to the natural source of the polymers, molecular compositions that are not well defined, and the lack of control over the polymer chemistry

to tune properties related to the application [23-25]. Quite naturally, therefore, many groups have turned to various forms of bioengineering to create designed biopolymers with tuneable properties [26-28].

Peptides of (nearly) arbitrary sequence can be easily prepared synthetically, and many groups are exploring the potential of peptide self-assembly to create gels that can act as scaffolds for cell growth [29, 30]. In particular, many groups are focusing on designing peptides that form stable fibers [31-36], since the collagen framework of the ECM is essentially a protein-fiber gel. Much longer designed polypeptides that form hydrogels, such as silk-elastin polymers [37-39], cannot be prepared synthetically, and have to be produced biosynthetically, via recombinant DNA technology. Much of this work is focussed on stimuli responsive hydrogels as scaffolds for cell growth [37-39].

We have previously designed a hydrophilic collagen-inspired polypeptide that behaves as a hydrophilic random chain, with an amino-acid composition close to that of collagen [40]. The 99 amino-acid long "C-block" sequence (and its multimers  $C_2$ ,  $C_4$ , etc.) can be produced at large scale by secreted expression by *Pichia pastoris* [40]. Simple bulk precipitation steps are sufficient to purify the polypeptides from the supernatant. By combining this collagen-inspired hydrophilic block with various bio-inspired self-assembly blocks, polypeptides can be obtained that form various types of hydrogels and that can be easily produced at large scale.

By attaching a collagen-inspired triple-helix forming sequence at both the N- and C-terminal end of the C-block, a telechelic polypeptide is obtained that forms very regular thermo-sensitive hydrogels with trifunctional nodes [41, 42]. Dilute, pH-sensitive fiber gels are formed by triblocks with the general structure  $C_2S_{48}^XC_2$ , where  $S^X$  is a silk-like sequence GAGAGAGX, where X is a corner residue that gives rise to a beta turn [43-46]. If X is chosen to be an ionizable residue, the folding of the silk block, and hence the formation of protein fibers and fiber gels, becomes pH dependent [47, 48]. All these polymers are amenable to biofunctional modifications that will make them very suitable for a broad range of biomedical applications.

---

In previous work [43-46, 49], we have especially explored the system  $C_2S_{48}^E C_2$ . This polymer forms fibers and fiber gels at low pH (pH 2) [43]. At low pH, the glutamic acid residues are uncharged, which allows the silk block to fold and stack. Both the fiber core dimensions as determined by X-ray [50] and atomistic computer simulations [51] suggest that the silk blocks adopt a so-called beta-roll fold [52, 53]. Nucleation and growth of fibers for  $C_2S_{48}^E C_2$  has also been studied in detail [46].

For application under physiological conditions (around pH 7.4), gels that form at low pH are of limited use. In the previous work, the production of a  $C_2S_{48}^H C_2$  triblock with X = His was mentioned [49], but the physical properties of hydrogels were not investigated in any detail. Since the  $pK_a$  of the histidine group is around pH = 7, it may be expected that this polymer should be soluble in monomeric form at low pH, and that it should form fibers and fiber gels upon changing the pH to values close to neutral or above. Hence this polymer is likely more interesting for medical application.

Here, we therefore present a detailed characterization of pH-dependent fiber- and gel-formation of the  $C_2S_{48}^H C_2$  triblock copolymer. The kinetics of fibril formation, fiber morphology and size are studied using both light scattering and atomic force microscopy as a function of pH. Next, we characterize the rheological properties of the dilute gels formed by these fibers that may be expected to be amenable to biofunctional modifications that will make them very suitable for a broad range of biomedical applications.



pMTL23-P2 [40] with *DraIII/Van91I* and inserted into the linearized vector, creating an adapted  $C_2$ -encoding block.

The sequence of both blocks was verified by DNA sequencing. Digestion with *BsaI/BanI* and directional ligation was used to prepare first diblocks  $C_2S_{24}^H$  and  $S_{24}^HC_2$ , and then triblock  $C_2S_{48}^HC_2$ . Finally, the triblock was cloned into expression vector pPIC9 (Invitrogen) using *EcoRI* and *NotI*. The resulting vector was linearized with *SaI* to promote homologous integration at the *his4* locus, and generation of the (Mut+) phenotype, upon transformation of *Pichia pastoris* GS115 by electroporation, as described previously [55].

### 3.2.2. Protein production and purification

The biopolymer was produced by methanol fed-batch fermentation of *P. pastoris* in 2.5 L Bioflo 3000 bioreactors (New Brunswick Scientific) as described previously [55]. The pH was maintained at 3 and the growth temperature at 30 °C. The methanol level was kept constant at ~ 0.2 % (w/v) during induction phase.

The purification of  $C_2S_{48}^HC_2$  was similar to the procedure described previously for  $C_2S_{48}^EC_2$  [43] and for  $C_2S_{48}^HC_2$  [49], with the exception that 45 % of ammonium sulphate saturation was used for protein precipitation and polymer pellet was dissolved in 50 mM formic acid in all steps. Protein was dialyzed using Spectra/Por 7 tubing (Spectrum Labs) with a 1 kDa molecular weight cut-off against 10 mM formic acid. The desalted protein was freeze-dried for storage until use.

Lyophilized product was characterized on SDS-PAGE using the NuPAGE Novex system (Invitrogen) with 10 % Bis-Tris gels, MES-SDS running buffer and SeeBlue Plus2 (Invitrogen) prestained molecular mass markers. Gels were stained with Coomassie SimplyBlue SafeStain (Invitrogen). N-terminal sequencing of six amino acids was done by Midwest Analytical (St. Louis, MO), on the main band in SDS-PAGE after blotting onto PVDF membrane, confirming the expected sequence.

Polysaccharide content, according to phenol-sulfuric acid sugar assay [56] was ~ 7 %.

The molecular mass distribution of the product was analysed by matrix-assisted laser desorption/ionization time-of-flight mass spectroscopy (MALDI-TOF MS). The analyses were performed on a 600  $\mu\text{m}$  AnchorChip target (Bruker) and with 2,5-dihydroxyacetophenone (Sigma-Aldrich) as matrix, using an Ultraflex mass spectrometer (Bruker). Samples were prepared and measured as described previously [41].

### 3.2.3. Atomic Force Microscopy (AFM)

Stock solutions of  $\text{C}_2\text{S}_{48}^{\text{H}}\text{C}_2$  were prepared by dissolving pure, lyophilized product to a concentration of approximately 10 g/L in 10 mM HCl (Merk, Germany), occasionally vortexed to allow complete dissolution of the protein. Stock solutions were neutralized with 10 mM NaOH (Merk, Germany) and diluted with 10 mM sodium phosphate buffer at the desired pH, to a final concentration of 5 g/L. The samples were incubated at room temperature to allow supramolecular assembly to occur. After 24 h samples were taken and diluted with  $\text{dH}_2\text{O}$  to a final product concentration of 0.2 g/L for AFM imaging. A drop (50  $\mu\text{l}$ ) of each sample was deposited onto clean mica wafer and incubated for 5 min. The wafer was washed then with 500  $\mu\text{l}$  of  $\text{dH}_2\text{O}$  to remove salts, and dried under a stream of nitrogen. The dry samples were analysed by a Nanoscope V in Scan Asyst™ imaging mode, using non-conductive silicon nitride probes (Veeco, NY, USA) with a spring constant of 0.32 N/m. Images were recorded between 0.200-0.990 Hz and further processed with NanoScope Analysis 1.20 software (Veeco Instruments Inc. 2010, USA).

### 3.2.4. Dynamic Light Scattering (DLS)

Light scattering measurements were performed using Zetasizer NanoZS apparatus (Malvern Instruments, UK), equipped with a 4 mW He-Ne ion laser, operating at a wavelength of 633 nm. All measurements were done at a fixed angle  $\vartheta$  of 173 ° at 25 °C.

The protein sample was freshly prepared by dissolving pure, lyophilized protein in 10 mM HCl to final concentration of 2 g/l and vortexing. The protein solution was then filtrated (10k, Millipore) and diluted with 10 mM sodium phosphate buffer of proper pH (pH 6, 7, 8, 9) to a final concentration of 0.2 g/l. DLS was started immediately after sample

preparation to follow the formation of the fibrils over a time period of 3 hours. The given light scattering intensity is the Derived Count rate as reported by DTS Software, version 5.10 beta 1. We checked that the decay of the autocorrelation function was dominated by a single component, and used the z-averaged hydrodynamic radii as reported by the DTS Software, version 5.10 beta 1.

### 3.2.5. Rheometry

Five different concentrations of protein (0.75, 1, 1.5, 2 and 3 %) and four different pH (6, 7, 8, 9) were tested. All the samples were prepared in the same way, by dissolving given amount of protein in 10 mM HCl and vortexing for 2 h to dissolve completely. Samples were filtrated and then concentrated using spin filters (Ultracel®-3k, Millipore) according to the instructions of the manufacturer. Concentrations after centrifugation were determined spectrophotometrically.

Rheological measurements were performed on an Anton Paar MCR 501 Rheometer equipped with a CC10/T200 (Anton Paar) Couette geometry, with bob and cup diameter of 10.002 and 10.845 mm, respectively. A solvent trap was used to minimize evaporation.

Frequency sweeps with angular frequency ( $\omega$ ) between 0.01-100 rad/s were performed at strain of 0.1 %. Strain sweeps were performed between 0.01-100 % deformation and frequency of 1 Hz. Based on initial frequency and strain sweep results, a 1 Hz and 0.1 % deformation was chosen for measuring the build up of the modulus in time. The temperature was controlled by Peltier elements that allowed fast cooling and heating.

## 3.3 Results and Discussion

### 3.3.1. pH dependency of fiber growth

The  $C_2S_{48}^HC_2$  triblock copolymer was produced in *Pichia pastoris* at high yield. Approximately 1.1 g of purified and desalted protein was recovered per L of clarified broth. See Fig.S1 for SDS-PAGE of the purified product. MALDI-TOF (Fig. S2) shows that the protein polymer is monodisperse. The observed mass of 66,076 Da is in good agreement

with the expected mass of 66,135 Da. The histidine residues in the GAGAGAGH repeats of the  $C_2S_{48}^HC_2$  triblock copolymer determine the pH-dependence of the polymers self-assembly. The  $pK_a$  for isolated histidine groups is  $pK_a = 6.1$ , so naively one might expect fiber formation to occur around neutral pH. However, the driving force for folding and stacking of the silk-like domain may be so large that assembly already starts at a lower pH, when not all histidine groups have been completely neutralized. If, in addition to interactions between neighboring GAGAGA beta strands, folding entails strong interactions between neighbouring histidine groups and these interactions may also affect the effective  $pK_a$ . For these reasons, we start by characterizing how the self-assembly kinetics depends on pH.

Dynamic light scattering (DLS) was used to investigate the kinetics of fiber growth at different pH values. Measurements were done at a fixed low protein concentration of 0.2 g/l, well below the gelation threshold. Figure 3.1 and Figure 3.2 show, respectively, the time-resolved light scattering intensity and the z-average hydrodynamic radius, for pH values between 5 and 8. As expected, the kinetics of fibril formation is strongly dependent on pH. In order to quantify the critical pH above which fiber formation starts, we have plotted the initial rate of increase of the z-average hydrodynamic radius versus pH in Fig. 3.3. The initial rate of increasing z-average  $R_h$  was done by linear fit in the first 3 h of fibril growth. The critical pH at which fibrils start forming ( $pH_c$ ) is  $\sim 5.6$ , much lower than the  $pK_a$  of the histidine groups.

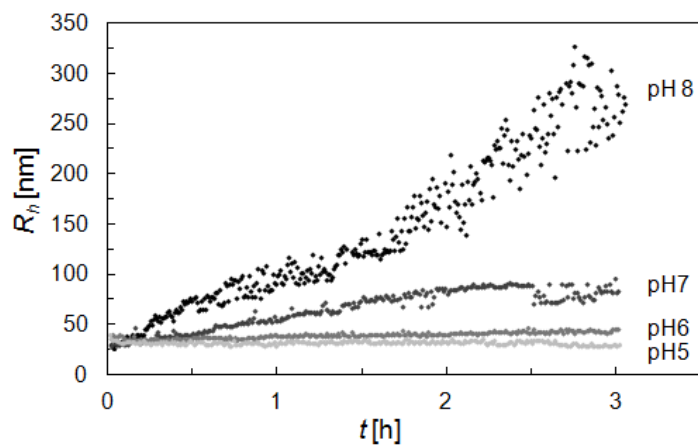


**Figure 3.1.** Influence of pH on the z-average hydrodynamic radius ( $R_h$ ) of  $C_2S_{48}^H C_2$  as a function of time  $t$ . The polymer concentration was 0.2 g/l in all samples.

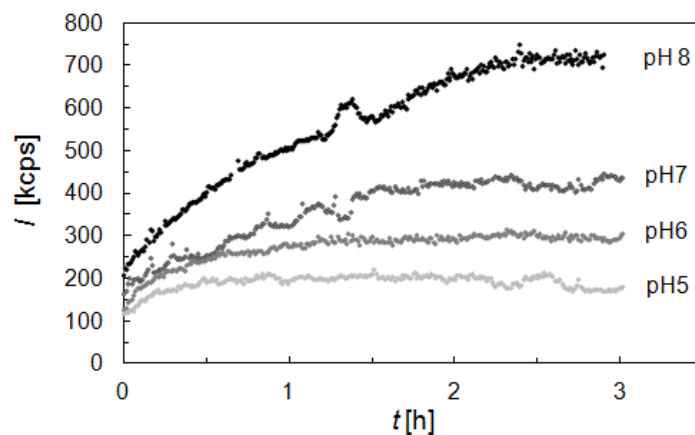


**Figure 3.2.** Influence of pH on the intensity  $I$  of scattered light of  $C_2S_{48}^H C_2$  as a function of time  $t$ . The  $C_2S_{48}^H C_2$  concentration was 0.2 g/l in all samples.

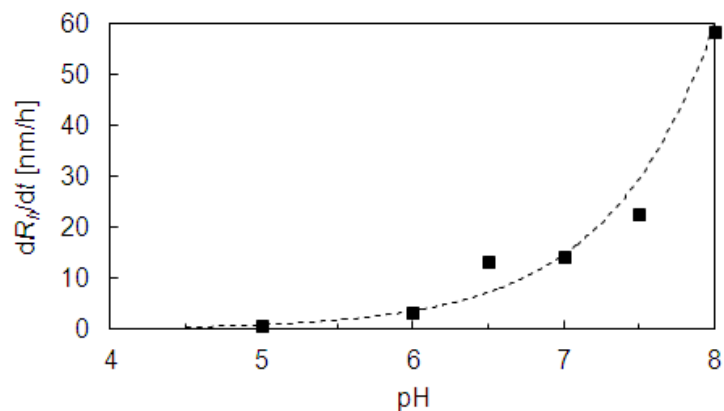


**Figure 3.3.** Initial rate of increase of hydrodynamic radius  $dR_H/dt$  as a function of pH. Fibril formation stops between pH 5 - 6.

Light scattering provides a first impression of the self-assembly kinetics, but shows neither the actual presence of fibers nor the fiber length and morphology. Therefore, AFM imaging was used. Fig. 3.4 shows images of self-assembled structures formed after 24 h, at different pH values. Fibrils with lengths of many microns were present at pH 7 and 8, whereas at pH 6, short fibrils with an average length of approximately 2.2  $\mu\text{m}$  were observed. At pH 5 hardly any fibrils were visible on the mica, and the few that were observed were short, with lengths below 500 nm. The pH dependence observed in the AFM images is completely consistent with that observed using DLS.

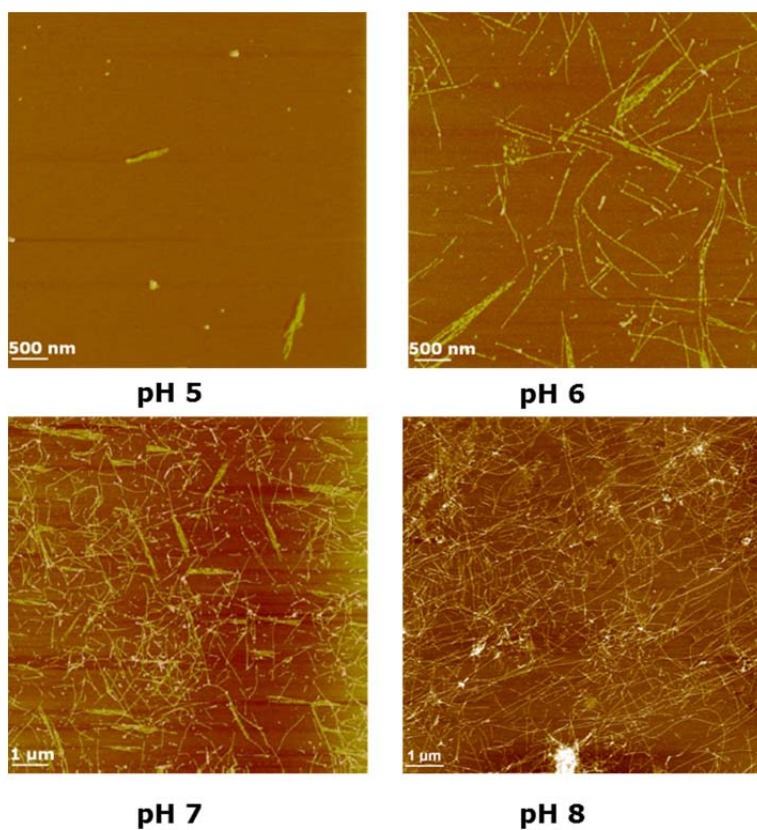


**Figure 3.4.** AFM images of 0.2 g/L  $C_2S_{48}^H C_2$  at different pH after 24 h incubation at room temperature

### 3.3.2. Gel Formation

With a view to future development of this type of polymers for application in medical gels, we characterized the rheological of hydrogels formed by the  $C_2S_{48}^H C_2$  fibers at higher concentrations, and focussed especially on the properties at pH 7. Gelation of the polypeptides is induced by raising the pH from pH 2 to pH 7. We have monitored the gelation process for a range of polypeptide concentrations using oscillation rheology, and the results are shown in Figure 3.5. For all concentrations tested, elastic behaviour (storage modulus  $G'$ ) eventually dominated over viscous behaviour (loss modulus  $G''$ ). The kinetics of gel formation and the final value of the moduli strongly depend on the

polypeptide concentration. The final values of the storage moduli are shown as a function of concentration in Figure 3.6. These moduli scale with concentration according to  $G'_0 = \alpha \cdot C^n$ , with a scaling exponent  $n \approx 1.5$ , and a prefactor  $\alpha = 16.1$ , where the storage modulus  $G'_0$  is in Pa and the polypeptide concentration  $C$  is in g/l. The hydrogels of the  $C_2S_{48}^H C_2$  studied here are quite different from the hydrogels of  $C_2S_{48}^E C_2$  studied before. At the same polypeptide concentration, the latter hydrogels have significantly higher moduli. Furthermore, the concentration dependence of the moduli of  $C_2S_{48}^E C_2$  is also steeper, having a scaling exponent  $n \approx 2.0$  [44]. Possibly,  $C_2S_{48}^H C_2$  forms shorter fibers than  $C_2S_{48}^E C_2$ , at higher concentration. Attractive interactions between the fibrils may have a strong impact on the rheology and also in this respect, the two systems may be different. For example, for a cross-linked network of semiflexible filaments [57], the predicted scaling exponent for the dependence of the storage modulus on concentration is  $n = 2.2$ , close to the value found for  $C_2S_{48}^E C_2$ , whereas for non-linked actin networks [58] the scaling exponent is experimentally found to be  $n = 1.4$ , close to the value we find for  $C_2S_{48}^H C_2$ .

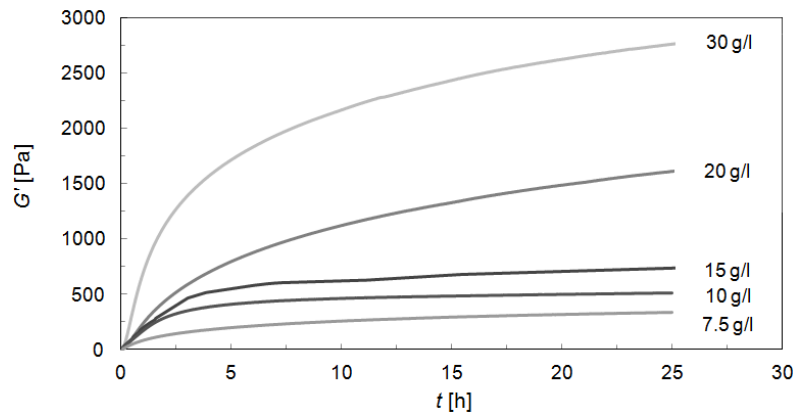


**Figure 3.5.** Development of storage moduli ( $G'$ ) as a function of time  $t$  at different concentrations of  $C_2S_{48}^H C_2$ . All measurements were recorded at pH 7 and 25 °C in a Couette configuration, at 1 Hz and 0.1 % deformation.

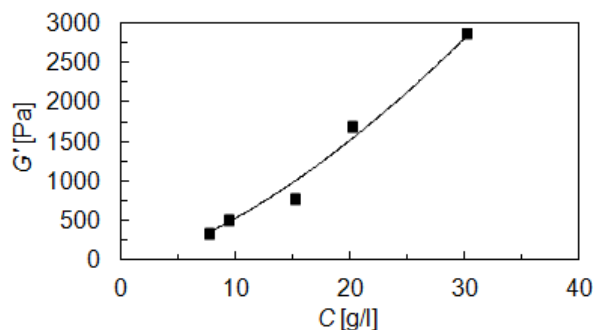


**Figure 3.6.** Storage modulus ( $G'$ ) as a function of concentration ( $C$ ) of  $C_2S_{48}^H C_2$  at pH 7 and 25 °C. The line is a power law fit through the data points with an exponent of 1.5 ( $y = 16.07x^{1.52}$ ).

With a view to possible future biomedical applications, we have also studied the growth and stability of the  $C_2S_{48}^H C_2$  hydrogels at the physiological temperature of 37 °C. The temperature increase affects the rheology properties and the final values of the storage modulus were somewhat lower at 37 °C than at 25 °C (250 Pa versus 500 Pa, for a 10 g/L sample). Furthermore, Figure 3.7 shows that higher ionic strength (150 mM) have a significant effect on the plateau elastic moduli ( $G' \approx 150$  Pa).

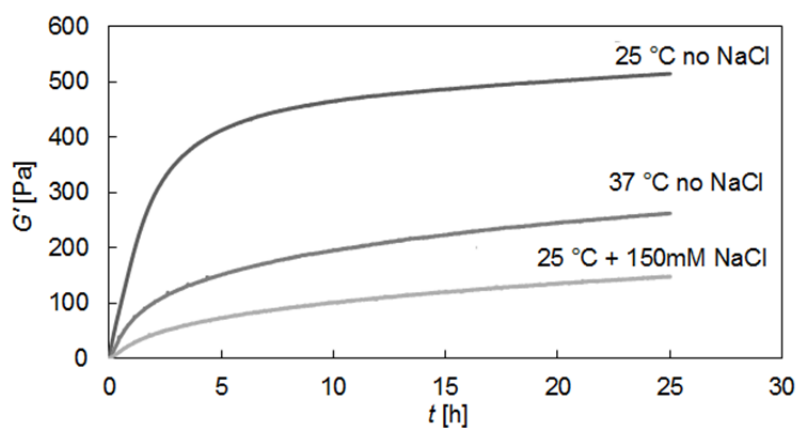


**Figure 3.7.** Storage modulus ( $G'$ ) for 10 g/l  $C_2S_{48}^H C_2$  at pH 7 as a function of time  $t$  (1 Hz,  $\gamma = 0.1$  %) at different temperatures and ionic strength.

### 3.3.3. pH dependence of gelation

For a selected concentration of  $C = 20$  g/l, we have also explored how pH affects gelation and final gel strength. Gelation was induced by raising the pH of the polypeptide value from  $\text{pH} = 2$  to the required pH value. The process of gelation was again followed by on-line measurement of the storage ( $G'$ ) modulus at 1 Hz at a strain of 0.1 %. Measured final storage moduli were plotted as a function of pH (Fig. 3.8). While naively one might expect to observe an increase in elastic moduli with increasing pH, we instead found a rather flat pH profile, with a slight optimum around  $\text{pH} = 7$ . Since many factors contribute to the gel modulus (fiber length, stiffness, concentration, physical cross-links, etc.) it is very possible that opposing pH dependencies exists. For example fiber length may increase with pH, but fiber stiffness or fiber physical cross-links may be reduced at higher pH. Such opposing or compensating pH dependencies may explain the rather flat pH profile of the modulus and the weak maximum at  $\text{pH} = 7$ .

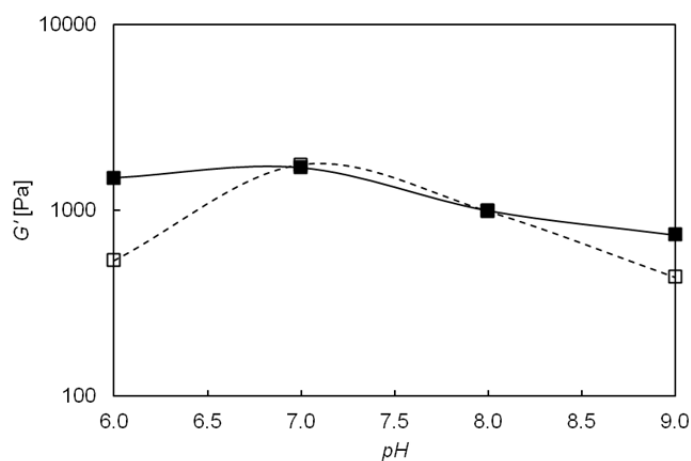


**Figure 3.8.** Storage modulus dependency on pH for 20 g/l  $C_2S_{48}^H C_2$  gel at 25 °C. Closed symbols: after 1<sup>st</sup> preparation. Open symbols: after mechanical failure and recovery for 24 h.

## 3.3.4. Nonlinear rheology

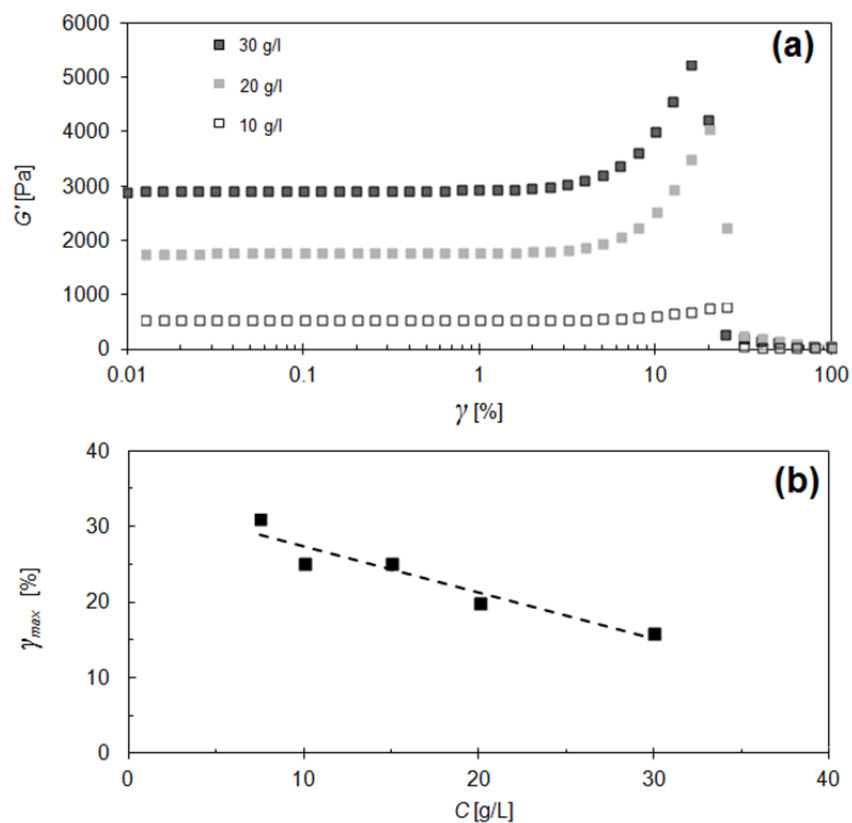


**Figure 3.9.** Strain sweep at 1 Hz for  $C_2S_{48}^H C_2$  gels; **(a)** Storage modulus ( $G'$ ) as a function of deformation ( $\gamma$ ) at various concentrations; **(b)** The deformation at which gels rupture ( $\gamma_{max}$ ) as a function of  $C_2S_{48}^H C_2$  concentration at pH 7 and 25 °C.

A hallmark for the rheology of gels of semiflexible fibers is strain stiffening [44, 57]. To test for possible strain stiffening,  $C_2S_{48}^H C_2$  gels at various concentrations and pH were exposed to a strain sweep, up to the point of mechanical failure. As is clear from Fig. 3.9a, all gels clearly showed an increase in the elastic modulus before failure, as was also found for the  $C_2S_{48}^E C_2$  hydrogels [44]. Figure 3.9b shows the maximum deformation ( $\gamma_{max}$ ) at which gels break down as a function of concentration. We find that stiffer gels break at lower strains, which is similar to actin gels [57, 59, 60]. The maximum strain stiffening, just before

failure, is a factor of about 2, independent of concentration. The strain stiffening notably depends on pH (Fig. 3.10), with gels that were made at lower pH values, breaking at lower strains.

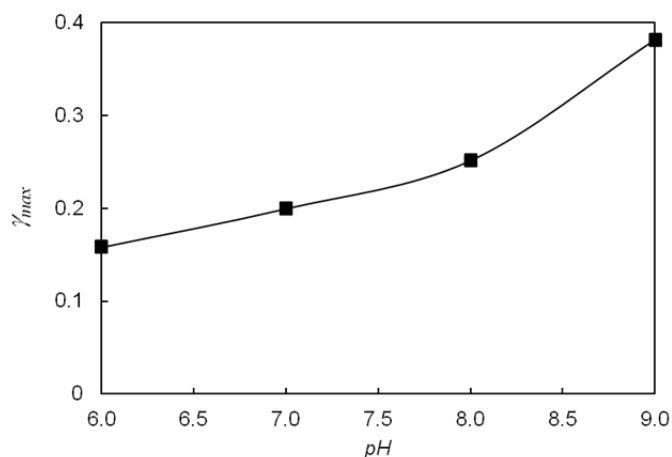


**Figure 3.10.** pH dependence of strain at failure for 20 g/l  $C_2S_{48}^H C_2$  gels at 25 °C.

Once broken, the networks slowly recover. A typical recovery curve is shown in Fig 3.11. Recovery is significantly faster than the initial gel formation, presumably because it merely involves fiber rearrangements and not fiber formation. Furthermore, recovery was found to be pH dependent (but not concentration dependent as it was checked for pH 7, data not shown), with complete recovery being found around pH 7, as shown in Fig. 3.11, and partial recovery at both lower and higher pH values. The inability to completely recover at pH values far away from pH 7 may point to long-lived physical cross-links between the fibers that may be pH-dependent. Indeed, the ability of these hydrogels to recover completely at pH 7 is in strong contrast with the  $C_2S_{48}^E C_2$  hydrogels that do not recover at all, once broken. In that case, stronger physical cross-links may have led both to a higher modulus and to an inability to recover from mechanical failure.

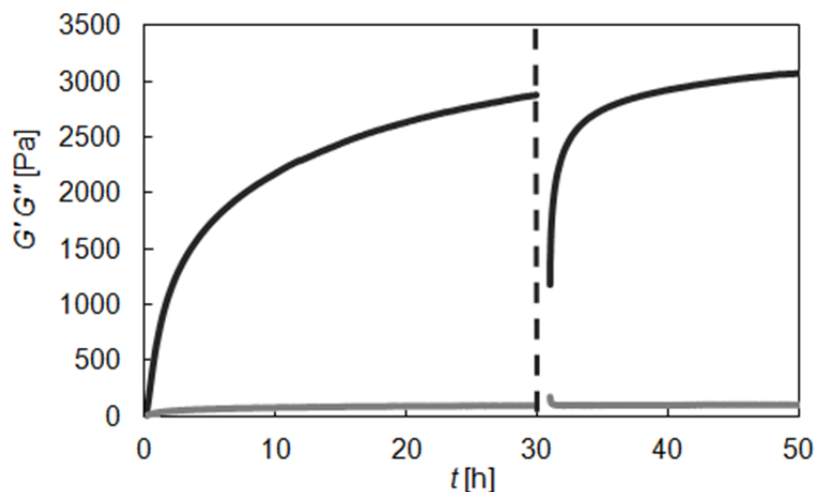


**Figure 3.11.** Time course of increase in storage  $G'$  (black curve) and loss  $G''$  (grey curve) moduli for 30 g/l  $C_2S_{48}^H C_2$  gel at pH 7 and 25 °C. At 30 h the gel was broken and the healing process was recorded in time. Measurement was made in a Couette configuration at 1 Hz and 0.1 % deformation.

### 3.4 Conclusion

The  $C_2S_{48}^H C_2$  polypeptides that we have studied here fulfill many requirements for use as a scaffold in biomedical applications: at physiological pH (and temperature, ionic strength) they form self-healing fiber gels starting at concentrations well below 10 g/l (a 0.5 wt% solution forms a gel with  $G' \approx 250$  Pa at pH 7). The collagen-like C block has already been shown to exhibit very low toxicity for cells [41, 61]. It is straightforward to bioengineer additional biofunctional domains into these polypeptides for tuning the relevant biomolecular interactions, and finally, they can easily be produced at a large scale. The latter is an important advantage e.g. over peptide hydrogels [32, 34, 62-65] for which the peptides are usually produced by chemical synthesis.

At the same time, our quantitative understanding and control over the rheology of these and other fiber-based hydrogels leaves a lot to be desired. Theoretical and experimental studies on the rheology of networks of cytoskeletal filaments, especially actin filaments, have highlighted the many length scales that are involved: the filament length, stiffness

and correlation length of the network [58, 60, 66-68]. Many different regimes exist, depending on the relative magnitudes of these lengths, and possibly non-affine deformations at higher strains lead to further complications [57, 68, 69]. Finally, in the limit of an uncross-linked network of semi-flexible filaments, the rheology shows an extreme sensitivity to trace amounts of cross-links between the fibers, either physical (reversible) or chemical (permanent) [67]. The latter point may be partly responsible for the large spread in moduli reported e.g. for uncrosslinked actin filament networks. Depending on the purification, preparation method and storage, 2 g/l of actin solution have given modulus from 10 Pa to 500 Pa [57, 66, 68].

Similarly, for better control and higher moduli of the hydrogels of the recombinant polypeptides it may be necessary to engineer additional physical interactions into the polypeptide sequences that control fiber bundling and cross-linking, in analogy with the many proteins that control the bundling and cross-linking of actin fibers in the living cell [70, 71].

---

## References

1. Wheeler, J.C., et al., *Evolution of hydrogel polymers as contact lenses, surface coatings, dressings, and drug delivery systems*. Journal of long-term effects of medical implants, 1996. **6**(3-4): p. 207.
2. Kwon, J.W., et al., *Biocompatibility of poloxamer hydrogel as an injectable intraocular lens: A pilot study*. Journal of Cataract & Refractive Surgery, 2005. **31**(3): p. 607-613.
3. Novikova, L.N., et al., *Alginate hydrogel and matrigel as potential cell carriers for neurotransplantation*. Journal of Biomedical Materials Research Part A, 2006. **77**(2): p. 242-252.
4. Balakrishnan, B., et al., *Evaluation of an in situ forming hydrogel wound dressing based on oxidized alginate and gelatin*. Biomaterials, 2005. **26**(32): p. 6335-6342.
5. Qiu, Y. and K. Park, *Environment-sensitive hydrogels for drug delivery*. Advanced Drug Delivery Reviews, 2001. **53**(3): p. 321-339.
6. Gupta, P., K. Vermani, and S. Garg, *Hydrogels: from controlled release to pH-responsive drug delivery*. Drug discovery today, 2002. **7**(10): p. 569-579.
7. Hoare, T.R. and D.S. Kohane, *Hydrogels in drug delivery: Progress and challenges*. Polymer, 2008. **49**(8): p. 1993-2007.
8. Lee, K.Y. and D.J. Mooney, *Hydrogels for tissue engineering*. Chemical reviews, 2001. **101**(7): p. 1869-1880.
9. Drury, J.L. and D.J. Mooney, *Hydrogels for tissue engineering: scaffold design variables and applications*. Biomaterials, 2003. **24**(24): p. 4337-4351.
10. Zheng Shu, X., et al., *In situ crosslinkable hyaluronan hydrogels for tissue engineering*. Biomaterials, 2004. **25**(7): p. 1339-1348.
11. Ferreira, L.S., et al., *Bioactive hydrogel scaffolds for controllable vascular differentiation of human embryonic stem cells*. Biomaterials, 2007. **28**(17): p. 2706-2717.
12. Kopecek, J., *Hydrogels: From soft contact lenses and implants to self assembled nanomaterials*. Journal of Polymer Science Part A: Polymer Chemistry, 2009. **47**(22): p. 5929-5946.
13. Keeley, R.D., et al., *The artificial nerve graft: a comparison of blended elastomer-hydrogel with polyglycolic acid conduits*. Journal of reconstructive microsurgery, 2008. **7**(02): p. 93-100.
14. de Jong, S.J., et al., *New insights into the hydrolytic degradation of poly(lactic acid): participation of the alcohol terminus*. Polymer, 2001. **42**(7): p. 2795-2802.
15. Deitzel, J.M., et al., *Controlled deposition of electrospun poly(ethylene oxide) fibers*. Polymer, 2001. **42**(19): p. 8163-8170.
16. Nuttelman, C.R., et al., *Attachment of fibronectin to poly(vinyl alcohol) hydrogels promotes NIH3T3 cell adhesion, proliferation, and migration*. Journal of Biomedical Materials Research, 2001. **57**(2): p. 217-223.
17. Hoffman, A.S., *Hydrogels for biomedical applications*. Advanced Drug Delivery Reviews, 2012. **64**(Supplement): p. 18-23.

18. Teles, H., et al., *Hydrogels of collagen-inspired telechelic triblock copolymers for the sustained release of proteins*. Journal of Controlled Release, 2010. **147**(2): p. 298-303.
19. Garvin, J., et al., *Novel system for engineering bioartificial tendons and application of mechanical load*. Tissue engineering, 2003. **9**(5): p. 967-979.
20. Whitlock, P.W., et al., *A naturally derived, cytocompatible, and architecturally optimized scaffold for tendon and ligament regeneration*. Biomaterials, 2007. **28**(29): p. 4321-4329.
21. Sell, S.A., et al., *The Use of Natural Polymers in Tissue Engineering: A Focus on Electrospun Extracellular Matrix Analogues*. Polymers, 2010. **2**(4): p. 522-553.
22. Lv, S., et al., *Towards constructing extracellular matrix-mimetic hydrogels: An elastic hydrogel constructed from tandem modular proteins containing tenascin FnIII domains*. Acta Biomaterialia, 2013. **9**(5): p. 6481-6491.
23. Schulz, S., *The Chemistry of Spider Toxins and Spider Silk*. Angewandte Chemie International Edition in English, 1997. **36**(4): p. 314-326.
24. Altman, G.H., et al., *Silk-based biomaterials*. Biomaterials, 2003. **24**(3): p. 401-416.
25. Eisoldt, L., A. Smith, and T. Scheibel, *Decoding the secrets of spider silk*. Materials Today, 2011. **14**(3): p. 80-86.
26. Alarcon, C.d.l.H., S. Pennadam, and C. Alexander, *Stimuli responsive polymers for biomedical applications*. Chemical Society Reviews, 2005. **34**(3): p. 276-285.
27. Dang, J.M. and K.W. Leong, *Natural polymers for gene delivery and tissue engineering*. Advanced Drug Delivery Reviews, 2006. **58**(4): p. 487-499.
28. Chen, Q., S. Liang, and G.A. Thouas, *Elastomeric biomaterials for tissue engineering*. Progress in Polymer Science, 2013. **38**(3-4): p. 584-671.
29. Holmes, T.C., *Novel peptide-based biomaterial scaffolds for tissue engineering*. TRENDS in Biotechnology, 2002. **20**(1): p. 16-21.
30. Genove, E., et al., *The effect of functionalized self-assembling peptide scaffolds on human aortic endothelial cell function*. Biomaterials, 2005. **26**(16): p. 3341-3351.
31. Fairman, R. and K.S. Åkerfeldt, *Peptides as novel smart materials*. Current Opinion in Structural Biology, 2005. **15**(4): p. 453-463.
32. MacPhee, C.E. and D.N. Woolfson, *Engineered and designed peptide-based fibrous biomaterials*. Current Opinion in Solid State and Materials Science, 2004. **8**(2): p. 141-149.
33. Rajagopal, K. and J.P. Schneider, *Self-assembling peptides and proteins for nanotechnological applications*. Current Opinion in Structural Biology, 2004. **14**(4): p. 480-486.
34. Woolfson, D.N. and M.G. Ryadnov, *Peptide-based fibrous biomaterials: some things old, new and borrowed*. Current Opinion in Chemical Biology, 2006. **10**(6): p. 559-567.
35. Yamada, M., et al., *Ile-Lys-Val-Ala-Val (IKVAV)-containing laminin  $\alpha$ 1 chain peptides form amyloid-like fibrils*. FEBS Letters, 2002. **530**(1-3): p. 48-52.

36. Yan, C. and D.J. Pochan, *Rheological properties of peptide-based hydrogels for biomedical and other applications*. Chemical Society Reviews, 2010. **39**(9): p. 3528-3540.
37. Dinerman, A.A., et al., *Swelling behavior of a genetically engineered silk-elastinlike protein polymer hydrogel*. Biomaterials, 2002. **23**(21): p. 4203-4210.
38. Jeong, B., S.W. Kim, and Y.H. Bae, *Thermosensitive sol-gel reversible hydrogels*. Advanced Drug Delivery Reviews, 2002. **54**(1): p. 37-51.
39. Hwang, D., et al., *Influence of polymer structure and biodegradation on DNA release from silk-elastinlike protein polymer hydrogels*. International Journal of Pharmaceutics, 2009. **368**(1-2): p. 215-219.
40. Werten, M.W.T., et al., *Secreted production of a custom-designed, highly hydrophilic gelatin in Pichia pastoris*. Protein Eng., 2001. **14**(6): p. 447-454.
41. Werten, M.W.T., et al., *Precision Gels from Collagen-Inspired Triblock Copolymers*. Biomacromolecules, 2009. **10**(5): p. 1106-1113.
42. Skrzyszewska, P.J., et al., *Physical gels of telechelic triblock copolymers with precisely defined junction multiplicity*. Soft Matter, 2009. **5**(10): p. 2057-2062.
43. Martens, A.A., et al., *Triblock Protein Copolymers Forming Supramolecular Nanotapes and pH-Responsive Gels*. Macromolecules, 2009. **42**(4): p. 1002-1009.
44. Martens, A.A., et al., *Dilute gels with exceptional rigidity from self-assembling silk-collagen-like block copolymers*. Soft Matter, 2009. **5**(21): p. 4191-4197.
45. Li, F., et al., *Formation of nanotapes by co-assembly of triblock peptide copolymers and polythiophenes in aqueous solution*. Soft Matter, 2009. **5**(8): p. 1668-1673.
46. Beun, L.H., et al., *Self-Assembly of Silk-Collagen-like Triblock Copolymers Resembles a Supramolecular Living Polymerization*. ACS Nano, 2011. **6**(1): p. 133-140.
47. Smeenk, J.M., et al., *Controlled Assembly of Macromolecular  $\beta$ -Sheet Fibrils*. Angewandte Chemie International Edition, 2005. **44**(13): p. 1968-1971.
48. Topilina, N.I., et al., *Bilayer Fibril Formation by Genetically Engineered Polypeptides: Preparation and Characterization*. Biomacromolecules, 2006. **7**(4): p. 1104-1111.
49. Yan, Y., et al., *Nanoribbons Self-Assembled from Triblock Peptide Polymers and Coordination Polymers*. Angewandte Chemie, 2008. **120**(22): p. 4260-4263.
50. Kim, H.J., et al., *Bone tissue engineering with premineralized silk scaffolds*. Bone, 2008. **42**(6): p. 1226-1234.
51. Keten, S. and M.J. Buehler, *Nanostructure and molecular mechanics of spider dragline silk protein assemblies*. Journal of The Royal Society Interface, 2010. **7**(53): p. 1709-1721.
52. Xu, M. and R.V. Lewis, *Structure of a protein superfiber: spider dragline silk*. Proceedings of the National Academy of Sciences, 1990. **87**(18): p. 7120-7124.
53. Keten, S. and M.J. Buehler, *Atomistic model of the spider silk nanostructure*. Applied physics letters, 2010. **96**(15): p. 153701-153701-3.
54. Werten, M.W.T., et al., *Biosynthesis of an Amphiphilic Silk-Like Polymer*. Biomacromolecules, 2008. **9**(7): p. 1705-1711.

55. Wertin, M.W.T., et al., *High-yield secretion of recombinant gelatins by Pichia pastoris*. Yeast, 1999. **15**(11): p. 1087-1096.
56. DuBois, M., et al., *Colorimetric Method for Determination of Sugars and Related Substances*. Analytical Chemistry, 1956. **28**(3): p. 350-356.
57. MacKintosh, F.C., J. Käs, and P.A. Janmey, *Elasticity of Semiflexible Biopolymer Networks*. Physical Review Letters, 1995. **75**(24): p. 4425-4428.
58. Hinner, B., et al., *Entanglement, Elasticity, and Viscous Relaxation of Actin Solutions*. Physical Review Letters, 1998. **81**(12): p. 2614-2617.
59. Janmey, P.A., et al., *Viscoelasticity of F-actin and F-actin/gelsolin complexes*. Biochemistry, 1988. **27**(21): p. 8218-8227.
60. Gardel, M.L., et al., *Elastic Behavior of Cross-Linked and Bundled Actin Networks*. Science, 2004. **304**(5675): p. 1301-1305.
61. Rozkiewicz, D.I., et al., *Covalent Microcontact Printing of Proteins for Cell Patterning*. Chemistry – A European Journal, 2006. **12**(24): p. 6290-6297.
62. Zhang, S., *Fabrication of novel biomaterials through molecular self-assembly*. Nature Publishing Group, 2003. **21**(10): p. 1171-1178.
63. Ryadnov, M.G. and D.N. Woolfson, *Engineering the morphology of a self-assembling protein fibre*. Nature materials, 2003. **2**(5): p. 329-332.
64. Ryadnov, M.G. and D.N. Woolfson, *Introducing Branches into a Self-Assembling Peptide Fiber*. Angewandte Chemie, 2003. **115**(26): p. 3129-3131.
65. Zhang, S. and X. Zhao, *Design of molecular biological materials using peptide motifs*. Journal of Materials Chemistry, 2004. **14**(14): p. 2082-2086.
66. Janmey, P.A., et al., *The mechanical properties of actin gels. Elastic modulus and filament motions*. Journal of Biological Chemistry, 1994. **269**(51): p. 32503-13.
67. Isambert, H. and A. Maggs, *Dynamics and Rheology of Actin Solutions*. Macromolecules, 1996. **29**(3): p. 1036-1040.
68. MacKintosh, F.C. and P.A. Janmey, *Actin gels*. Current Opinion in Solid State and Materials Science, 1997. **2**(3): p. 350-357.
69. Head, D.A., A.J. Levine, and F.C. MacKintosh, *Distinct regimes of elastic response and deformation modes of cross-linked cytoskeletal and semiflexible polymer networks*. Physical Review E, 2003. **68**(6): p. 061907.
70. Tilney, L.G., et al., *Regulation of actin filament cross-linking and bundle shape in Drosophila bristles*. The Journal of cell biology, 2000. **148**(1): p. 87-99.
71. Welch, M.D. and R.D. Mullins, *Cellular Control Of Actin Nucleation*. Annu. Rev. Cell Dev. Biol, 2002. **18**: p. 247-88.

## Additional Information

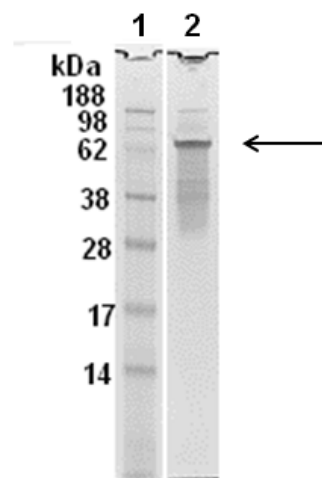


**Figure 3.12.** SDS PAGE of purified  $C_2S_{48}^H C_2$ : **Lane 1:** molecular mass marker, **Lane 2:** purified product (pellet after second precipitation with ammonium sulfate at 45% saturation dissolved in 50 mM formic acid and dialyzed against 10 mM formic acid). The arrows point to the product band.

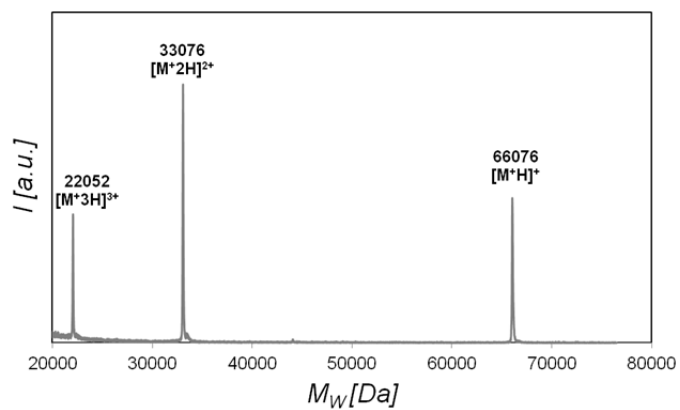


**Figure 3.13.** MALDI-TOF of purified  $C_2S_{48}^H C_2$ . The various charged- molecular ions are indicate



## Chapter 4

---

# Modulation of mechanical properties of hydrogels composed of protein-based polymers using cross-linking enzymes

---

We explore the use of enzymatic cross-linking to modulate the mechanical properties of hydrogel forming, *de novo* designed recombinant polypeptides. The polypeptides feature a collagen-inspired hydrophilic block whose lysine and glutamine residues we attempt to covalently couple using microbial transglutaminase (mTGase). We find that the collagen-inspired hydrophilic blocks are poor substrates for mTGase, but the few cross-links that are introduced have a remarkably strong effect on the mechanical properties of the hydrogels. For triblock polypeptides consisting of a silk-like self-assembly block flanked by collagen-inspired hydrophilic block, that forms fiber gels around neutral pH, we find that the introduction of a low amount of cross-links can increase the modulus of the gels by a factor of five, without changing the self-healing nature of the gels. For triblock polypeptides consisting of a collagen-inspired hydrophilic block flanked by triple helix-forming segments (that form thermo-sensitive hydrogels) we find qualitatively new behaviour, viz. shape memory. Our study suggests that engineered enzymatic cross-linking sites could be a powerful tool obtain yet more control over structures formed by *de novo* designed recombinant polypeptides.

Submitted as: M.D. Golinska, F.A. de Wolf, M.A. Cohen Stuart, J. van der Gucht and R. de Vries;  
Cross-linking enzymes for modulation of mechanical properties of hydrogels composed of protein-based polymers



## 4.1 Introduction

After ribosomal synthesis, many proteins undergo some form of enzymatic or non-enzymatic post-translational modification (PTM), that influences the structural or functional properties of the protein. For example, PTM can influence the activity, stability and targeting of the protein, and also its (signalling or non-signalling) interaction with other cellular molecules such as proteins, nucleic acids or lipids [1-4].

PTM is a very useful tool in protein engineering, in particular the establishment of new covalent bonds by inteins [5], sortases [6, 7], transglutaminases [8, 9], or oxidative enzymes such as tyrosinase [8, 10], lysyl oxidase [11], and horse radish peroxidase [12]. PTM principles can be used *in vitro* for artificial site-specific incorporation of functional groups [6, 12, 13], for peptide cyclization, or for the improvement of protein purification [6, 14], receptor activity, or selectivity and affinity towards ligands [7]. Artificial PTM has also been used for stabilization of self-assembling peptide hydrogels, and for enhancement of their elasticity and mechanical strength [9, 11, 15].

In particular, microbial transglutaminase (mTGase), is widely used to cross-link proteins and protein-based materials [16-19]. Transglutaminases (EC 2.3.2.13, amine  $\gamma$ -glutamyl transferases) catalyze protein cross-linking by acyl-transferase reactions between the  $\gamma$ -carboxamide group of glutamine (Gln) and the  $\epsilon$ -amino group of lysine (Lys), and by formation of a  $\epsilon$ -( $\gamma$ -glutamyl)lysine isopeptide bond between the proteins. Microbial transglutaminase (mTGase) is produced by a variety of *Streptoverticillium mobaraense* and shows a catalytic activity that is, unlike human transglutaminase,  $\text{Ca}^{2+}$  ion-independent, a crucial feature for many industrial applications. Its activity is particularly sensitive to the environment of the Gln residue. While the natural targets of mTGase are still unknown, the sequence requirements for the environment of the Gln residue are starting to be elucidated [20, 21].

We have previously designed and produced a range of block copolymer-like proteins with hydrogel-forming capacity and with blocks inspired by structural proteins

such as collagen and silk. One of the modules used as a block in such proteins is a hydrophilic stretch of 99 amino acids that adopts random coil conformation irrespective of the ambient pH and temperature, and has a collagen-/gelatin-inspired amino acid composition. One or more of these so-called 'C'-blocks were combined with one or more silk-inspired pH-responsive blocks, and/or with thermoresponsive triple helix forming blocks, so as to obtain proteins capable of stimulus-responsive self-organization into supramolecular structures and hydrogels. By attachment of collagen-like triple-helix forming (Pro-Gly-Pro)<sub>n</sub> blocks (denoted as T<sub>n</sub>) to both (N- and C-terminal) ends of a C-block oligomer (C<sub>m</sub>), a telechelic polypeptide (T<sub>n</sub>C<sub>m</sub>T<sub>n</sub>) is obtained that forms precisely-defined thermo-sensitive hydrogels [22, 23]. A silk-inspired, pH-responsive block that we have used is GAGAGAGX (denoted as S<sub>n</sub><sup>X</sup>, where X can be for example Glu, His or Lys. Attachment of for example a C<sub>2</sub> block to both ends of an S<sub>n</sub><sup>X</sup> block results in a C<sub>2</sub><sup>P</sup>S<sub>n</sub><sup>X</sup>C<sub>2</sub><sup>P</sup> triblock protein that forms stiff molecular tapes (fibers) at pH values where the X residue becomes uncharged [24-27]. These C<sub>m</sub>S<sub>n</sub><sup>X</sup>C<sub>m</sub> fibers start forming hydrogels already at low concentrations (below 1 wt %).

It is well known that animal gelatin is a good substrate for mTGase [28-30]. We reasoned that our C-blocks may also be amenable to modification by this enzyme, because they contain, like animal gelatin, ~ 33 mol-% Gly, ~ 22 mol-% Pro, a number of Lys residues, and high Gln content. If cross-linking by mTGase is sufficiently efficient, this would give us an extra possibility to influence the properties of C-block containing polymer-like proteins, biosynthetic, "post-translational" handle on hydrogels composed of protein-based polymers. For example, it could be used to create injectable hydrogels [31-33], to obtain additional control over the mechanical properties of hydrogels, or to prepare shape-memory hydrogels that feature a combination of covalent and stimulus-responsive physical cross-links. While a permanent shape is conferred to the gel by means of the covalent (chemical) cross-links, a temporary, deformed state, can be imposed by the physical cross-links. Switching off the physical cross-links leads to a return of the shape of the hydrogels to its original permanent shape. Shape-memory materials, including

shape memory hydrogels, find applications as implants, controlled drug delivery systems, biosensors or temperature responsive stents (tubes) [34-36].

We therefore explored the suitability of the collagen-like, hydrophilic "C" block as a substrate for mTGase and studied the modulation, by mTGase-mediated cross-linking, of the mechanical properties of hydrogels of  $C_2^P S_{48}^H C_2^P$  and  $T_9 C_4 T_9$ , both of which contain C-blocks. Among else, we studied the extent to which the modulus of dilute  $C_2^P S_{48}^H C_2^P$  gels can be increased by treatment with mTGase, with a view to the preparation of stiff protein fiber hydrogels at low protein concentration. Finally, we investigated whether mTGase can be used to create shape memory gels with the thermoresponsive  $T_9 C_4 T_9$ .

## 4.2 Materials and Methods

### 4.2.1. Recombinant protein-based polymer

Recombinant protein-based polymers  $C_4^R$  [22, 23],  $C_4^P$  [37],  $C_2^P S_{48}^H C_2^P$  [27, 38] and  $T_9 C_4^R T_9$  [22, 23] were produced and purified as described before.

### 4.2.2. Enzyme purification

In all experiments, Activa<sup>®</sup> YG transglutaminase from Ajinomoto was used with further purification according to Lantto *et.al* [39]. The original Ajinomoto product contains, among others, lactose, yeast extract, maltodextrin, vegetable oils. The enzyme was dissolved in 30 mM sodium acetate buffer at pH 5.5 and applied to Streamline SP XL cation-exchanger beads (GE Healthcare Bio-Science AB), and kept for 20 h in 4 °C. The beads with bound enzyme were washed 15 times with 30 mM sodium acetate buffer at pH 5.5 and finally eluted with 500 mM sodium phosphate buffer with 1 M NaCl at pH 8. During ultrafiltration (Millipore Ultrafiltration Disc Membranes, 10k 76 mm) the elution buffer was replaced with a 10 mM sodium phosphate buffer, pH 8, and simultaneously, the enzyme was concentrated. The activity of the mTGase stock solutions thus obtained was determined using Microbial Transglutaminase Assay Kit (Zedira GmbH). The activity was determined according to the instructions of the assay manufacturer, and found to be 0.57 U/ml. The

enzyme concentration was determined to be 1.2 mg/ml by UV spectroscopy at 280 nm using an extinction coefficient  $\epsilon = 1.898 \text{ ml}/(\text{mg}\cdot\text{cm})$ , based on Pace, *et al* [40, 41].

#### 4.2.3. Cross-linking reactions

Reactions catalysed by mTGase were performed at 37 °C in 10 mM sodium phosphate buffer pH 7.5 for 24 h at the indicated enzyme to substrate ratio (which was 1:20 by weight for most experiments).

#### 4.2.4. Light Scattering

Protein-based polymer samples were prepared freshly for each light scattering experiment, by dissolving pure, lyophilized  $C^R_4$  protein in 10 mM sodium phosphate buffer pH 7.5 to final concentrations of 10, 20, 25 and 30 g/l, and vortexing. Solutions were filtered (Ultrafree-MC Centrifugal Filter Units with Microporous PVDF Membrane, 0.22  $\mu\text{m}$ , Millipore) and the desired amount of mTGase was added from a mTGase stock solution of 1.2 mg/ml. Light scattering measurements were performed using a Zetasizer NanoZS (Malvern Instruments, UK), equipped with a 4 mW He-Ne ion laser, operating at a wavelength of 633 nm. All measurements were taken at a fixed angle  $\vartheta$  of 173 ° and 37 °C. Quantities reported are the light scattering intensity (Derived Count Rate) and z-averaged hydrodynamic radii, as reported by Malvern DTS Software, version 5.10 beta 1.

#### 4.2.5. OPA analysis of lysine residues

Quantification of (unreacted) lysine groups was performed using OPA (ortho-phthaldialdehyde) analysis as described before [42-44]. The OPA reagent was prepared immediately before use each time by dissolving 20 mg OPA in 500  $\mu\text{l}$  methanol, followed by addition of 12.5 ml 0.1 M sodium tetraborate buffer, 2.5 ml 10% SDS, 100 mg 2-(dimethylamino)ethanethiol hydrochloride (DMA) and  $\text{dH}_2\text{O}$  to a final volume of 25 ml. Protein samples were prepared with concentrations ranging from 5 to 20 g/l in 10 mM sodium phosphate buffer at pH 7.5. 5  $\mu\text{l}$  of each concentration was added to 300  $\mu\text{l}$  of OPA reagent and incubated for 10 min. The protein was washed five times with  $\text{dH}_2\text{O}$  using

centrifugal filters (Amicon Ultra-0.5, Ultracel-3 Membrane, 3 kDa, Merck Millipore) to remove the ammonia released upon reaction of OPA with free lysine residues that had remained unprocessed by mTGase. Dialysis somewhat changed the protein concentration of the samples, and this change in concentration was estimated from the change in volume of the sample, under the assumption that no protein was lost during the dialysis. Subsequently, for the dialysed samples, the absorbance at 340 nm was measured in a 96 well plate in a Safire microplate spectrophotometer (Tecan). A standard curve was obtained, using the same protocol as above, with L-leucine ( $M_w = 131.18$  g/l, Pierce) as a reference, in a concentration range of 0.4 mM to 6 mM.

#### 4.2.6. Rheology

All rheological measurements were performed using an Anton Paar MCR 501 Rheometer equipped with a CC10/T200 (Anton Paar) Couette geometry, with bob and cup diameter of 10.002 and 10.845 mm, respectively. A solvent trap was used to minimize evaporation. The temperature of the rheometer was controlled via Peltier elements.

Samples of the fiber-forming  $C_2^p S_{48}^H C_2^p$  were prepared by dissolving a given amount of protein in 10 mM HCl and vortexing for 2 h for complete dissolution. Samples were then filtered and concentrated using spin filters (Ultracel<sup>®</sup>-3k, Millipore) according to the instructions of the manufacturer. Concentrations after centrifugation were determined spectrophotometrically at 230 nm. The pH of the concentrated samples was adjusted to pH 7.5 by adding small amounts of 1 M NaOH. Subsequently, samples were diluted to their final concentrations with 10 mM sodium phosphate buffer pH 7.5. Finally mTGase was added (from a stock solution of 1.2 mg/ml), and the mixture was immediately transferred to the preheated (37 °C) couette cell. Strain sweeps were performed between 0.01-100 % deformation at a frequency of 1 Hz. Based on initial frequency- and strain-sweep results, a 1 Hz and 0.1 % deformation was chosen for measuring the build-up of the modulus, during fiber formation and cross-linking.

Samples of  $T_9C_4^R T_9$  were prepared by dissolving given amounts of protein during 30 min in 10 mM sodium phosphate buffer, at pH 7.5 and 55 °C, at which temperature triple helices are not present. Solutions were then cooled to 37 °C, mTGase was added from a stock solution of 1.2 mg/ml, and the mixture was transferred to the couette cell that was preheated to 37 °C. During the entire process of chemical gel formation and subsequent physical gel formation, storage and loss moduli were measured at a frequency of 1 Hz and at 1 % deformation. First, chemical (mTGase-induced) network formation was allowed to proceed for 15 h. Next, the temperature was lowered to 20 °C and the additional formation of physical cross-links due to triple helix formation was monitored for another 20 h. To verify reversibility of the system, the temperature was then again increased to 37 °C at which temperature the triple helices melted again, and the viscoelastic response was followed for another 15 h before a second decrease of temperature was applied to check if the system will recover to the previously observed value.

For shape-memory experiments, permanent chemical (mTGase-induced) gels of  $T_9C_4^R T_9$  were allowed to form during 2 h in the rheometer at 37 °C. Subsequently, still at 37 °C, a 25 % shear strain was applied and the temperature was lowered to 5, 10, or 20 °C, keeping the deformation at the same level of 25 % for 15 h to allow for the formation of a temporary physical network constraining the chemical network a strain of 25 %. After 15 h the load (stress) was taken away and the response of the system was monitored at various temperatures, by measuring the strain relaxation. Finally the gel was heated back to 37 °C for 10 h to check strain recovery.

All rheological experiments with  $T_9C_4^R T_9$  were performed on samples containing 55 g/l (1.4 mM)  $T_9C_4^R T_9$  and 0.42 g/l mTGase.

---

## 4.3 Results and discussion

### 4.3.1 Collagen-like C block as a substrate for mTGase

The two varieties  $C^R$  [22] and  $C^P$  [37] of the random coil block  $C$  have identical molar mass, but slightly different sequence. The  $C^P$  has a glycine (G) in every third position, similar to collagen, but  $C^R$  has glycines at irregular positions. Single blocks of both protein-based polymers consist of 99 amino acids with 33 residues of glycine (G), 22 of proline (P), 16 of glutamine (Q), 12 of asparagine (N), 8 of serine (S), 4 of glutamic acid (E), 3 of lysine (K), and 1 of alanine (A). The tetramers  $C_4^R$  and  $C_4^P$  used in this study consist of 401 amino acids and have a molar mass of 37 kDa.

First we explored the suitability of both  $C_m^R$  and  $C_m^P$  as a substrate for mTGase. Using the tetramers ( $C_4^R$  and  $C_4^P$ ). Both have 12 lysines and 64 glutamines. Figure 1 shows the hydrodynamic radius and light scattering intensity after 24 h of incubation of 10 g/l of  $C_4^R$  with various concentration of mTGase at 37 °C. Both the scattering intensity and the hydrodynamic radius increase with increasing enzyme concentration. The hydrodynamic radius increases from about 6 nm (the expected hydrodynamic size for a single  $C_4^R$  coil) to about 65 nm (indicative of large clusters consisting of many  $C_4^R$  coils joined together) at the highest concentration of enzyme. Saturation, or at least a distinct break in the curves, appears to occur at a weight ratio of enzyme to substrate of about 1/100. Apparently, for the C-blocks, very high concentrations of enzyme are needed to achieve maximal conversion speed. For further experiments, we use a fixed weight ratio of enzyme to substrate of 1/20, corresponding to an enzymatic activity of 0.114 U per mg/ml of protein-based polymer.

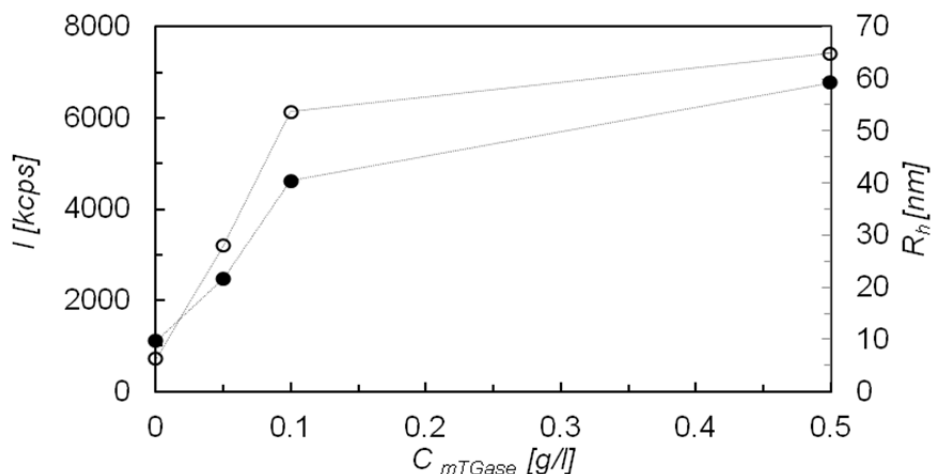


**Figure 4.1** Intensity of scattered light  $I$  (closed symbols) and Z-average hydrodynamic radius  $R_h$  (open symbols) versus concentration  $C_{mTGase}$  of mTGase.

The light scattering is very biased towards small fractions of large scattering objects, hence the larger clusters of  $C_4^R$  polymers that are detected after 24 h of cross-linking possibly only make up a small mass fraction of the total reaction product. In order to estimate the average number of cross-links per polymer, we have examined, using *o*-phthalaldehyde (OPA), the percentage of lysines in  $C_4^R$  and  $C_4^P$  that was processed by mTGase for quantitative analysis of amino groups. Two controls were used to check the assay itself: a  $S_{48}^H$  protein-based polymer (the silk-like midblock of the fiber forming triblock  $C_2^P S_{48}^H C_2^P$ ) that does not have any lysine residues and bovine apo- $\alpha$ -lactalbumin that is known to be quite accessible to modification by mTGase [45]. In all cases, prior to adding OPA, proteins were cross-linked with mTGase and incubated for 24 h at 37 °C. Results for the  $S_{48}^H$  control that should only give one amino group per polymer (the terminal amino group) indicate that the accuracy of the assay (about  $\pm 2$  amino groups, at least in our hands) is not very high. For bovine apo- $\alpha$ -lactalbumin, a significant decrease of the number of amino groups was indeed observed, after cross-linking with mTGase. For both  $C_4^R$  and  $C_4^P$  however, the observed decrease was not significant. Apparently, only very few lysines per  $C_4$  were modified by mTGase, under the conditions used in our assay.

Even though only a few cross-links seemed to be formed per per  $C_4$ , the effect of mTGase on hydrogels of  $C_2S_{48}^HC_2$  and  $T_9C_4T_9$  were very strong, as we will show below.

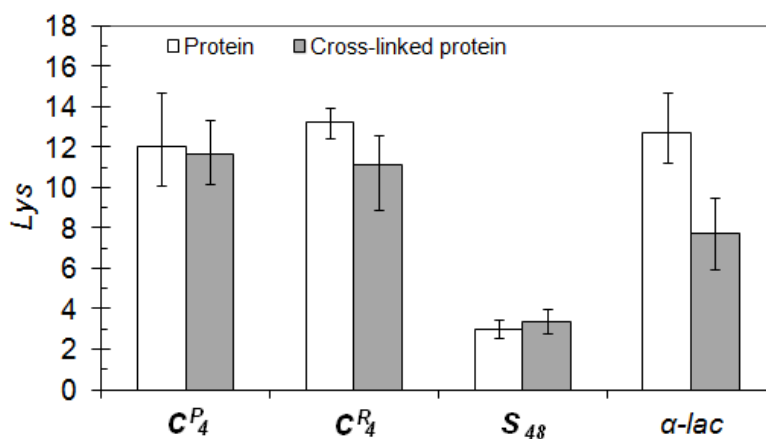


**Figure 4.2.** Number of amino groups per protein before and after cross-linking with mTGase at weight ratio of enzyme to substrate of 1/20, after 24 h of incubation at 37 °C. The  $S_{48}^H$  and apo- $\alpha$ -lactalbumin proteins were used respectively, as a negative and positive control for determining mTGase induced cross-linking via the OPA assay. The error bars show the standard deviations.

### 4.3.2. Enhancement of mechanical properties of dilute $C_2^P S_{48}^H C_2^P$ fiber gels

As a first possible application of mTGase cross-linking, we studied the effect of mTGase on gels consisting of  $C_2^P S_{48}^H C_2^P$  fibers. The  $C_2^P S_{48}^H C_2^P$  protein consists of approximately 800 amino acids and has a molecular weight of about 66 kDa. The histidine residues in the silk-like block are positively charged at low pH, where  $C_2^P S_{48}^H C_2^P$  is soluble. Neutralization, at  $\text{pH} > 6$ , of the histidines in the silk-like middle-block leads to fiber formation and, at concentrations above 10 g/L, to the formation of transparent, self-healing fiber-based hydrogels [38]. As we have shown above, the hydrophilic side-chains of these fibers are amenable to mTGase-induced cross-linking. mTGase-mediated enhancement of the mechanical properties of  $C_2^P S_{48}^H C_2^P$  gels was studied at a  $C_2^P S_{48}^H C_2^P$  concentration just sufficed to form gels (10 g/l). Figure 3 shows that, in the absence of mTGase, the shear modulus  $G'$ , at 37 °C, rose to about 270 Pa in 24 h, when the pH of the polymer solution was increased to pH 7.5. The same experiment is repeated, but now with added mTGase

(after the quench to pH 7). In the presence of increasing amounts of mTGase, the modulus rose faster, and increased to a higher values (5 times larger than in the absence of mTGase, at a weight ratio of enzyme to substrate of 1/20), As is shown in Fig. 3.

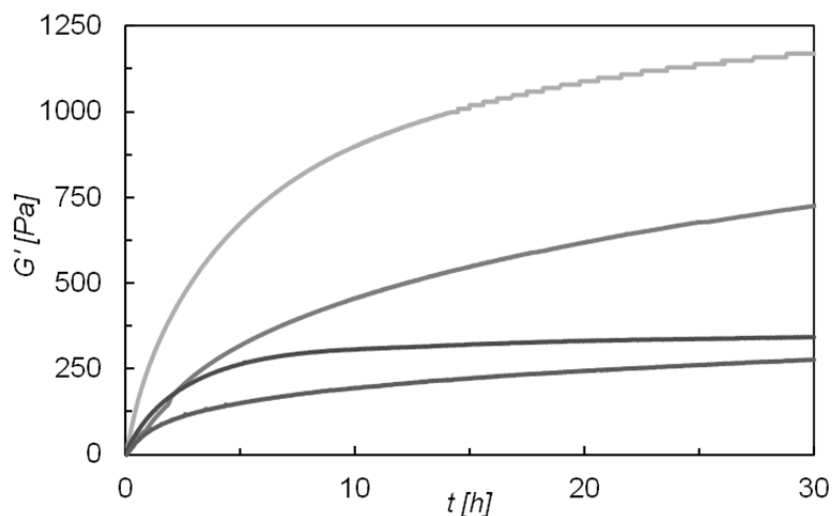


**Figure 4.3** Development of the storage modulus,  $G'$  of a 10 g/l  $C_2S_{48}^H C_2^P$  gel at different mTGase concentrations, after adjustment of the pH from a low value to pH 7.5. Concentration of mTGase from top to the bottom: 0.5 g/l, 0.1 g/l, 0.05 g/l, no enzyme. Temperature: 37 °C.

As we have shown previously [26],  $C_2S_{48}^E C_2^P$ -based hydrogels (consisting of polymers in which the histidine residues are replaced with glutamic acid residues, such that the gels only form at low pH) are strain hardening and show a clear increase of storage modulus ( $G'$ ) before mechanical failure, reminiscent of biological fiber gels composed for example of F-actin. This property appears to be preserved after enzymatic cross-linking. Figure 4 shows results of strain sweep experiments with 10 g/l  $C_2S_{48}^H C_2^P$  gels prepared by adjustment of the pH to 7.5 and incubation of the polymers with varying enzyme concentrations during 24 h at 37 °C. In agreement with observations on other polymer gels [46-48] and on  $C_2S_{48}^E C_2^P$  gels [26], Figure 4 shows that stiffer  $C_2S_{48}^H C_2^P$  gels break at lower strains.

In previous chapter, we have shown that  $C_2^P S_{48}^H C_2^P$  [38] but not  $C_2^P S_{48}^E C_2^P$  [26] hydrogels have a modulus that fully recovers after mechanical failure. Remarkably, as illustrated in Fig. 5, the property of self-healing is preserved when  $C_2^P S_{48}^H C_2^P$  fiber gels are cross-linked using mTGase. Consistent with the conclusion of the previous section that the C-blocks are not a very good substrate for mTGase, and that only a few cross-links per polymer chain are formed (still can mean a significant number of cross-links per fiber), this presumably indicates that not all fibers are joined by cross-linking so that self-healing via rearrangements of fiber clusters and free fibers is still possible, even though such cross-linking does lead to a strong increase of the storage modulus.

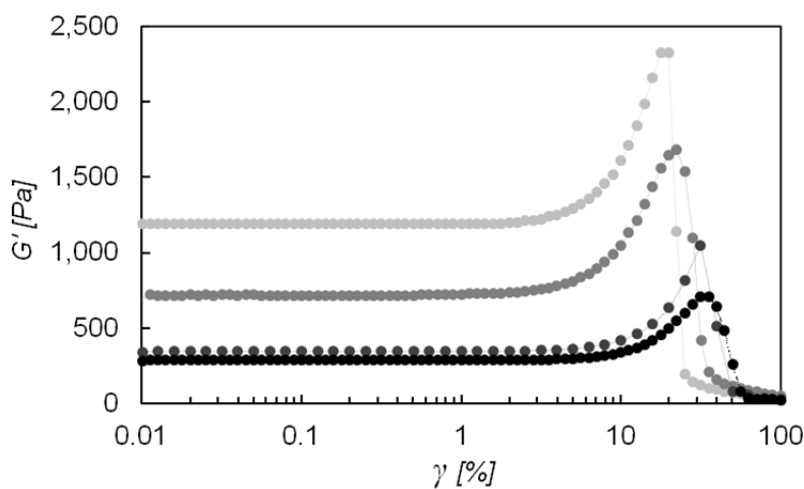


**Figure 4.4** Strain sweep at 1 Hz for 10 g/l  $C_2^P S_{48}^H C_2^P$  enzymatically cross-linked gels; storage modulus ( $G'$ ) as a function of deformation ( $\gamma$ ) at various mTGase concentrations. Concentration of mTGase from top to the bottom: 0.5 g/l, 0.1 g/l, 0.05 g/l, no enzyme. Temperature: 37 °C.

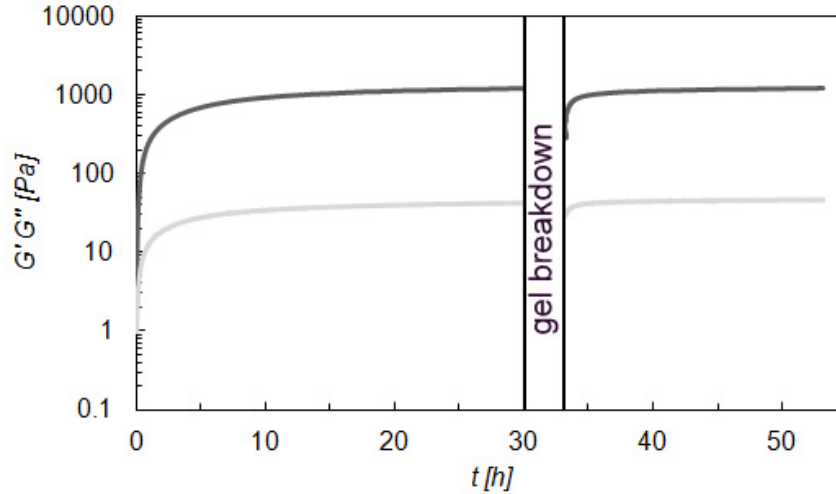


**Figure 4.5.** Time course of increase in storage  $G'$  (black curve) and loss  $G''$  (grey curve) moduli for 10 g/l  $C_2^p S^H_{48} C_2^p$  gel cross-linked with 0.5 g/l mTGase at pH 7.5 and 37 °C. After 30 h the gel was broken by applying 100 % deformation and the healing process was recorded in time. Measurement was made in a Couette configuration at 1 Hz and 0.1 % deformation.

### 4.3.3. $T_9 C_4^R T_9$ shape memory gels obtained after TGase treatment

The thermoresponsive telechelic polymer  $T_9 C_4^R T_9$  (461 amino acids, molar mass of 42 kDa) [22] has collagen-like (Pro-Gly-Pro) end blocks that form triple helical junctions with a melting temperature of about 42 °C at  $\sim 1.4$  mM protein [23]. After previous work in which we used the toxic chemical crosslinker glutaraldehyde (GA), we presently explored the use of mTGase to prepare essentially biocompatible  $T_9 C_4^R T_9$  shape memory gels. The  $T_9 C_4^R T_9$  concentration (55 g/l, or 1.4 mM) was chosen so as to facilitate comparison with our previous work [23, 49], and a fixed enzyme to substrate ratio of 1/20 by weight was used. First, a mTGase-crosslinked gel was allowed to form during 15 h at 37 °C. As is shown in Fig. 6, this first stage leads to a final storage modulus of  $G' \approx 600$  Pa. Via  $G' = c_{sub} \cdot k_B \cdot T$ , this corresponds to a density of elastically active subchains of  $c_{sub} = 0.25$  mM. Since the molar concentration of  $T_9 C_4^R T_9$  chains is 1.4 mM, this again confirms that the degree of cross-linking is low: on average, only one in 5 to 6 chains is elastically active, that might be because of many intra-chain crosslinks that do not contribute to the

modulus. At a temperature of 37 °C, the percentage of  $T_9$  blocks taking part in trimeric junctions is too low to obtain a percolating  $T_9C^R_4T_9$  network [23] and accordingly, incubation of  $T_9C^R_4T_9$  at this temperature, in the absence of mTGase, did not result in development of a measurable elasticity (see Fig. 6). When the temperature was lowered to 20 °C, to allow for the additional formation, in the course of 20 h, of a physical network of triple helial junctions, the storage modulus further increases to a final value of  $G' \approx 1600$  Pa (fig. 6). During the same period, the control sample without enzyme developed a modulus of merely  $G' \approx 200$  Pa, indicating that the combination of chemical and physical cross-links is highly synergistic. The physical-chemical network has a much higher elastic modulus ( $G' \approx 1600$  Pa) than the combined modulus of the chemical and physical networks ( $G' \approx 800$  Pa). Probably this is due to the presence of fewer loops or dangling ends that weaken the gel. The fully reversible nature of the physical cross-links was confirmed using a number of cycles of heating and cooling (Fig. 7). Again, despite the fact that the C-blocks are not particularly good substrates for mTGase, mTGase treatment had a remarkably large effect.

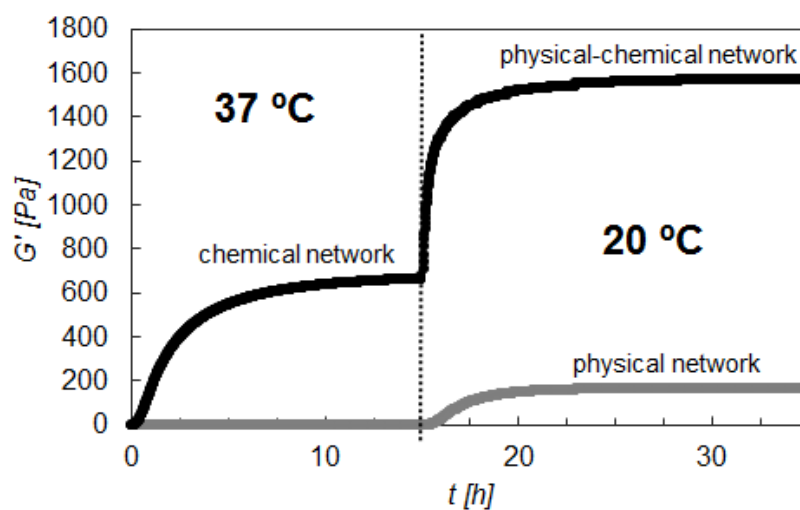


**Figure 4.6.** Development of storage moduli  $G'$  in 55 g/l  $T_9C^R_4T_9$  (grey curve) and 55 g/l  $T_9C^R_4T_9$  crosslinked with mTGase (black curve, enzyme to substrate ratio 1/20 by weight, enzyme was added at  $t = 0$ ). During the first 15 h, the temperature was 37 °C, and during the next 20 h, the temperature was kept at 20 °C.

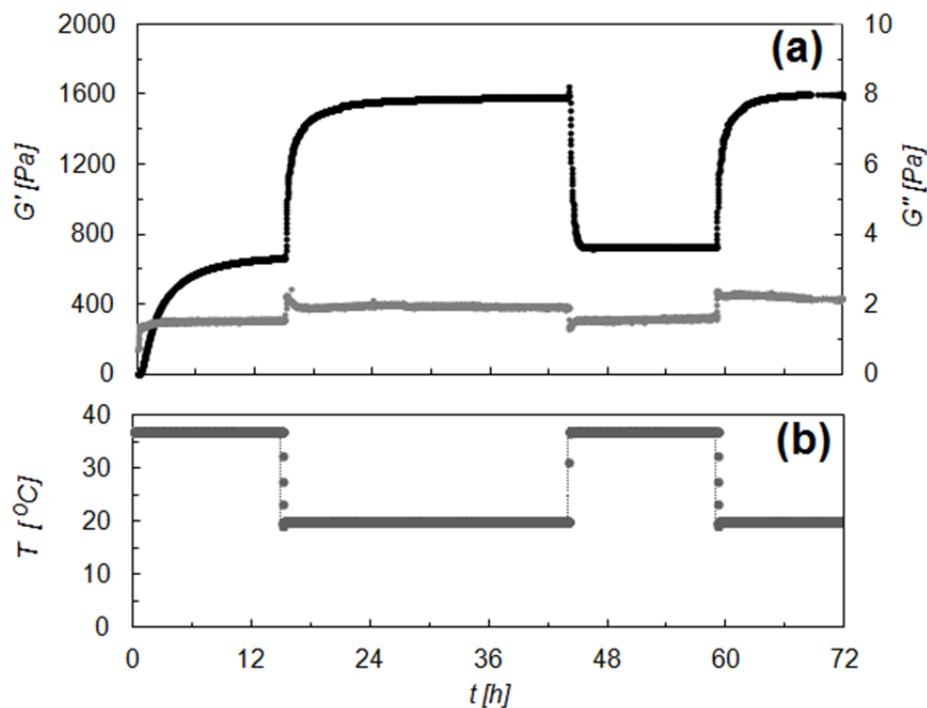


**Figure 4.7.** Time-resolved effect of temperature changes on the viscoelastic properties of a 55 g/l  $T_9C^R_4T_9$  hydrogel supplemented with with 0.42 g/l mTGase at  $t = 0$  (a) Storage modulus  $G'$  (black points) and loss modulus  $G''$  (grey points), and (b) applied temperature  $T$ .

Relaxation of  $T_9$  triple helical nodes is known to be strongly temperature dependent [49] hence shape memory behaviour was tested at different temperatures. Samples were mixed with mTGase and kept at 37 °C for 2 h to allow for enzyme-mediated formation of a covalently-bonded ('chemical') network. When the gel was formed, a 25 % shear strain was applied for 1 h at 37 °C. Next, the temperature was lowered to 5, 10, or 20 °C, while maintaining the shear-induced deformation during 15 h to allow the formation of triple helical, thermoreversible ('physical') junctions that fix the chemical gel in its temporary deformed state. After this step, the load (stress) is taken away, the strain relax and return of the gel to its permanent shape (0 % strain of the chemical network) is recorded. Results for the strain relaxation are shown in Fig. 8. The physical network first shows an

immediate relaxation to about 10 % strain. This initial relaxation is larger than for hydrogels of  $T_9C_4^R T_9$  crosslinked with glutaraldehyde (GA), which showed a lower degree of initial relaxation, viz. to 18% [49]. The initial relaxation is caused by readjustment of the mechanical equilibrium between the two networks. The remaining 10 % strain is constrained by the physical network for a time that strongly depends on the temperature (Fig. 8), as was also shown for  $T_9C_4^R T_9$  shape memory gels prepared using glutaraldehyde cross-linking [49].

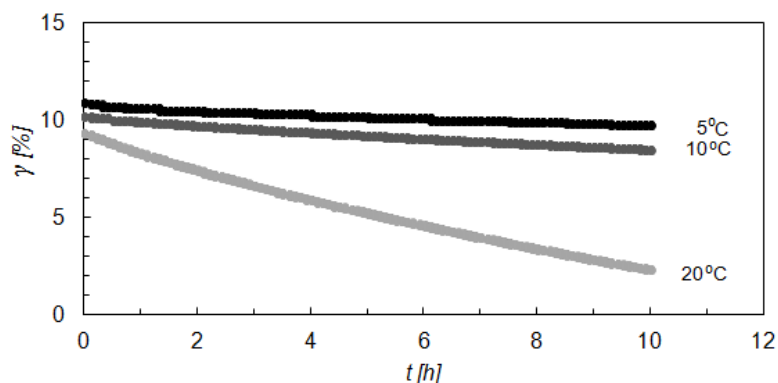


**Figure 4.8.** Strain relaxation of enzymatically cross-linked 55 g/l  $T_9C_4^R T_9$  gels, covalently cross-linked by incubating for 2 h at 37 °C with mTGase at an enzyme to substrate ratio of 1/20 by weight. The chemical network was strained to 25 % and kept at the indicated temperature for 15 h, to allow for the formation of a physical network, before strain relaxation was started at  $t = 0$ .

#### 4.4 Discussion

We have shown that despite the fact that the collagen-like "C" module is not a particularly good substrate for cross-linking by mTGase, the enzyme nevertheless has quite dramatic effects on hydrogels composed of protein-based block copolymers that contain this module as one of their blocks. The use of mTGase leads to a five-fold increase in the modulus of  $C_2^P S_{48}^H C_2^P$  fiber gels, and can be used to create biocompatible protein-based shape memory gels without recurrence to toxic chemical crosslinkers. This report has only been a first exploration of possibilities. It is clear that if the sequence of the hydrophilic block is tuned to allow for more efficient enzymatic cross-linking, this kind of "post-

translational" modifications can be a powerful tool to further control of nano- and microstructures formed by genetically engineered, protein-based polymers.

The low reactivity of the  $C^R$  and  $C^P$  block sequences is consistent with the current (rather incomplete) knowledge on mTGase sequence specificity. Reactivity most sensitively depends on the environment of the Gln residue [50, 51], and to a lesser extent on the environment of the Lys residue [52]. As for the environment of the Lys residue, it has been reported that an adverse effect on substrate activity is found if the Lys amino donor is surrounded (on either side: -1, +1 or -2) by glycine, aspartic acid, proline, histidine or tryptophan [52, 53]. In both  $C^R$  and  $C^P$  block sequences all 12 lysine residues would then be subject to such an adverse effect. The situation is more clear for the Gln environment, for which reactive sequences have recently been analyzed in quite some details [50, 54, 55]. A consensus motif is described by Sugimura [56]: (i) the -3 position to the glutamine is an aromatic amino acid, (ii) the -1, + 1, and + 2 to the glutamine residues are leucine, arginine, and proline, respectively, and (iii) tyrosine is present at the C-terminal side. In the collagen-like blocks only proline residues are present and just 8 (for  $C^R_4$ ) or 3 (for  $C^P_4$ ) out of 64 glutamines have in + 2 position proline, that could explain their low reactivity.

This and other information on the selectivity of cross-linking enzymes can possibly be used to construct highly reactive peptide pairs for mTGase and other enzymes, that can be included in protein-based polymer designs, such as the ones that we consider here. Indeed, there is already some progress in the design of peptide tags optimized for use with various cross-linking enzymes. Conversely, mTGase variants with increased affinity for existing protein-based polymer blocks could be obtained by modern screening and directed evolution techniques.

Higher degrees of enzymatic cross-linking than have been achieved with our "C" block and mTGase will certainly be useful to increase the range of variation of mechanical properties of protein-based polymer hydrogels. In shape memory applications, stiffer gels will require stronger physical bonds to constrain the permanent deformations of the covalent network. This could e.g. be achieved with longer triple-helical end blocks, e.g.  $T_{12}$  or  $T_{16}$

[57, 58] or by using an interpenetrating polymeric network (IPN) of collagen with a different polymer that are entangled with each other [59, 60]. Also, if enzymatic cross-linking is sufficiently fast, the addition of enzyme may be used as a trigger for injectable protein-based hydrogels [61]. In summary, mTGase and other cross-linking enzymes can be a powerful tool in engineering the properties of hydrogels composed of designed protein-based polymers, in particular if the emerging information on sequence specificity of these enzymes is taken into full consideration when designing such polymers.

## References

1. Uy, R. and F. Wold, *Posttranslational covalent modification of proteins*. Science, 1977. **198**(4320): p. 890-896.
2. Beevers, L., *Post-translational modifications*, in *Nucleic Acids and Proteins in Plants I*. 1982, Springer. p. 136-168.
3. Mann, M. and O.N. Jensen, *Proteomic analysis of post-translational modifications*. Nature biotechnology, 2003. **21**(3): p. 255-261.
4. Jensen, O.N., *Modification-specific proteomics: characterization of post-translational modifications by mass spectrometry*. Current Opinion in Chemical Biology, 2004. **8**(1): p. 33-41.
5. Tan, L.P. and S.Q. Yao, *Intein-mediated, in vitro and in vivo protein modifications with small molecules*. Protein and peptide letters, 2005. **12**(8): p. 769-775.
6. Popp, M.W.-L. and H.L. Ploegh, *Making and Breaking Peptide Bonds: Protein Engineering Using Sortase*. Angewandte Chemie International Edition, 2011. **50**(22): p. 5024-5032.
7. Bolscher, J.G.M., et al., *Sortase A as a tool for high-yield histatin cyclization*. The FASEB Journal, 2011. **25**(8): p. 2650-2658.
8. Yang, X., Y. Liu, and G.F. Payne, *Crosslinking Lessons From Biology: Enlisting Enzymes for Macromolecular Assembly*. The Journal of Adhesion, 2009. **85**(9): p. 576-589.
9. Davis, N.E., et al., *Modular enzymatically crosslinked protein polymer hydrogels for in situ gelation*. Biomaterials, 2010. **31**(28): p. 7288-7297.
10. Lewandowski, A.T., et al., *Tyrosine-based "Activatable Pro-Tag": Enzyme-catalyzed protein capture and release*. Biotechnology and Bioengineering, 2006. **93**(6): p. 1207-1215.
11. Bakota, E.L., et al., *Enzymatic Cross-Linking of a Nanofibrous Peptide Hydrogel*. Biomacromolecules, 2011. **12**(1): p. 82-87.
12. Minamihata, K., M. Goto, and N. Kamiya, *Site-Specific Protein Cross-Linking by Peroxidase-Catalyzed Activation of a Tyrosine-Containing Peptide Tag*. Bioconjugate chemistry, 2011. **22**(1): p. 74-81.
13. Sakamoto, T., et al., *Enzyme-Mediated Site-Specific Antibody-Protein Modification Using a ZZ Domain as a Linker*. Bioconjugate chemistry, 2010. **21**(12): p. 2227-2233.
14. Matsunaga, S., et al., *Biotinylated-sortase self-cleavage purification (BISOP) method for cell-free produced proteins*. BMC Biotechnology, 2010. **10**(1): p. 42.
15. Moreira Teixeira, L.S., et al., *Enzyme-catalyzed crosslinkable hydrogels: Emerging strategies for tissue engineering*. Biomaterials, 2012. **33**(5): p. 1281-1290.
16. Huang, Y.-P., et al., *Cross-linking of contractile proteins from skeletal muscle by treatment with microbial transglutaminase*. Journal of Biochemistry, 1992. **112**(2): p. 229-234.

17. Sakamoto, H., Y. Kumazawa, and M. Motoki, *Strength of protein gels prepared with microbial transglutaminase as related to reaction conditions*. Journal of Food Science, 1994. **59**(4): p. 866-871.
18. Zhu, Y., et al., *Microbial transglutaminase - a review of its production and application in food processing*. Applied Microbiology and Biotechnology, 1995. **44**(3-4): p. 277-282.
19. Halloran, D.M.O., et al., *Characterization of a microbial transglutaminase cross-linked type II collagen scaffold*. Tissue engineering, 2006. **12**(6): p. 1467-1474.
20. Ando, H., et al., *Purification and characteristics of a novel transglutaminase derived from microorganisms*. Agricultural and Biological Chemistry, 1989. **53**(10): p. 2613-2617.
21. Fleckenstein, B., et al., *Gliadin T Cell Epitope Selection by Tissue Transglutaminase in Celiac Disease: Role of Enzyme specificity and pH Influence on the Transamidation versus Deamidation reactions*. Journal of Biological Chemistry, 2002. **277**(37): p. 34109-34116.
22. Wertén, M.W.T., et al., *Precision Gels from Collagen-Inspired Triblock Copolymers*. Biomacromolecules, 2009. **10**(5): p. 1106-1113.
23. Skrzyszewska, P.J., et al., *Physical gels of telechelic triblock copolymers with precisely defined junction multiplicity*. Soft Matter, 2009. **5**(10): p. 2057-2062.
24. Li, F., et al., *Formation of nanotapes by co-assembly of triblock peptide copolymers and polythiophenes in aqueous solution*. Soft Matter, 2009. **5**(8): p. 1668-1673.
25. Martens, A.A., et al., *Triblock Protein Copolymers Forming Supramolecular Nanotapes and pH-Responsive Gels*. Macromolecules, 2009. **42**(4): p. 1002-1009.
26. Martens, A.A., et al., *Dilute gels with exceptional rigidity from self-assembling silk-collagen-like block copolymers*. Soft Matter, 2009. **5**(21): p. 4191-4197.
27. Yan, Y., et al., *Nanoribbons Self-Assembled from Triblock Peptide Polymers and Coordination Polymers*. Angewandte Chemie, 2008. **120**(22): p. 4260-4263.
28. Fuchsbauer, H.L., et al., *Influence of gelatin matrices cross-linked with transglutaminase on the properties of an enclosed bioactive material using  $\beta$ -galactosidase as model system*. Biomaterials, 1996. **17**(15): p. 1481-1488.
29. Babin, H. and E. Dickinson, *Influence of transglutaminase treatment on the thermoreversible gelation of gelatin*. Food Hydrocolloids, 2001. **15**(3): p. 271-276.
30. Crescenzi, V., A. Francescangeli, and A. Taglienti, *New Gelatin-Based Hydrogels via Enzymatic Networking*. Biomacromolecules, 2002. **3**(6): p. 1384-1391.
31. Kurisawa, M., et al., *Injectable biodegradable hydrogels composed of hyaluronic acid-tyramine conjugates for drug delivery and tissue engineering*. Chemical Communications, 2005. **0**(34): p. 4312-4314.
32. Jin, R., et al., *Enzyme-mediated fast in situ formation of hydrogels from dextran-tyramine conjugates*. Biomaterials, 2007. **28**(18): p. 2791-2800.
33. Lee, F., J.E. Chung, and M. Kurisawa, *An injectable hyaluronic acid-tyramine hydrogel system for protein delivery*. Journal of Controlled Release, 2009. **134**(3): p. 186-193.

34. Lendlein, A. and S. Kelch, *Shape-memory polymers as stimuli-sensitive implant materials*. *Clinical Hemorheology and Microcirculation*, 2005. **32**(2): p. 105-116.
35. Yakacki, C.M., et al., *Unconstrained recovery characterization of shape-memory polymer networks for cardiovascular applications*. *Biomaterials*, 2007. **28**(14): p. 2255-2263.
36. Neffe, A.T., et al., *Polymer Networks Combining Controlled Drug Release, Biodegradation, and Shape Memory Capability*. *Advanced Materials*, 2009. **21**(32-33): p. 3394-3398.
37. Werten, M.W.T., et al., *Secreted production of a custom-designed, highly hydrophilic gelatin in Pichia pastoris*. *Protein Engineering*, 2001. **14**(6): p. 447-454.
38. Golinska, M.D., et al., *Dilute self-healing hydrogels of silk-collagen-like block copolypeptides at neutral pH*. *Biomacromolecules*, 2013.
39. Lantto, R., et al., *Enzyme-Aided Modification of Chicken-Breast Myofibril Proteins: Effect of Laccase and Transglutaminase on Gelation and Thermal Stability*. *Journal of agricultural and food chemistry*, 2005. **53**(23): p. 9231-9237.
40. Pace, C.N., et al., *How to measure and predict the molar absorption coefficient of a protein*. *Protein Science*, 1995. **4**(11): p. 2411-2423.
41. Yokoyama, K.-i., et al., *In vitro refolding process of urea-denatured microbial transglutaminase without pro-peptide sequence*. *Protein Expression and Purification*, 2002. **26**(2): p. 329-335.
42. Church, F.C., et al., *Spectrophotometric Assay Using o-Phthaldialdehyde for Determination of Proteolysis in Milk and Isolated Milk Proteins*. *Journal of Dairy Science*, 1983. **66**(6): p. 1219-1227.
43. Vigo, M.S., et al., *Spectrophotometric assay using o-phthaldialdehyde for determination of reactive lysine in dairy products*. *Food Chemistry*, 1992. **44**(5): p. 363-365.
44. Dinnella, C., et al., *Spectrophotometric assay using o-phthaldialdehyde for the determination of transglutaminase activity on casein*. *Food Chemistry*, 2002. **78**(3): p. 363-368.
45. Nieuwenhuizen, W.F., et al., *Modification of Glutamine and Lysine Residues in Holo and Apo  $\alpha$ -Lactalbumin with Microbial Transglutaminase*. *Journal of agricultural and food chemistry*, 2003. **51**(24): p. 7132-7139.
46. Fairman, R. and K.S. Åkerfeldt, *Peptides as novel smart materials*. *Current Opinion in Structural Biology*, 2005. **15**(4): p. 453-463.
47. MacPhee, C.E. and D.N. Woolfson, *Engineered and designed peptide-based fibrous biomaterials*. *Current Opinion in Solid State and Materials Science*, 2004. **8**(2): p. 141-149.
48. Rajagopal, K. and J.P. Schneider, *Self-assembling peptides and proteins for nanotechnological applications*. *Current Opinion in Structural Biology*, 2004. **14**(4): p. 480-486.
49. Skrzyszewska, P.J., et al., *Shape-memory effects in biopolymer networks with collagen-like transient nodes*. *Biomacromolecules*, 2011. **12**(6): p. 2285-2292.

50. Ohtsuka, T., et al., *Comparison of substrate specificities of transglutaminases using synthetic peptides as acyl donors*. *Bioscience, biotechnology, and biochemistry*, 2000. **64**(12): p. 2608-2613.
51. Lee, J.-H., et al., *Glutamine (Q)-peptide screening for transglutaminase reaction using mRNA display*. *Biotechnology and Bioengineering*, 2013. **110**(2): p. 353-362.
52. Lee, D.-S., et al., *Identification of the  $\epsilon$ -( $\gamma$ -glutamyl) lysine cross-linking sites in  $\alpha$ -lactalbumin polymerized by mammalian and microbial transglutaminases*. *Journal of agricultural and food chemistry*, 2002. **50**(25): p. 7412-7419.
53. Grootjans, J.J., P.J.T.A. Groenen, and W.W. de Jong, *Substrate Requirements for Transglutaminases: Influence of the amino acid residue preceding the amine donor lysine in a native protein*. *Journal of Biological Chemistry*, 1995. **270**(39): p. 22855-22858.
54. Matsumura, Y., et al., *Enhanced susceptibility to transglutaminase reaction of  $\alpha$ -lactalbumin in the molten globule state*. *Biochimica et Biophysica Acta (BBA) - Protein Structure and Molecular Enzymology*, 1996. **1292**(1): p. 69-76.
55. Sato, H., et al., *Further Studies on the Site-Specific Protein Modification by Microbial Transglutaminase*. *Bioconjugate chemistry*, 2001. **12**(5): p. 701-710.
56. Sugimura, Y., et al., *Identification of preferred substrate sequences of microbial transglutaminase from *Streptomyces mobaraensis* using a phage-displayed peptide library*. *Archives of Biochemistry and Biophysics*, 2008. **477**(2): p. 379-383.
57. Silva, C.I.F., et al., *Secreted production of collagen-inspired gel-forming polymers with high thermal stability in *Pichia pastoris**. *Biotechnology and Bioengineering*, 2011. **108**(11): p. 2517-2525.
58. Silva, C.I.F., et al., *Tuning of Collagen Triple-Helix Stability in Recombinant Telechelic Polymers*. *Biomacromolecules*, 2012. **13**(5): p. 1250-1258.
59. Suri, S. and C.E. Schmidt, *Photopatterned collagen-hyaluronic acid interpenetrating polymer network hydrogels*. *Acta Biomaterialia*, 2009. **5**(7): p. 2385-2397.
60. Hoffman, A.S., *Hydrogels for biomedical applications*. *Advanced drug delivery reviews*, 2012. **64**(Supplement): p. 18-23.
61. Hatefi, A. and B. Amsden, *Biodegradable injectable in situ forming drug delivery systems*. *Journal of Controlled Release*, 2002. **80**(1): p. 9-28.

Appendix

GPPGESPGPQ PGGPQNPQSG EGQGNPNPNK NGPSQGGQPQ GGGSPGSGEP PNPNGPQNG  
 QKPGGQNGP GNGQEGNGQ QNGGSGSGP GSPPGKPPGQ PAGESPGPQP GGPQNPQSGE  
 GQGNPNPNKN GPSQGGQPQG GGSPGSGEPP NPNPGPQNGQ KPGGQNGPG NGQEGNGQQ  
 NGGGSGSGPG SPPGKPPGQP AGESPGPQPG GPQNPQSGEG QGNPNPNKNG PSQGGQPQGG  
 GSPGSGEPPN PNPGPQNGQK PGGQNGPQN GQEGNGQON GGGSGSGPGS PPGKPPGQPA  
 GESPGPQPG PQNPQSGEGQ GNGPNPNKNGP SQGGQPQGGG SPGSGEPPNP NPGPQNGQKP  
 GGQNGPQNG QQEGNGQQNG GGSQSGPGSP PGKPPGQPAG G

Figure 4.9. Sequence of  $C_4^R$  protein polymer [22]

GPPGEPGNPG SPGNQGPQN KGSFGNPGQP GNEGQPGQPG QNGQPGEPGS NGPQGSQGNP  
 GKNGQPGSPG SQGSPGNQGS PGQPNPGQP GEQKPGNQG PAGEPGNPGS PGNQGPQGNK  
 GSPGNPGQPG NEGQPGQPGQ NGQPGEPGSN GPQGSQGNPG KNGQPGSPGS QGSPGNQGSF  
 GQPNPGQPG EQKPGNQP AGEFGNPGSP GNQGPQGNKG SPGNPGQPN EGQPGQPGQN  
 GQPGEPGSNG PQGSQGNPGK NGQPGSPGSQ GSPGNQSGSP QPNPGQPGQE QKPGNQGPA  
 GEPGNPGSP NQGPQGNKGS PGNPGQPGNE GQPGQPGQNG QPGEPGSNGP QGSQGNPGKN  
 GQPGSPGSQ SPGNQGSQPG PGNPGQPGQE GKPGNQGPA G

Figure 4.10. Sequence of  $C_4^P$  protein polymer [37]

YVEFLGAGA PGEFGNPGSP GNQGPQGNK SPGNPGQPN EGQPGQPGQN QPGEPGSNG  
 PQSQGNPGK NGQPGSPSQ GSPGNQSGP QPNPGQPGQE QKPGNQGPA GEPGNPGSPG  
 NQGQPGNKG SPGNPGQPGNE GQPGQPGQNG QPGEPGSNGP QGSQGNPGKN GQPGSPGSQ  
 SPGNQGSQPG PGNPGQPGEQ GKPGNQGPA EGAGAGAGHG AGAGAGHGAG AGAGHGAGAG  
 AGHGAGAGAG HGAGAGAGHG AGAGAGHGAG AGAGHGAGAG AGHGAGAGAG HGAGAGAGHG  
 AGAGAGHGAG AGAGHGAGAG AGHGAGAGAG HGAGAGAGHG AGAGAGHGAG AGAGHGAGAG  
 AGHGAGAGAG HGAGAGAGHG AGAGAGHGAG AGAGHGAGAG AGHGAGAGAG HGAGAGAGHG  
 AGAGAGHGAG AGAGHGAGAG AGHGAGAGAG HGAGAGAGHG AGAGAGHGAG AGAGHGAGAG  
 AGAGAGHGAG AGAGHGAGAG AGHGAGAGAG HGAGAGAGHG AGAGAGHGAG AGAGHGAGAG  
 GEPGNPGSP NQGPQGNKGS PGNPGQPGNE GQPGQPGQNG QPGEPGSNGP QGSQGNPGKN  
 GQPGSPGSQ SPGNQGSQPG PGNPGQPGEQ GKPGNQGPA EPNPGSPGN QGQPGNKGSP  
 GNPGQPGNEG QPGQPGQNGQ PGEFGSNGP QSQGNPGKNG QPGSPGSQGS PGNQGSQPGP  
 GNPGQPGEQ KPNQGPAGE GA

Figure 4.11. Sequence of  $C_2^P S_{48}^H C_2^P$  protein polymer [27]

GPPGAPGPPG PPGPPGPPGP PGPPGPPGPP GPAGESPGPQ PGGPQNPGSG EGQGNPNPNK  
 NGPSQGGQPQ GGGSPGSSEP PNPNPQPQNG QKPGGQQNGP GNGQQEGNGQ QNGGGSQSGP  
 GSPPGKPPGQ PAGESPGPQP GGPQNPGSGE GQGNPNPNKN GPSQGGQPQG GGSPPSGEPP  
 NPNPQPQNGQ KPGGQQNGPG NGQQEGNGQQ NGGGSQSGPG SPPGKPPGQP AGESPGPQPG  
 GPQNPGSSEG QGNPNPNKNG PSQGGQPQGG GSPSGEPPN PNPQPQNGQK PGGQQNGPGN  
 GQQEGNGQQN GGGSQSGPGS PPGKPPGQPA GESPPQPQGG PQNPGSGEGQ GNGPNPNKNGP  
 SQGGQPQGGG SPGSSEPPNP NPGPQNGQKP GGQQNGPQNG QQEGNGQQNG GGSQSGPGSP  
 PGKPPGQPAG APGPPGPPGP PGPPGPPGPP GPPGPPGPPAG G

**Figure 4.12.** Sequence of  $T_9C^R_4T_9$  protein polymer [22, 23]



# Chapter 5

---

## Pearl-necklace complexes of flexible polyanions with neutral-cationic diblock copolymers

---

In this chapter, we study the complexation of very asymmetric diblock copolymers (consisting of a cationic block of 12 lysines connected to a 400 amino acid long hydrophilic polypeptide block with a net charge that is nearly zero) with oppositely charged sodium poly(acrylic acid) (NaPAA) with a range of molar masses between 2 - 1300 kg/mol. For shorter NaPAA chains, spherical complex coacervates micelles are formed, but for long NaPAA chains, with molar masses in excess of 250 kg/mol, Atomic Force Microscopy indicates the presence of pearl-necklace structures. Complexes most likely consist of only a single NaPAA chain, complexed to multiple diblocks. Hence, the size of the complexes can be fully controlled via the NaPAA molar mass. The occurrence of pearl-necklace complexes at higher NaPAA molar masses is attributed to the packing frustration that arises due to the small size of the cationic block of the diblock copolymers.

Publish as: M.D. Golinska , F.A. de Wolf, M.A. Cohen Stuart , A. Hernandez-Garcia and R. de Vries; Pearl-necklace complexes of flexible polyanions with neutral-cationic diblock copolymers, *Soft Matter*, **2013**, 9, 6406-6411



---

## 5.1 Introduction

Electrostatic complexes of macroions have been studied for many decades, starting with early work on the interactions between oppositely charged flexible polyelectrolytes [1, 2] and on interactions between flexible polyelectrolytes and oppositely charged globular proteins [3, 4]. The topic has seen sustained interest in recent years with many studies on, among others, protein-polysaccharide complexes [5], complexes of DNA/RNA with polycations [6], on polymer coatings fabricated by electrostatic layer-by-layer self-assembly of oppositely charged macroions [7-9] and on polyelectrolyte brushes interaction with oppositely charged macroions such as proteins [10, 11].

In solution, oppositely charged macroions often exhibit macroscopic phase separation when the electrostatic attraction is strong enough. When large uncharged hydrophilic blocks are connected to (at least) one of the complexing macroions, macroscopic phase separation is prevented or frustrated, and instead, microphase separation occurs. For example, diblock copolymers consisting of a charged block connected to a neutral hydrophilic block, form so-called complex coacervate core micelles, when mixed with oppositely charged macroions [12], with a core consisting of the macroion complex (often a complex coacervate) and a corona consisting of the neutral hydrophilic blocks.

Using recombinant DNA technology, we have recently produced completely monodisperse and very asymmetric charged-neutral diblock copolymers, consisting of a cationic block of 12 lysines ( $B^{K12}$ ), connected to 4 repeats of a large hydrophilic and net uncharged polypeptide of 100 amino acids ("C-block"). This very asymmetric  $C_4B^{K12}$  diblock copolymer uniformly coats double stranded semiflexible DNA to form a self-assembled bottle-brush polymer [13].

It is interesting to consider what would happen if these very asymmetric charged-neutral diblock copolymers are complexed with an oppositely charged *flexible* polyelectrolyte with much lower persistence length than the semiflexible DNA that we have studied before. The chain length of this flexible homopolyelectrolyte is defining the structure of the

complexes. For very long flexible polyanions, spherical complex coacervates micelles can no longer be formed since the radius of the corresponding complex coacervate core would exceed the (rather small) stretched length of the charged block on the diblock copolymer. In this case, it may be expected that local complex coacervates only develop up to length scales on the order of the length of charged block of the diblock copolymer.

Here we study the complexation of the very asymmetric  $C_4B^{K12}$  diblock copolymer with the flexible polyanion sodium poly(acrylic acid) for a range of molar masses, up to  $2 \cdot 10^6$  g/mol. Complexes are characterized using dynamic light scattering (DLS), static light scattering (SLS) and atomic force microscopy (AFM). As we will show, complexes with these very asymmetric charged-neutral diblocks are distinctly different from complexes with the less asymmetric charged-neutral diblocks that have been studied before [14-18]: the large neutral block in combination with the short charged block prevents full charge neutralization in complexes. Complexes most likely involve only single homopolyelectrolyte chains (as we have previously also found for complexes with semiflexible DNA). Finally, for very high molar mass homopolyelectrolytes, the complexes exhibit pearl-necklace configurations reminiscent of the pearl-necklace configurations of partially collapsed hydrophobic polyelectrolytes.

## 5.2 Materials and methods

### 5.2.1. Materials

Na-PAA with molar masses ( $M_w$ ) of 2000 - 1300000 g/mol were purchased from Polysciences, Inc. and have reported polydispersities  $D_p = M_w/M_n$  between 1.3 and 2.15. The  $C_4B^{K12}$  diblock was produced and purified as described before [13].

### 5.2.2. Sample preparation

Aqueous solutions of Na-PAA (up to 0.1 g/L) and  $C_4B^{K12}$  (up to 5 g/L) were prepared by dissolving known amount of the polymers in 10 mM phosphate buffer pH 7. All polymers were filtered using 0.22  $\mu\text{m}$  pore size centrifugal filters with low-binding Durapore<sup>®</sup> PVDF membrane (Ultrafree-MC, Millipore) and mixed at different bulk charge ratio's  $f_{+/}$  and final PAA and  $C_4B^{K12}$  weight concentrations  $C_{\text{PAA}}$  and  $C_{\text{diblock}}$ . The ratio  $f_{+/}$  is defined as a total number of positively charged lysine groups of the  $B^{K12}$  blocks over to the total number of (negatively) chargeable acrylic acid groups. All experiments were performed at 25 °C.

### 5.2.3. Light Scattering

Dynamic light scattering (DLS) experiments were performed on a Zetasizer Nano ZS (Malvern Instruments, UK) with a 5 mW He-Ne ion laser operating at a wavelength  $\lambda = 633$  nm and at fixed scattering angles of 173° and 12.3°, at a temperature of 25 °C. The reported hydrodynamic radius  $R_h$  is the peak position of the dominant peak in the distribution analysis performed on the DLS autocorrelation functions by the Malvern DTS software, version 5.10 beta 1. For each sample, reported values are the average of 10 measurements of 60 s.

Static light scattering experiments were performed on an ALV-125 goniometer, combined with a 300 mW Cobolt Samba-300 DPSS laser operating at a wavelength of  $\lambda = 532$  nm, an ALV optical fiber with a diameter of 50  $\mu\text{m}$ , and an ALV/SO Single Photon Detector.

Temperature was maintained at  $25 \pm 0.1$  °C using a Haake F8-C35 thermostatic bath. Measurements were taken at multiple scattering angles  $\vartheta$  ranging from  $50^\circ$  to  $140^\circ$ , corresponding to a scattering vector:

$$q = \frac{4\pi n_s}{\lambda} \sin(\theta / 2) \quad (5.1)$$

where  $n_s = 1.333$  is the refractive index of the solvent (water). Absolute scattering intensities (Rayleigh Ratio's)  $R_\vartheta$  were calculated from the relative scattered intensities of the sample ( $I_{sample}$ ), solvent ( $I_{solvent}$ ) and toluene reference ( $I_{toluene}$ ) according to:

$$R_\vartheta = \frac{I_{sample}(\vartheta) - I_{solvent}(\vartheta)}{I_{toluene}(\vartheta)} \frac{n_s^2}{n_{tol}^2} R_{toluene} \quad (5.2)$$

The absolute scattering of the reference toluene is  $R_{toluene} = 2.10 \times 10^{-3} \text{ m}^{-1}$  [19] and the toluene refractive index is  $n_{toluene} = 1.496$  [20]. Guinier plots [21] were used to extract the scattering at zero angle and the radius of gyration, using

$$\ln R_\vartheta \approx \ln R_{\vartheta=0} - \frac{R_g^2}{3} q^2 \quad (5.3)$$

The weight averaged molar mass  $M_w$  of the PAA in solution was estimated from scattering experiments at a range of concentrations  $C_{PAA}$ , from

$$R_{\vartheta=0} = K_R C_{PAA} M_w \quad (5.4)$$

$$K_R = \frac{4\pi^2 n_s^2}{\lambda N_{Av}} \left( \frac{dn}{dc} \right)_{PAA}^2 \quad (5.5)$$

where the Rayleigh constant  $K_R$  involves the PAA refractive index increment  $(dn/dc)_{PAA} = 0.14 \text{ cm}^3 \text{ g}^{-1}$  [22], and  $N_{Av}$  is Avogadro's constant. Molar masses were estimated for each concentration of  $C_{PAA}$  and then extrapolated to zero concentration.

When estimating the mass of the complexes, we need to take into account the differential scattering contrast of the PAA and the diblocks. The amino acid composition of the  $C_4B^{K12}$  diblock is very close to that of gelatin, hence we use a value of  $(dn/dc)_{diblock} = 0.18 \text{ cm}^3 \text{ g}^{-1}$  [23], such that the contrast ratio is:

$$\zeta = \frac{(dn/dc)_{diblock}}{(dn/dc)_{PAA}} = 1.3 \quad (5.6)$$

Next assume that the scattering in mixtures is caused by PAA-diblock complexes (complex weight concentration  $C_{complex}$ ) coexisting with excess  $C_4B^{K12}$  diblock polymer (concentration  $C_{diblock,free}$ ):

$$R_{\theta=0} = R_{\theta=0,complex} + R_{\theta=0,diblock} \quad (5.7)$$

$$R_{\theta=0,complex} = K_{R,complex} C_{complex} M_{complex} \quad (5.8)$$

$$R_{\theta=0,diblock} = K_{R,diblock} C_{diblock,free} M_{diblock} \quad (5.9)$$

It is convenient to introduce some further notation. The total mass ratio of diblock copolymers to PAA is

$$\Gamma = C_{diblock}/C_{PAA} \quad (5.10)$$

The mass ratio of bound diblock copolymers to PAA is

$$\Gamma_{bound} = C_{diblock,bound} / C_{PAA} = \frac{M_{diblock} N_{diblock}}{M_{PAA}} \quad (5.11)$$

where  $N_{diblock}$  is the number of diblock copolymers bound to a single PAA molecule. The scaled difference of the mass of total and bound diblock copolymers is:

$$\Delta\Gamma = \Gamma - \Gamma_{bound} \quad (5.12)$$

And the contrast of the complexes is estimated as:

$$\left(\frac{dn}{dc}\right)_{complex} = w_{PAA} \left(\frac{dn}{dc}\right)_{PAA} + w_{diblock} \left(\frac{dn}{dc}\right)_{diblock} = \left(\frac{dn}{dc}\right)_{PAA} \frac{1 + \Gamma_{bound} \zeta}{1 + \Gamma_{bound}} \quad (5.13)$$

where  $w_{PAA}$  and  $w_{diblock}$  are the weight fractions of PAA and diblock copolymer in the complexes. Assuming the complexes consist of a single PAA chain complexed with many diblock copolymers, the ratio of the scattering by complexes over the scattering of the PAA is:

$$\frac{R_{\theta=0,complex}}{R_{\theta=0,PAA}} = (1 + \Gamma_{bound} \zeta)^2 \quad (5.14)$$

If the scattering of free diblocks can be neglected, this can be used to extract values of  $\Gamma_{bound}$  from measured (zero angle) scattering intensities. The ratio of the scattering of the free diblocks over that of the complexes is:

$$\frac{R_{\theta=0,diblock}}{R_{\theta=0,complex}} = \zeta^2 \frac{M_{diblock}}{M_{PAA}} \frac{\Delta\Gamma}{(1 + \Gamma_{bound} \zeta)^2} \quad (5.15)$$

Typically, the contribution of the free diblocks to the scattering is negligible. For example, assuming that about 50 % of the PAA charge is neutralized and that the concentration of free diblocks equals the concentration of diblocks that are bound to PAA, then  $\Delta\Gamma = \Gamma_{bound} \approx 17$ . In this case, for  $M_{PAA} = 800$  kg/mol, the scattering of the free diblocks amounts to only 0.3 % of the total scattering. This implies that when performing DLS on the complexes coexisting with excess diblock copolymer, one typically only observes the diffusion of the complexes.

#### 5.2.4. Atomic Force Microscopy (AFM)

Samples for AFM were prepared by diluting the complexes at a PAA concentration  $C_{PAA} = 0.01$  g/L used for light scattering 5, 8, 10 or 20 times with filtrated dH<sub>2</sub>O. A drop of sample (5  $\mu$ l) was immediately placed on a freshly cleaved mica wafer and left for 5 min, followed

by washing with 1 ml of filtrated dH<sub>2</sub>O to removed salts and nonabsorbed particles. Next the sample was slowly dried under a nitrogen steam. To validate the reproducibility of observed morphology, multiple images were collected on at least three independently prepared samples during different days. Samples were analyzed using a Digital Instruments NanoScope V. The imaging was conducted using silicon nitride cantilevers (Veeco, NY, USA) with a nominal spring constant of 0.32 N/m. The ScanAsyst™ image mode was used in air at room temperature. Images were processed using NanoScope Analysis 1.20 software.

### 5.3 Results and discussion

For less asymmetric charged-neutral diblocks, complexation with oppositely charged homopolyelectrolytes leads to spherical complex coacervate core micelles consisting of multiple homopolyelectrolytes and multiple charged-neutral diblock copolymers [24]. These systems typically show a peak in the scattering intensity at a charge ratio  $f_{+/-} = 1$ , indicating dissolution of the large complex coacervate cores of the micelles at excess charge conditions. We have performed dynamic light scattering as a function of the charge stoichiometry  $f_{+/-}$  for fixed low concentrations of Na-PAA of two molar masses (20 kg/mol and 245 kg/mol), at low ionic strength (10 mM pH 7 Phosphate buffer). As can be seen in Figure 5.1a, for the Na-PAA complexed with increasing amounts of  $C_4B^{K12}$ , there is no peak in the scattered intensity as a function of charge stoichiometry  $f_{+/-}$ . Instead, the scattering intensity increases with increasing  $f_{+/-}$ , leveling off only at large values of  $f_{+/-}$ . Figure 5.1b shows the hydrodynamic radii  $R_h$  of the PAA's and their complexes with  $C_4B^{K12}$ , as a function of  $f_{+/-}$ . For both Na-PAA homopolymers, the hydrodynamic size of the complexes rapidly increases from 8.5 nm to 20 nm for Na-PAA<sub>20k</sub>- $C_4B^{K12}$  and from 29.5 nm to 44 nm for Na-PAA<sub>245.2k</sub>- $C_4B^{K12}$ . Saturation of the hydrodynamic radius already occurs at about  $f_{+/-} = 0.5$ , as opposed to saturation of the scattered intensity that levels off much slower, and still increases weakly at  $f_{+/-} \gg 1$ . As is shown using numerical estimates in the Materials and Methods, the scattering intensity of the excess diblock copolymers is negligible as compared to that of the complexes, hence only a single diffusion size is found with DLS.

These results are very similar to what was observed for  $C_4B^{K12}$  complexation with the semiflexible polyelectrolyte DNA. For that case it was found from the absolute molar mass of the complexes that they were slightly undercharged, single DNA chain complexes, i.e. not all DNA negative charge was being compensated by the positive charges on the  $B^{K12}$  block, even at a large excess of the  $C_4B^{K12}$  diblocks. This was attributed to the large steric repulsion among the  $C_4$  blocks that form a bottle-brush around the DNA. It is very likely that a similar mechanism operates when the  $C_4B^{K12}$  binds to oppositely charged flexible polyelectrolytes such as PAA.

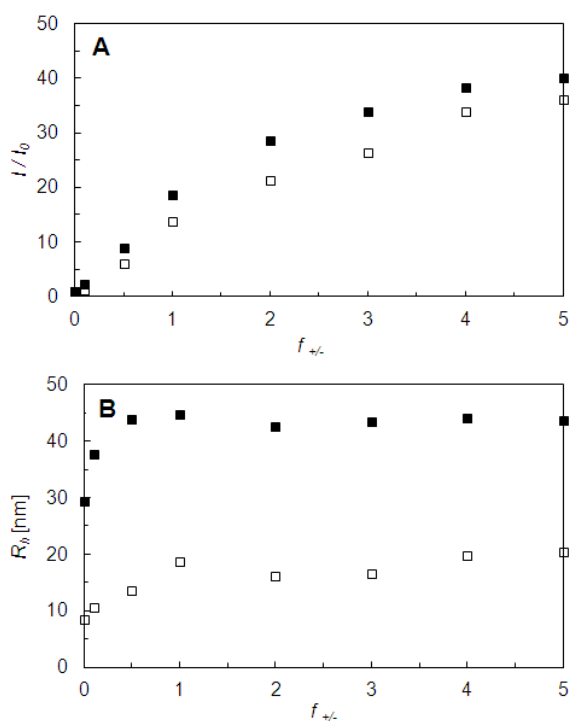


**Figure. 5.1** Light scattering (scattering angle  $\vartheta = 173^\circ$ , wavelength  $\lambda = 633\text{nm}$ ) of 0.01 mg/ml PAA solutions of two molar masses (20 kg/mol (○) and 245.2 kg/mol (●)), complexed with increasing amounts of the diblock copolymer  $C_4B^{K12}$  (expressed in terms of the charge ratio  $f_{+/-}$ ). A) Scattered intensity  $I$ , scaled by scattered intensity  $I_0$  at  $f_{+/-} = 0$ . B) Effective hydrodynamic radius  $R_h$ .

---

For the case of semiflexible DNA we observed that the  $C_4B^{K12}$  diblock copolymers uniformly coated single DNA molecules. If the  $C_4B^{K12}$  diblock copolymers also associate with single PAA molecules, one would expect a distinct scaling of the micellar size with molar mass of the PAA molecules. Results of dynamic light scattering measurements on complexes of the  $C_4B^{K12}$  diblock copolymers with Na-PAA homopolymers of a range of molar masses (at  $f_{+,-} = 1$ ) are shown in Fig. 5.2, together with the corresponding sizes of the bare Na-PAA chains. To confirm that angular dependence of the scattering does not influence the results, we have also performed the same experiments at a much smaller scattering angle of  $\vartheta = 12.3^\circ$ , and this give identical results, albeit with somewhat higher standard deviations (data not shown). Furthermore, to test for non-equilibrium effects, we have followed the scattering of the complexes in time, measuring from immediately after preparation, up to 24 hours after preparation, and found no changes in the scattering (data not shown). For the bare Na-PAA chains, we find a scaling for the hydrodynamic size  $R_h$  with molar mass  $M$ , of  $R_h \propto M^\nu$ ,  $\nu \approx 0.5$ . Ideal chain as opposed to full excluded volume scaling ( $\nu \approx 0.6$ ) is observed probably because the majority of the samples are at rather low molar mass. Furthermore, the salt concentration is rather low (10 mM) such that there is significant electrostatic stiffening, leading to long, slender effective segments with small excluded volume interactions. For the complexes we observe  $R_h \propto M^\nu$ ,  $\nu \approx 0.3$ . This can be explained by a combination of a rather constant corona size, plus a core volume that grows linearly with the length of the Na-PAA polyanion, giving a predicted scaling exponent of  $\nu = 1/3$ . Hence, the PAA molar mass dependence is fully consistent with the hypothesis that the complexes consist of a single Na-PAA polyanion, complexed with multiple  $C_4B^{K12}$  diblock copolymers, though it not directly proves that it is true.

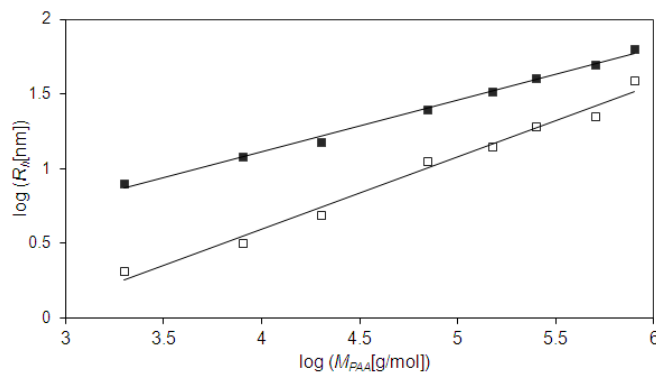


**Figure 5.2.** Hydrodynamic radius,  $R_h$  of complex Na-PAA with diblock at  $f_{+/-} = 1$  (filled squares) and free Na-PAA (open squares) obtained from DLS at  $\vartheta = 173^\circ$ .

For an estimate of the degree of charge neutralization of the  $f_{+/-} = 1$  complexes, via the absolute molar mass of the complexes, we have turned to static light scattering. Fig. 5.3 shows the Guinier plots for both bare 800 kg/mol PAA (at  $C_{PAA} = 0.1$  g/L) and 800 kg/mol PAA complexed with the  $C_4B^{K12}$  diblock copolymer at a bulk charge ratio  $f_{+/-} = 1$  ( $C_{PAA} = 0.01$  g/L and  $C_{diblock} = 0.34$  g/L). Molar masses of bare PAA and of complexes were determined by performing Guinier plots for different concentrations ( $C_{PAA} = 0.005$  g/L, 0.01 g/L and 0.03 g/L) and extrapolating the estimated molar masses to zero PAA concentration.

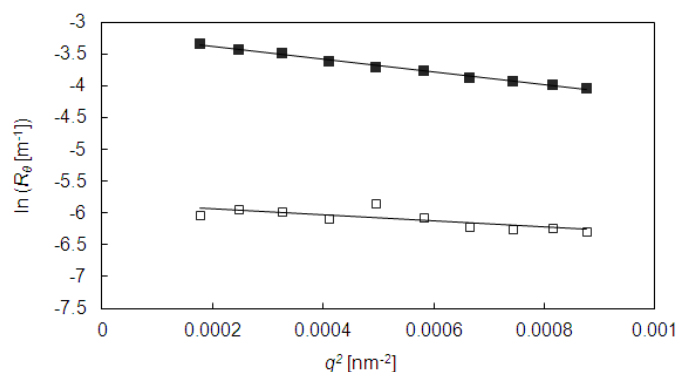


**Figure 5.3.** Guinier plots of SLS data for complex 800 kg/mol Na-PAA with diblock at  $f_{+/-} = 1$  (filled squares) and free 800 kg/mol Na-PAA (open squares)

---

The molar mass of the bare PAA obtained from light scattering is found to be within 10 % of the expected value of 800 kg/mol. Gyration radii obtained for the bare PAA and the complex are quite close to each other. For the bare PAA,  $R_g = 60$  nm, whereas for the complex,  $R_g = 73$  nm. These values are similar to the hydrodynamic radii at 800 kg/mol in Fig 5.2. As is very clear from that figure, the sizes of the free PAA chains and the complexes indeed start approaching each other at the highest PAA molar masses.

If we assume the core of the complexes indeed consists of a single PAA chain, we can estimate the ratio  $\Gamma_{bound}$  of the mass of diblock copolymers bound to PAA, over the mass of PAA from the ratio of the scattered intensities of the complexes and the bare PAA at zero scattering angle (see 5.2. Materials and Methods). From such an analysis, it is found that  $\Gamma_{bound} \approx 11$ . For full charge neutralization of the PAA charges by the polylysines of the cationic blocks, the expected mass ratio is  $\Gamma_{max} = 34$ , such that the estimated degree of charge neutralization at a bulk charge ratio  $f_{+/-} = 1$ , is  $\alpha = \Gamma_{bound} / \Gamma_{max} \approx 0.3$ . For the case of DNA [13] it was estimated that around 80 - 90% of the DNA charges could be neutralized by binding the  $C_4B^{K12}$  diblock copolymers at low salt but apparently the lower linear charge density of the PAA pushes the maximal degree of charge neutralization that can be achieved even further down to about 30 %. Results of the analysis of the static light scattering are summarized in Table 5.1.

**Table 5.1.** Radius of gyration for the bare PAA,  $R_{g,0}$ ; radius of gyration for the complex,  $R_{g,c}$ ; the molar mass of 800 kg/mol PAA obtained from light scattering,  $M_{w,0}$ ; mass ratio of bound diblock copolymers to PAA,  $\Gamma_{bound}$ ; estimated degree of charge neutralization at a bulk charge ratio  $f_{+/-} = 1$ ,  $\alpha = \Gamma_{bound} / \Gamma_{max}$ . Values of  $R_{g,0}$ ,  $R_{g,c}$  and  $M_{w,0}$  are found by extrapolation to zero concentration.

$R_{g,0}$	60 nm
$R_{g,c}$	73 nm
$M_{w,0}$	710 kg/mol
$\Gamma_{bound}$	11
$\alpha = \Gamma_{bound} / \Gamma_{max}$	0.3

If we assume the core of the complexes indeed consists of a single PAA chain, we can estimate the ratio  $\Gamma_{bound}$  of the mass of diblock copolymers bound to PAA, over the mass of PAA from the ratio of the scattered intensities of the complexes and the bare PAA at zero scattering angle (see 5.2. Materials and Methods). From such an analysis, it is found that  $\Gamma_{bound} \approx 11$ . For full charge neutralization of the PAA charges by the polylysines of the cationic blocks, the expected mass ratio is  $\Gamma_{max} = 34$ , such that the estimated degree of charge neutralization at a bulk charge ratio  $f_{+/-} = 1$ , is  $\alpha = \Gamma_{bound} / \Gamma_{max} \approx 0.3$ . For the case of DNA [13] it was estimated that around 80 - 90% of the DNA charges could be neutralized by binding the  $C_4B^{K12}$  diblock copolymers at low salt but apparently the lower linear charge density of the PAA pushes the maximal degree of charge neutralization that can be achieved even further down to about 30 %. Results of the analysis of the static light scattering are summarized in Table 5.1.

Finally, atomic force microscopy (AFM) was used to visualize the structure of the complexes in more detail. Figure 5.4 shows a typical image of  $C_4B^{K12}$  and Na-PAA

complexes. Whereas at low PAA molar mass (250 kg/mol and below) single micelles are observed, complexes with PAA of higher molar mass (800 kg/mol and above) show a pearl-necklace structure, with individual complexes consisting of typically  $4 \pm 1$  connected micelles per chain for 800 kg/mol PAA. Assuming a degree of charge neutralization of  $\alpha = 0.3$ , as estimated from static light scattering, this corresponds to about  $50 C_4B^{K12}$  diblock copolymers per micellar core.

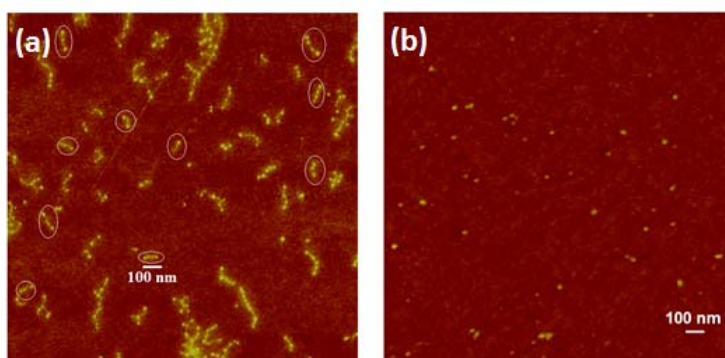


**Figure 5.4.** AFM images in air of Na-PAA complexed with  $C_4B^{K12}$  protein diblock copolymer at  $f_{+/-} = 1$  pH 7, deposited on mica. **a)**  $M_{PAA} = 800$  kg/mol, white ellipses surround hypothetical single-chain pearl-necklace complexes with around 3 - 5 complex coacervate micelles per complex. **b)**  $M_{PAA} = 250$  kg/mol.

Some numerical estimates may be helpful to explain the splitting into a pearl-necklace structure at higher PAA molar mass. As suggested in the introduction, the splitting most likely arises because of the frustration that is associated with the very short cationic block: the stretched length of the cationic block basically sets the maximum radius for the complex coacervate core of the micelles. While a cylindrical complex coacervate core would also have satisfied the frustration due to the short cationic block, in this case apparently the interfacial tension at the core/corona interface is too large for that, such that the pearl-necklace configuration has a lower free energy.

It is straightforward to estimate beyond which PAA molar mass the radius  $R_c$  of a single PAA chain complex coacervate increases beyond the stretched length  $R_{c,max} \approx 5$  nm of the

cationic block. The polyanion chains consist of  $N^-$  monomers of volume  $v_0^-$ , the cationic block of the diblock consists of  $N^+$  monomers of volume  $v_0^+$ . The core of the micelle is assumed to consist of a single polyanion chain and  $m^+$  diblocks, such that the degree of charge neutralization of the core complex is given by  $f = m^+ N^+ / N^- \approx 0.3$ . The volume fraction of water in the complex coacervate core is  $\Phi_w$ . Mass balance leads to a simple estimate of the core radius  $R_c$ :

$$R_c = \left( \frac{3}{4\pi} \frac{2 - \phi_w}{1 - \phi_w} N^- (v_0^- + f v_0^+) \right)^{1/3} \quad (5.16)$$

For the estimates, we use parameter values indicated in Table 5.2. The only parameter that is not known accurately is the water content  $\Phi_w$ . For bulk polyelectrolyte complex coacervates very few values are available, here we use a water content of 60 % as was determined recently for polyelectrolyte complexes [25]. Results for the number of diblocks  $m_+$  per complex, and for the core radius as a function of the PAA molar mass, are given in table 5.3. These estimates suggest that the boundary  $R_c \approx R_{c,max}$  occurs at a PAA molar masses of order (100 kg/mol). Given the rough nature of these estimates, this may be considered to be at least consistent with the AFM observation that the transition between single-core and pearl-necklace micelles occurs between PAA molar masses of 250 kg/mol and 800 kg/mol.

Another quantity of interest is the surface grafting density  $\sigma$  of neutral  $C_4$  blocks on the surface of the micellar core,  $\sigma = m^+ / 4\pi R_c^2$ . If  $\sigma R_0^2 \gg 1$ , where  $R_0$  is the unperturbed radius of the neutral block, the neutral blocks may be expected to be highly stretched. Clearly, for single-core micelles corona-chain stretching increases quite dramatically with PAA molar mass, and this may also favor the formation of a pearl-necklace structure, in addition to the inability of the cationic block to fill complex coacervate cores with radii larger than  $R_{c,max}$ .

**Table 5.2.** Estimated parameters of volume of anionic chain of PAA monomers,  $u_0^-$ ; volume of cationic diblock monomers,  $u_0^+$ ; volume fraction of water in the complex coacervate core,  $\Phi_w$ ; unperturbed radius of the neutral block,  $R_0$ .

$u_0^-$	0.1 nm <sup>3</sup>
$u_0^+$	0.2 nm <sup>3</sup>
$f$	0.3
$\Phi_w$	0.6
$R_0$	6 nm

**Table 5.3.** Estimated number of diblocks ( $m_+$ ) per complex, number of polyanion monomers ( $N^-$ ), dimensionless surface grafting density ( $\sigma R_0^2$ ) and the core radius ( $R_c$ ) as a function of the PAA molar mass ( $M_{PAA}$ )

$M_{PAA}$ (kg/mol)	$N^-$	$m^+$	$R_c$ (nm)	$\sigma R_0^2$
1	14	1	1.5	1.3
10	139	12	3.3	3.2
100	1,389	116	7.0	6.8
1000	13,889	1157	15.2	14.4

#### 4. Conclusion

We have shown that the packing frustration that arises as a consequence of the very short cationic block of our  $C_4B^{K12}$  diblock copolymer, leads to novel single-chain electrostatic pearl-necklace complexes with long PAA, reminiscent of pearl-necklace configurations of hydrophobic polyelectrolytes [26-28]. Whereas for the latter case, obtaining definite experimental proof of the theoretically predicted pearl necklaces conformations has been challenging, in the present case the pearl-necklace nature of the complexes was immediately evident from straightforward AFM experiments. As opposed to complex coacervate core micelles prepared with less asymmetric charged-neutral diblocks, our complexes appear to have only a single homopolyelectrolyte in the complex coacervate core which implies full control of the coacervate core size via the homopolyelectrolyte molar mass, up to the point where packing frustration starts leading to pearl-necklace configurations. Finally, the results emphasize the distinct differences between complexes of these highly asymmetric diblocks with flexible as opposed to semi-flexible homopolyelectrolytes. Whereas for the latter case the homopolyelectrolytes are simply decorated with diblocks, leading to a bottle-brush structure, for flexible polyelectrolytes, local collapse of the partly neutralized homopolyelectrolyte cannot be prevented by the long neutral blocks of the  $C_4B^{K12}$  diblock copolymer.

---

## References

1. Bungenberg de Jong, H.G., *Contributions to the theory of vegetable tanning I. Dehydration of lyophilic sols and gels by tannins and its bearing on the theory of vegetable tanning*. Recueil des Travaux Chimiques des Pays-Bas, 1923. **42**(5): p. 437-472.
2. Kruyt, H.R., *Colloid Science*, ed. H.G. Bungenberg de Jong. Vol. 2. 1949, New York: Elsevier Pub. Co. .
3. Morawetz, H. and W.L. Hughes, *The Interaction of Proteins with Synthetic Polyelectrolytes. I. Complexing of Bovine Serum Albumin*. The Journal of Physical Chemistry, 1952. **56**(1): p. 64-69.
4. Cooper, C.L., et al., *Polyelectrolyte-protein complexes*. Current Opinion in Colloid & Interface Science, 2005. **10**(1-2): p. 52-78.
5. Turgeon, S.L., C. Schmitt, and C. Sanchez, *Protein-polysaccharide complexes and coacervates*. Current Opinion in Colloid & Interface Science, 2007. **12**(4-5): p. 166-178.
6. Thomas, M. and A.M. Klibanov, *Non-viral gene therapy: polycation-mediated DNA delivery*. Applied Microbiology and Biotechnology, 2003. **62**(1): p. 27-34.
7. Lvov, Y., et al., *Assembly of Multicomponent Protein Films by Means of Electrostatic Layer-by-Layer Adsorption*. Journal of the American Chemical Society, 1995. **117**(22): p. 6117-6123.
8. Decher, G., *Fuzzy Nanoassemblies: Toward Layered Polymeric Multicomposites*. Science, 1997. **277**(5330): p. 1232-1237.
9. Ladam, G., et al., *Protein Adsorption onto Auto-Assembled Polyelectrolyte Films*. Langmuir, 2001. **17**(3): p. 878-882.
10. Wittemann, A. and M. Ballauff, *Secondary Structure Analysis of Proteins Embedded in Spherical Polyelectrolyte Brushes by FT-IR Spectroscopy*. Analytical Chemistry, 2004. **76**(10): p. 2813-2819.
11. Rosenfeldt, S., et al., *Interaction of proteins with spherical polyelectrolyte brushes in solution as studied by small-angle x-ray scattering*. Physical Review E, 2004. **70**(6): p. 061403.
12. Cohen Stuart, M.A., et al., *Assembly of polyelectrolyte-containing block copolymers in aqueous media*. Current Opinion in Colloid & Interface Science, 2005. **10**(1-2): p. 30-36.
13. Hernandez-Garcia, A., et al., *Coating of Single DNA Molecules by Genetically Engineered Protein Diblock Copolymers*. Small, 2012. **8**(22): p. 3491-3501.
14. Gucht, J.v.d., et al., *Polyelectrolyte complexes: Bulk phases and colloidal systems*. Journal of Colloid and Interface Science, 2011. **361**(2): p. 407-422.
15. de Vos, W.M., et al., *Ultradense Polymer Brushes by Adsorption*. Angewandte Chemie International Edition, 2009. **48**(29): p. 5369-5371.
16. Lindhoud, S., et al., *Structure and Stability of Complex Coacervate Core Micelles with Lysozyme*. Biomacromolecules, 2007. **8**(7): p. 2219-2227.

17. Hofs, B., A. de Keizer, and M.A. Cohen Stuart, *On the Stability of (Highly Aggregated) Polyelectrolyte Complexes Containing a Charged-block-Neutral Diblock Copolymer*. The Journal of Physical Chemistry B, 2007. **111**(20): p. 5621-5627.
18. Loh, P., et al., *Collapse of Linear Polyelectrolyte Chains in a Poor Solvent: When Does a Collapsing Polyelectrolyte Collect its Counterions?* Macromolecules, 2008. **41**(23): p. 9352-9358.
19. Wu, H., *Correlations between the Rayleigh ratio and the wavelength for toluene and benzene*. Chemical Physics, 2010. **367**(1): p. 44-47.
20. Dean, J.A., *Lange's Handbook of Chemistry*. 15th ed. 1998: McGraw-Hill. 1291.
21. Glatter, O. and O. Kratky, *Small-Angle X-Ray Scattering*. 1982: Academic Press
22. Morcellet, M. and C. Loucheux, *Preferential solvation of poly(acrylic acid) and its sodium salt in water/dioxane mixtures: A comparison with poly( $\alpha$ -L-glutamic acid)*. Die Makromolekulare Chemie, 1978. **179**(10): p. 2439-2450.
23. Altgelt, K., A.J. Hodge, and F.O. Schmitt, *Gamma Tropocollagen: A Reversibly Denaturable Collagen Macromolecule*. Proceedings of the National Academy of Sciences of the United States of America, 1961. **47**(12): p. 1914-1924.
24. van der Burgh, S., A. de Keizer, and M.A. Cohen Stuart, *Complex Coacervation Core Micelles. Colloidal Stability and Aggregation Mechanism*. Langmuir, 2004. **20**(4): p. 1073-1084.
25. Spruijt, E., et al., *Binodal Compositions of Polyelectrolyte Complexes*. Macromolecules, 2010. **43**(15): p. 6476-6484.
26. Lord Rayleigh, F.R.S., *On the equilibrium of liquid conducting masses charged with electricity*. Philos. Mag., 1882. **14**(87): p. 184-186.
27. Baigl, D., M. Sferrazza, and C.E. Williams, *On the pearl size of hydrophobic polyelectrolytes*. Europhys. Lett., 2003. **62**(1): p. 110-116.
28. Limbach, H.J., C. Holm, and K. Kremer, *Structure of polyelectrolytes in poor solvent*. Europhys. Lett., 2002. **60**(4): p. 566.

# Chapter 6

---

## General Discussion

---



## 6.1 Protein-based polymers for biomedical hydrogels

### 6.1.1. Introduction

The field of developing new biomaterials is growing rapidly. By using genetic engineering it is possible to clone and express fusions of multiple domains of natural or modified proteins in almost limitless combinations. However, their usefulness in real applications depends on production yield, cost effective purification, and application scope of these proteins. Protein polymers inspired by- or based on natural structural proteins such as collagen, elastin, silk, etc. are particularly interesting as biomaterial hydrogels in regenerative medicine, since they are similar not only to the natural extracellular matrix (ECM) but also to other proteins in the human body [1, 2]. The aim of this thesis is to design, produce and characterized stimuli sensitive recombinant protein polymers. Our motivation for this study is to understand the mechanism of their self- and co-assembly that could be used for future design of biomaterials with precisely defined behavior and function. The relevant physical-chemical properties of various protein-based hydrogels were analyzed at different environmental conditions. For example, silk-collagen like block copolymers, can be used as a tissue engineering scaffold, as they are able to form gels under physiological conditions, at relatively low concentrations (1 %). They are produced at g/L levels secreted expression by *Pichia pastoris* and their properties can be tuned by pH, temperature, ionic strength or enzymatic cross-linking. Both collagen and silk blocks are non-toxic, biodegradable and biocompatible, that gives them huge advantages over synthetic systems.

This chapter highlights current progress in the development of protein-based polymers that form hydrogels, their application potential, and advantages of these materials over other biomaterials. It is summarizing not only specific requirement that have to be met, but we also argue why recombinant proteins are indeed promising systems for biomedical applications. In this discussion, first we define what exactly we mean by "biomaterials" in the context of this thesis, and next zoom in on different types of hydrogels that are useful

in the pharmaceutical and medical industries, based on a set of relevant selection criteria. After that we review current studies on recombinant protein-polymer systems and discuss possible next steps towards real applications of these materials.

### **6.1.2 Definition**

Within the context of this thesis, and this chapter in particular, biomaterials are defined to be materials used in prosthesis or medical devices that are in contact with living organisms, body fluids, or cells. Depending on the specific applications, such biomaterials have to meet a range of specific criteria and requirements. Many of them are composed of polymers, and in this chapter we will focus on biomaterials composed of a specific class of (bio)polymers: bio-inspired polypeptide and proteins (high molecular weight polymers composed of amino acid repeating sequence linked together by characteristic peptide bonds) that form hydrogels with potential biomedical and pharmaceutical applications. Hydrogels have ability to swell in water and preserve a significant amount of it within their structure, leading to soft and rubber-like consistency that contributes to their biocompatibility [3], as they are able to resemble properties of living tissues much better than other biomaterials. However, at higher water contents preserving the required mechanical strength becomes a critical factor.

### **6.1.3. Polymer types**

Classification of polymers that form hydrogels can be done based on preparation methods, ionic charges, source of the materials, degree of swelling, rate of biodegradation or the nature of cross-linking. Since we want to argue that recombinant protein-polymers have specific application advantages, we here focus on a classification by source of material. Basically there are four main groups of polymer materials that can be distinguished: natural polymer, synthetic polymers, engineered biopolymers, and finally, hybrid hydrogels composed of combinations of bio- and synthetic polymers.

*Synthetic polymers*

Synthetic polymer hydrogels are the biggest group of materials currently used in biomedical applications. There are numerous reports about new chemical structures for which the market is expanding rapidly [4]. A very important class of polymers are the biodegradable poly( $\alpha$ -hydroxy acids) that can be used for implants, as 3D polymer scaffolds for cell growth, or for fracture fixation. These include: poly(glycolide) (PGA), poly(lactic acid) (PLA) and poly(ethylene glycol) (PEG) [5]. Poly(glycolide) is one of the first polymers for which biodegradability and usefulness as a biomaterial were studied in detail. PGA is highly crystalline with high tensile modulus and low solubility in organic solvents. In view of its fiber forming ability, it was used extensively for developing sutures, or as a scaffold matrix for tissue regeneration. It features good biodegradability, mechanical properties and cell viability [6]. Alternatively, PLA is a chiral molecule that exists in two stereoisomeric (optically active) forms L and D. It is hydrophobic and its *in vivo* degradation is relatively slow (from weeks to years, depending on the molecular weight). Because of its high mechanical strength PLA has been used in orthopedic devices and hard tissue implants. The DL-lactic acid racemic mixture has been study in target drug delivery [5]. Finally, PEG is fiber-forming polymer with high hydrolytic instability [5], used mainly as a suture material in surgery [7]. It is also used as a material to treat burns and skin damage or as sponges/tampons for packing the surface of bleeding organs [8, 9].

The synthesis of hydrogels based on synthetic polymers is typically done by cross-linking polymerization [10], cross-linking of polymer precursors [11] or cross-linking via polymer-polymer reactions [12, 13]. For all of these approaches, side reactions are taking place that may result in unreacted pendant groups, entanglements, cycles, loops or other imperfections in structure and chemistry. Other disadvantages of synthetic hydrogels are that is not always possible to achieve the required mechanical properties, fast response to external stimuli, and biocompatibility [14].

### *Natural biopolymers*

Proteins (amino acid polymers) are a key structural component of human body, present in tissues, and arranged in well-defined three-dimensional structures. Natural protein-based materials have long been preferred materials for tissue engineering scaffolds, drug delivery and sutures [15], being obviously biocompatible and having very favorable biodegradation properties [16].

One example is *albumin*, found in blood plasma. This globular, non-glycosylated protein can be used as a coating for biomaterials in contact with blood by attaching it to the surfaces of the biomaterials [17, 18]. It has been also used as a carrier matrix for injectable drug/gene delivery systems [19], coating material for cardiovascular devices [20] and in diagnostics for imaging tissues and organs (radiolabeled) [21]. The most abundant protein present in human body is *collagen*. It is the major component of skin, tendon and bone providing strength and structural stability to various tissues. A denaturated form of collagen is *gelatin* that is obtained by a partial hydrolysis of collageneous tissues. Collagen and gelatin are an ideal materials for tissue engineering and wound dressing, as it can serve as a natural substrate for cell attachment, proliferation and differentiation [22, 23]. They have also been used for localized delivery of low molecular weight drugs/antibiotics [24]. The main sources of collagen are bovine, or Achilles tendons. One of the few limitations of natural collagen-based materials (as compared to other materials) is a mild immunogenicity, that varies depending on donor species, processing techniques and implementation site. Other problems in using natural collagen-based materials include high cost and risk of contamination.

Next to proteins, polysaccharides also perform key structural roles in the human body, and have been used extensively as biomaterials. One example of a polysaccharide used as biomaterial in medical applications is *chitin*, a polysaccharide found in the exoskeletons of insects and internal shells of cephalopods (squids and octopuses). The extraction of natural chitin is usually done from those sources. Chitosan is prepared from chitin by deacetylation, produce by treating chitin with the alkali sodium hydroxide. Both, chitin

and chitosan, are biodegradable and can promote cell growth, and hence can be used as wound dressing, in contact lenses, as hemostatic agents, and as drug delivery vehicles or injectable materials [25-28].

Other polysaccharides and proteins obtained from natural source (such as fibrinogen, hyaluronic acid, alginate, casein, starch, etc.) were also investigated to prepare biodegradable matrices, drug delivery devices, etc. [29-32].

#### *Engineered biopolymers*

Some of the disadvantages of using proteins from natural sources in biomaterials (control of purity, reproducibility, limited control over relevant material properties) can be remedied by using proteins produced using recombinant DNA technology, which offers the possibility not only to obtain very pure protein materials, but also to engineer the amino acid sequence of the proteins. The biosynthesis of peptides and proteins (natural, modified or *de novo* designed) can be done by recombinant organisms such as bacteria, yeast, fungi, plant, insects or mammalian cells. This approach is widely used in industry as it offers production of long peptides (over 40 amino acids) and proteins with relatively low cost for large-scale production [33]. Recombinant production of peptides and proteins allows for the construction of proteins or protein-based polymers with endless combinations of blocks of precisely defined composition and structure [34]. A range of polypeptides that include self-assembly blocks have been designed and produced specifically as tissue engineering scaffolds or drug delivery systems [35, 36]. Recombinant protein-based polymers with sequences inspired by structural proteins such as collagen, elastin, silk, etc., are gaining increasing attention in the biomedical field [36].

#### *Biopolymer-synthetic polymer hybrid gels*

Another way of trying to combine the best properties of both biological and synthetic polymers is to design hybrid polymer materials. Hybrid hydrogels can be created that combine biological macromolecules and synthetic polymers, interconnected either

covalently or noncovalently [37]. The introduction of protein- or peptide fragments into hybrid hydrogel structures allows, among others, for tuning of degradability [38, 39], for response to external stimuli such as temperature [40, 41], or for response to the presence of biologically active molecules (e.g. antigens, antibodies) [42, 43]. Other biomolecules have also been cross-linked to water-soluble synthetic polymers, e.g. oligodeoxyribonucleotides [44] and dextran polysaccharides [45].

#### **6.1.4. Examples of biomedical applications of hydrogels**

Potential biomedical applications of the hydrogels that have already been mentioned include: scaffolds in tissue engineering, artificial extracellular matrix, sustained-release drug delivery systems, biosensors or implantable devices. As proteins are a major component of human tissues, protein-based materials have been carefully investigated for all of these applications. Below we discuss a selection of these applications in somewhat more detail.

##### *Tissue engineering*

Tissue damage or loss of tissue (as a result of disease, accident, or failure) are major causes of illness, disability and death. Treatments sometimes require transplantation of tissues and organs. Tissues can be isolated from the same patient, or from another individual. Both cases have serious risks for complications such as donor-site morbidity, immunoincompatibility, infections and more. Many of these risks can be minimized by engineering and developing tissues *in vitro* that are able to meet specific needs [46]. A range of implants have been designed to replace diseased or damaged parts of body e.g., artificial skin [47, 48], breast [49], nerve [50] or other soft tissues [51-55]. The materials used for these implants should have the proper mechanical properties, biocompatibility, biodegradability, etc. The most widely used polymers for these applications are biopolymer materials from natural sources (collagen, gelatin, or polysaccharides) or biodegradable synthetic polymers (PLLA, PEG, PGA). Hydrogels are also used as dressings for burns or other hard-to-heal wounds. In this case, the hydrogel material should fulfill additional

requirements such as easy application and removal, allowing for diffusive exchange of gas between tissues and environment, controlled release of drugs, antimicrobial agents, or other wound repair agents [56].

#### *Drug delivery system*

A final important application of hydrogels that we want to introduce here are microgels for drug delivery. This application requires understanding the diffusion of small molecular weight molecules, peptides or proteins in the gels, in order to be able to carefully control the release of encapsulated drugs [57]. The preparation of drug delivery vehicle can be done by physical entrapment of the drug by noncovalent association to the scaffold (through physical bonds) or by immobilization of the drug to the hydrogel chains through covalent bonds [58]. When using physical entrapment, drug release can be controlled via the mesh size of the network that restricts diffusion rate of encapsulated drug. For the case of covalent immobilization, done by direct incorporation of the drug into polypeptide chain, drugs release depends on network degradation [59].

## **6.2. Criteria of selection**

When thinking about possible future applications of recombinant protein-based polymers it is crucial to know about the range of possible constraints on biomaterials that come with specific applications. The literature on this topic is large but scattered. Below we discuss some of the most important general constraints that biomaterials have to meet.

### **6.2.1. Biocompatibility**

Biocompatibility is one of the most important criteria, but also a very broad one that includes all responses of organism to biomaterial. For biodegradable materials, biocompatibility extends to degradation products that should also be non-toxic, non-carcinogenic, do not cause any inflammatory or allergenic reactions, embolisms (blood clots, a fat globule or a gas bubble in the bloodstream, which can cause a blockage), or

tissue necrosis. Typically, hydrogels have weak interaction with proteins [60] and this is a favorable factor in the acceptance of foreign objects by organisms.

*Blood response:* biomaterials that might have, or are design to have, contact with blood, have to be evaluated for blood-biomaterial interactions. The most important issues are protein adsorption, platelet reactions, intrinsic coagulation, fibrinolytic activity, erythrocytes and, leucocytes activation [61]. Not only the biomaterial structure is an important factor influencing the blood response, but also the presence of antithrombotic agents [62]. Blood - material interaction may cause thrombus formation that lead to emboli formation (death or biomaterial failure) [63]. They may also cause changes in the structure of proteins, including denaturation [62]. Activation of plasma proteins and/or blood cells may leads to inflammatory reactions, or thrombosis (formation of a blood clot) [64].

*Tissue response:* The major response of tissues after local injury, insult or infection is the inflammatory process. Inflammation may occur when the implemented material is in contact with living tissue [65]. It is characterized by an increased concentration of lymphocytes and leukocytes and by exudation around the implant [66]. Inflammation can be biological, chemical or physical and involves many proteins, tissues and cells [64]. Chemical inflammation is caused by substances (or breakdown products thereof) that are released by the biomaterial and that are identified by the organism as being foreign. Physical stimuli for inflammation include certain surface properties, size, shape or configuration of biomaterial. This type of inflammation leads to cell ingestion, fibrous encapsulation or fibrous ingrowths [67]. Biological inflammation is caused by microorganisms. A mild inflammation response can lead to healing and effective implant response, but when the organism is responding with severe inflammation, tissue necrosis, granulomas or oncogenesis may occur [64].

In summary the ideal material does not cause thrombosis, destruction of cells, tissues or enzymes, modification of plasma proteins, depletion of electrolytes, adverse immune

responses or allergenic reactions [68]. It should be porous, allowing for the removal of contaminants that may be a source of inflammation reactions [69].

### **6.2.2. Desirable physical properties**

The physical properties of biomedical hydrogels depend on the specific application and type of material. Generally, biomedical hydrogels should have soft and tissue-like mechanics, with proper elasticity and strength, along with ability to absorb aqueous solutions without losing shape and mechanical properties [70]. Moreover, they should have high permeability (*in vivo*) for low molecular weight metabolites and ions that can be released through hydrogels to the surrounding tissue in a controlled manner [71]. The 3D structure of hydrogel in swollen state is preserved either by physical (e.g. hydrogen bonding) or chemical (covalent, atomic, ionic) cross-linking. This cross-linking may take place *in vitro* (during preparation) or *in vivo* (after application in human body) [72]. Rheological characterization of the physical properties of biomedical hydrogels should include final bulk viscoelastic properties, but also flow behavior and the development of rheological properties during gelation [73, 74]. Finally, it should also be established that the mechanical and other properties are maintained by the biomaterial *in vivo* over the required period of time.

### **6.2.3. Surface properties**

Surface properties of biomedical hydrogels are key factor as the initial interactions between material and cell are protein adsorption and cell adhesion. It is known that chemical composition and surface morphology (smooth, rough, porous) can influence the response of cells. An important feature of biomaterials are its surface modifications, that should provide suitable chemical and physical properties to the surrounding tissues and cells, in order to become biocompatible. The main issues that should be considered during designing are surface hydrophobicity/hydrophilicity, wettability, charge, polarity, or heterogeneity in the distribution of reactive groups [5]. Many approaches have been proposed to find optimal surface modifications, including for hydrogel materials. These

modifications should not significantly influence bulk material properties. One of the approaches is immobilization of ECM components (e.g. collagen, gelatin, or fibronectin) or synthetic peptides (e.g. RGD sequence), which improve adhesion, differentiation and proliferation properties of the surrounding cells on the material surface [75-77].

### 6.2.4 Biodegradation

Biodegradation is another important property of hydrogels. Often the biodegradation of polymers can be tuned by varying the nature and ratio of monomeric units. This tunability is used extensively in the development of novel drug delivery systems with tuned drug release. Some parameters that influence biodegradation are listed in table 6.1.

**Table 6.1.** Factors that play a role in biodegradation.

Factor	Biodegradation	
	increase	slow down
water permeability	easy	difficult
chemical structure	hydrolytically unstable bonds	hydrolytically stable bonds
hydrophobicity	hydrophilic	hydrophobic
molecular weight	smaller	bigger
morphology	amorphous	crystalline
glass transition temperature	lower than body temp (rubbery behavior under in vivo)	higher than body temp (glassy behavior under in vivo)
geometrical factors	high surface to volume ratio	low surface to volume ratio
degradation products, environmental factors	site of implantation, injection, pH, ionic strength, temperature	
additives	enzymes	
structure	shape, size	

Biodegradable polymers have the crucial advantage over the non-degradable materials that they do not need to be removed from body by surgery. The degradation products are normally excreted from the human body via natural pathways, which may lead to a faster recovery of the patient.

#### **6.2.5. Easy processing methods**

The preparation of biomaterials for any application involves many processing steps: synthesis steps, a series of purification steps, possibly freeze drying, product fabrication and sterilization steps. Details of such steps vary with (bio)macromolecule type, physicochemical properties and final application. For competitive final products, processing techniques should be as easy, cost-efficient, time-saving as possible, and not lead to unwanted changes in the materials such as its bioactivity, biodegradation or biocompatibility. The selection of proper processing method is crucial for materials used in biomedical application and has to be chosen with care.

### **6.3. Recombinant polymers for medical hydrogels**

Recombinant protein and peptides are new biological materials for tissue engineering scaffolds or drug delivery. Fibrous proteins, like collagen, elastin, silk or combination of those, offer the advantages of natural well-defined structural scaffolds with limitless possibilities of controlling functionality by using genetic manipulation. Through the design and expression of artificial genes, it is possible to prepare recombinant proteins with specific domains/blocks that are able to self-assemble into specific patterns, in order to modulate cellular behavior [78]. Additionally, functional elements such as cell binding sites or enzymatic domains can be introduced into these recombinant proteins to further broaden their applicability. Protein engineering has several advantages over the use of proteins isolated from natural starting materials. These include less variability of material (due to isolation from different hosts or tissues), more options to control mechanical properties, and a decreased risk of transmittable diseases [79]. In comparison to synthetic

polymers, they allow complete control of the composition, sequence and length of the blocks. Recombinant protein-based materials can be design to mimic the desired features of their natural equivalent thus exhibit similar biocompatibility and biodegradability in contrast to synthetic materials. One of the drawbacks of recombinant protein production is the choice of building blocks that are limited to the naturally occurring amino acids. Nevertheless, this still provide endless possible combinations when designing new materials.

For example, it was shown that elastin-like systems, based on repeating pentapeptide sequence (VPGXG, where X can be any natural amino acid except proline) can be easily engineered to accomplish mechanical behavior comparable to the native elastin proteins [80]. Interestingly, recombinant elastin-like proteins exhibit termoresponsive behavior that can be tune by amino acid at X position, molecular weight, and concentration [81]. Elastins can be crosslink by radiation [80, 82], or chemical means [83]. Preparation of fibers can be done using electrospinning [84]. Additionally, different oligopeptides containing either RGD or REDV domains can be introduced to stimulate adhesion of endothelial cells used for tissue-engineered vascular grafts [85-87]. Elastin-like polymers are very promising biomaterials that show excellent biocompatibility because of their resemblance to natural elastins and biodegradability to native amino acids [88].

A key structural protein that is used in many biomedical applications is collagen. It is used in interventions on various kinds of tissues e.g. cylindrical tubes (blood vessel regeneration) [89], microporous scaffolds (wound dressing) [90], or microbeads (adipogenic differentiation of stem cells) [91]. When aiming to produce porous bone tissue scaffold, collagen and collagen-like proteins are often used in combination with calcium phosphates that provide extra strength [92]. For improving interactions of collagen and collagen-like proteins with cells, specific peptides or growth factors (e.g. BMP-2) can be included or attached [93-95]. Collagen-like hydrogels can be also combined with proteoglycans to be used as artificial skin that improves wound healing [96].

Another natural structural protein that has inspired many (bio)material scientists is silk. Biosynthesis is probably the only method that allows for the production of high molecular weight proteins with silk-like sequences. Silks are remarkable biomedical materials with extraordinary mechanical properties. They are biodegradable, biocompatible and non-immunogenic, extremely strong, light and stable. Because of these properties they are often applied in tissue engineering or blood vessels [97].

Recombinant technology not only allows for the construction of novel proteins inspired by a single natural protein or protein domain, but also for the creation of chimeric constructs that combine (possibly multiple repeats) of two or three motifs. In such chimeric constructs, the block composition can be used to tune the final properties of the material. For example, elasticity can be increased by including elastin-like blocks, strength by including silk-like blocks, and cell-binding domains to modulate the biological activity of the material. Part of this thesis deals with silk-elastin polymers. Previous studies on silk-elastin like proteins (SELP) have demonstrated high tensile strength, excellent elasticity and non-toxicity to the cells [98, 99]. Combinations of SELPs with bioactive domains may be used to modulate the biological activity of these materials [100-102].

In our group we have been working with a range of different types of protein block copolymers. For example, dilute, pH-sensitive fiber gels have been formed, which are based on triblocks composed of silk-collagen-like proteins [103-106]. The silk block was designed in such a way that it contains ionizable residue, and that the formation of protein fibers and fiber gels becomes pH dependent [107, 108]. Fibril formation has also been studied for silk-elastin diblock and triblocks composed of silk-collagen-elastin motifs [109]. Finally, collagen-like blocks were also combined with self-assembly motifs to obtain bio-inspired and highly regular thermo-sensitive hydrogels: by attaching triple-helix forming sequences onto both ends of a collagen-like block [110, 111].

The field of recombinant protein is growing rapidly and many research groups are aiming to construct materials for biomedical applications. As a genetic engineering is very

powerful technology, it provides excellent tools to design and construct polymer scaffolds with a wide range of attractive properties.

#### 6.4. Conclusions and future perspective

In this study, we design, produce and characterize a number of self-assembling and hydrogel forming protein-based polymers that can be applied in biomedical applications. Some of them have promising properties such as  $C_2S_{48}^HC_2$  (Chapter 3) or enzymatically cross-linked  $C_2S_{48}^HC_2$  and  $T_9R_4T_9$  (Chapter 4) and are good candidate for tissue engineering scaffolds. Others, such as  $S_{24}E_{40}$  and  $S_{12}C_4E_{40}$  (Chapter 2), still need more characterization and investigation to elucidate their application potential. Nevertheless, all of the work in this thesis illustrates that recombinant proteins polymers are good alternative to animal-derived or synthetic materials, with precisely controlled molecular composition and predictable physicochemical properties. While there is already preliminary evidence that shows that many of our polypeptide building blocks are not immunogenic, many more tests need to be done in the future to truly establish the potential of these materials for tissue engineering *in vitro* and finally *in vivo*.

Future studies should elucidate the interaction of hydrogel systems such as ours and living organisms. More modifications will certainly be needed, for example by attaching biological units (heparin or its fragments, albumin, streptokinase etc.) onto hydrogel surfaces to mimic natural interfaces. Furthermore, the attachment of specific synthetic peptides sequence (e.g. RDG, KQAGDV, PHSRN [112, 113]) can strongly enhance cell adhesion, proliferation and differentiation therefore improving biocompatibility. Other biological molecules that could be incorporated include nucleic acids, enzymes, antibodies, or antigens. This could lead to novel biomaterials with applications in drug targeting, diagnostic biosensors or bioassays and more.

Future study should (still) focus on improving viscoelastic properties of protein hydrogels. This can be done, for instance, by introducing motifs into the polymer sequence that could allow more efficient enzymatic cross-linking. Another possibility is to biologically modify

blocks length and composition, or insert another type of block with different stimuli response (pH, temperature, UV).

To sum up, hydrogel biomaterials have a very promising future. Numerous new designs for better controls of morphology, self-assembly and stimuli-sensitivity may still be expected. Hopefully, this will also lead to a better understanding of the key issue underlying the design of recombinant polypeptides for biomaterials, namely the relation between primary sequence and ultimate biomaterial properties.

## References

1. Murphy, W.L. and D.J. Mooney, *Molecular-scale biomimicry*. Nat Biotech, 2002. **20**(1): p. 30-31.
2. Pradhan, S. and M.C. Farach-Carson, *Mining the extracellular matrix for tissue engineering applications*. Regenerative medicine, 2010. **5**(6): p. 961-970.
3. Bruck, S.D., *Aspects of three types of hydrogels for biomedical applications*. Journal of Biomedical Materials Research, 1973. **7**(5): p. 387-404.
4. Ratner, B.D. and A.S. Hoffman. *Synthetic hydrogels for biomedical applications*. in *Hydrogels for Medical and Related Applications, ACS symposium series*. 1976. ACS Publications.
5. Piskin, E., *Biodegradable polymers as biomaterials*. Journal of Biomaterials Science, Polymer Edition, 1995. **6**(9): p. 775-795.
6. Nair, L.S. and C.T. Laurencin, *Biodegradable polymers as biomaterials*. Progress in polymer science, 2007. **32**(8): p. 762-798.
7. Isaacs, J., I. Klumb, and C. McDaniel, *Preliminary investigation of a polyethylene glycol hydrogel "nerve glue"*. Journal of Brachial Plexus and Peripheral Nerve Injury, 2009. **4**(1): p. 1-5.
8. Barvič, M., K. Kliment, and M. Zavadil, *Biologic properties and possible uses of polymer-like sponges*. Journal of Biomedical Materials Research, 1967. **1**(3): p. 313-323.
9. Corkhill, P.H., C.J. Hamilton, and B.J. Tighe, *Synthetic hydrogels VI. Hydrogel composites as wound dressings and implant materials*. Biomaterials, 1989. **10**(1): p. 3-10.
10. Odian, G., *Principles of Polymerization, 4th Edition* 2004, NJ: Wiley, Hoboken. 832.
11. Yeh, P.Y., P. Kopečková, and J.i. Kopeček, *Biodegradable and pH-sensitive hydrogels: Synthesis by crosslinking of N, N-dimethylacrylamide copolymer precursors*. Journal of Polymer Science Part A: Polymer Chemistry, 1994. **32**(9): p. 1627-1637.
12. Ghandehari, H., et al., *Biodegradable and pH sensitive hydrogels: synthesis by a polymer-polymer reaction*. Macromolecular Chemistry and Physics, 1996. **197**(3): p. 965-980.
13. Wang, D., et al., *Novel aromatic azo-containing pH-sensitive hydrogels: synthesis and characterization*. Macromolecules, 2002. **35**(20): p. 7791-7803.
14. Kopeček, J. and J. Yang, *Hydrogels as smart biomaterials*. Polymer International, 2007. **56**(9): p. 1078-1098.
15. Kiraly, R.J. and Y. Nose, *Natural Tissue as a Biomaterial*. Artificial Cells, Blood Substitutes and Biotechnology, 1974. **2**(3): p. 207-224.
16. Meinel, L., et al., *The inflammatory responses to silk films in vitro and in vivo*. Biomaterials, 2005. **26**(2): p. 147-155.
17. Keogh, J.R. and J.W. Eaton, *Albumin binding surfaces for biomaterials*. The Journal of laboratory and clinical medicine, 1994. **124**(4): p. 537-545.

18. Kottke-Marchant, K., et al., *Effect of albumin coating on the in vitro blood compatibility of Dacron® arterial prostheses*. Biomaterials, 1989. **10**(3): p. 147-155.
19. Chuang, V.T.G., U. Kragh-Hansen, and M. Otagiri, *Pharmaceutical strategies utilizing recombinant human serum albumin*. Pharmaceutical research, 2002. **19**(5): p. 569-577.
20. Uchida, M., et al., *Reduced platelet adhesion to titanium metal coated with apatite, albumin-apatite composite or laminin-apatite composite*. Biomaterials, 2005. **26**(34): p. 6924-6931.
21. Klibanov, A.L., *Targeted delivery of gas-filled microspheres, contrast agents for ultrasound imaging*. Advanced drug delivery reviews, 1999. **37**(1): p. 139-157.
22. Sai K, P. and M. Babu, *Collagen based dressings - a review*. Burns, 2000. **26**(1): p. 54-62.
23. Vin, F., L. Teot, and S. Meaume, *The healing properties of Promogran in venous leg ulcers*. Journal of Wound Care, 2002. **11**(9): p. 335-341.
24. Friess, W., *Collagen-biomaterial for drug delivery*. European Journal of Pharmaceutics and Biopharmaceutics, 1998. **45**(2): p. 113-136.
25. Francis Suh, J.K. and H.W.T. Matthew, *Application of chitosan-based polysaccharide biomaterials in cartilage tissue engineering: a review*. Biomaterials, 2000. **21**(24): p. 2589-2598.
26. Ishihara, M., et al., *Photocrosslinkable chitosan as a dressing for wound occlusion and accelerator in healing process*. Biomaterials, 2002. **23**(3): p. 833-840.
27. Molinaro, G., et al., *Biocompatibility of thermosensitive chitosan-based hydrogels: an in vivo experimental approach to injectable biomaterials*. Biomaterials, 2002. **23**(13): p. 2717-2722.
28. Nettles, D.L., S.H. Elder, and J.A. Gilbert, *Potential use of chitosan as a cell scaffold material for cartilage tissue engineering*. Tissue engineering, 2002. **8**(6): p. 1009-1016.
29. Aprahamian, M., et al., *A new reconstituted connective tissue matrix: Preparation, biochemical, structural and mechanical studies*. Journal of Biomedical Materials Research, 1987. **21**(8): p. 965-977.
30. Elvira, C., et al., *Starch-based biodegradable hydrogels with potential biomedical applications as drug delivery systems*. Biomaterials, 2002. **23**(9): p. 1955-1966.
31. Augst, A.D., H.J. Kong, and D.J. Mooney, *Alginate hydrogels as biomaterials*. Macromolecular Bioscience, 2006. **6**(8): p. 623-633.
32. Song, F., et al., *Novel casein hydrogels: formation, structure and controlled drug release*. Colloids and Surfaces B: Biointerfaces, 2010. **79**(1): p. 142-148.
33. Kyle, S., et al., *Recombinant self-assembling peptides as biomaterials for tissue engineering*. Biomaterials, 2010. **31**(36): p. 9395-9405.
34. Kim, W., *Recombinant protein polymers in biomaterials*. Frontiers in bioscience: a journal and virtual library, 2012. **18**: p. 289-304.
35. Torchilin, V.P. and A.N. Lukyanov, *Peptide and protein drug delivery to and into tumors: challenges and solutions*. Drug Discovery Today, 2003. **8**(6): p. 259-266.

- 
36. Werkmeister, J.A. and J.A.M. Ramshaw, *Recombinant protein scaffolds for tissue engineering*. Biomedical Materials, 2012. **7**(1): p. 012002.
  37. Vandermeulen, G.W.M. and H.-A. Klok, *Peptide/protein hybrid materials: Enhanced control of structure and improved performance through conjugation of biological and synthetic polymers*. Macromolecular Bioscience, 2004. **4**(4): p. 383-398.
  38. Ulbrich, K., J. Strohalm, and J. Kopeček, *Polymers containing enzymatically degradable bonds. VI. Hydrophilic gels cleavable by chymotrypsin*. Biomaterials, 1982. **3**(3): p. 150-154.
  39. Rejmanová, P., et al., *Polymers containing enzymatically degradable bonds, 8. Degradation of oligopeptide sequences in N-(2-hydroxypropyl)methacrylamide copolymers by bovine spleen cathepsin B*. Die Makromolekulare Chemie, 1983. **184**(10): p. 2009-2020.
  40. Wang, C., R.J. Stewart, and J. Kopeček, *Hybrid hydrogels assembled from synthetic polymers and coiled-coil protein domains*. Nature, 1999. **397**(6718): p. 417-420.
  41. Tang, A., et al., *The coiled coils in the design of protein-based constructs: hybrid hydrogels and epitope displays*. Journal of Controlled Release, 2001. **72**(1-3): p. 57-70.
  42. Miyata, T., N. Asami, and T. Urugami, *A reversibly antigen-responsive hydrogel*. Nature, 1999. **399**(6738): p. 766-769.
  43. Lu, Z.-R., P. Kopečková, and J. Kopeček, *Antigen Responsive Hydrogels Based on Polymerizable Antibody Fab' Fragment*. Macromolecular Bioscience, 2003. **3**(6): p. 296-300.
  44. Nagahara, S. and T. Matsuda, *Hydrogel formation via hybridization of oligonucleotides derivatized in water-soluble vinyl polymers*. Polymer Gels and Networks, 1996. **4**(2): p. 111-127.
  45. de Jong, S.J., et al., *Novel Self-assembled Hydrogels by Stereocomplex Formation in Aqueous Solution of Enantiomeric Lactic Acid Oligomers Grafted To Dextran*. Macromolecules, 2000. **33**(10): p. 3680-3686.
  46. Laurencin, C.T., et al., *Tissue Engineering: Orthopedic Applications*. Annual Review of Biomedical Engineering, 1999. **1**(1): p. 19-46.
  47. Yannas, J.F.B.I.V., et al., *Successful use of a physiologically acceptable artificial skin in the treatment of extensive burn injury*. Annals of surgery, 1981. **194**(4): p. 413.
  48. Michaeli, D. and M. McPherson, *Immunologic study of artificial skin used in the treatment of thermal injuries*. Journal of Burn Care & Research, 1990. **11**(1): p. 21-26.
  49. Tullie, L., et al., *Breast augmentation with collagen injections*. BMJ Case Reports, 2011. **2011**.
  50. Yannas, I.V., et al., *Polymeric template facilitates regeneration of sciatic nerve across 15 mm gap*. Trans Soc Biomater, 1985. **8**: p. 146.
  51. Wallace, D.G. and S.B. Wade, *Collagen implant material and method for augmenting soft tissue*, 1984, Google Patents.

52. Pachence, J.M., *Collagen-based devices for soft tissue repair*. Journal of Biomedical Materials Research, 1996. **33**(1): p. 35-40.
53. Nehrer, S., et al., *Canine chondrocytes seeded in type I and type II collagen implants investigated in vitro*. Journal of Biomedical Materials Research, 1997. **38**(2): p. 95-104.
54. Frenkel, S.R., et al., *Chondrocyte transplantation using a collagen bilayer matrix for cartilage repair*. Journal of Bone & Joint Surgery, British Volume, 1997. **79**(5): p. 831-836.
55. Takeshita, K., W. Bowen, and G. Michalopoulos, *Three-dimensional culture of hepatocytes in a continuously flowing medium*. In Vitro Cellular & Developmental Biology - Animal, 1998. **34**(6): p. 482-485.
56. Schneider, A., J.A. Garlick, and C. Egles, *Self-Assembling Peptide Nanofiber Scaffolds Accelerate Wound Healing*. PLoS ONE, 2008. **3**(1): p. e1410.
57. Gombotz, W.R. and D.K. Pettit, *Biodegradable Polymers for Protein and Peptide Drug Delivery*. Bioconjugate Chemistry, 1995. **6**(4): p. 332-351.
58. Kumar Malik, D., et al., *Recent Advances in Protein and Peptide Drug Delivery Systems*. Current Drug Delivery, 2007. **4**(2): p. 141-151.
59. Romano, N.H., et al., *Protein-engineered biomaterials: nanoscale mimics of the extracellular matrix*. Biochimica et Biophysica Acta (BBA)-General Subjects, 2011. **1810**(3): p. 339-349.
60. Hoffman, A.S., *Principles governing biomolecule interactions at foreign interfaces*. Journal of Biomedical Materials Research, 1974. **8**(3): p. 77-83.
61. Gorbet, M.B. and M.V. Sefton, *Biomaterial-associated thrombosis: roles of coagulation factors, complement, platelets and leukocytes*. Biomaterials, 2004. **25**(26): p. 5681-5703.
62. Courtney, J.M., et al., *Biomaterials for blood-contacting applications*. Biomaterials, 1994. **15**(10): p. 737-744.
63. Hu, W.-J., et al., *Molecular basis of biomaterial-mediated foreign body reactions*. Blood, 2001. **98**(4): p. 1231-1238.
64. Anderson, J.M., *Biological responses to materials*. Annual Review of Materials Research, 2001. **31**(1): p. 81-110.
65. Anderson, J.M., A. Rodriguez, and D.T. Chang. *Foreign body reaction to biomaterials*. in *Seminars in immunology*. 2008. Elsevier.
66. Šprincl, L., J. Vacík, and J. Kopeček, *Biological tolerance of ionogenic hydrophilic gels*. Journal of Biomedical Materials Research, 1973. **7**(1): p. 123-136.
67. Franz, S., et al., *Immune responses to implants - A review of the implications for the design of immunomodulatory biomaterials*. Biomaterials, 2011. **32**(28): p. 6692-6709.
68. Bruck, S.D., *Polymeric Materials: Current Status of Biocompatibility*. Artificial Cells, Blood Substitutes and Biotechnology, 1973. **1**(1): p. 79-98.
69. Roorda, W.E., et al., *Synthetic hydrogels as drug delivery systems*. Pharmaceutisch Weekblad, 1986. **8**(3): p. 165-189.

- 
70. Yaszemski, M.J., et al., *Tissue Engineering And Novel Delivery Systems* 2003: CRC Press. 620.
  71. Peppas, N.A., et al., *Physicochemical foundations and structural design of hydrogels in medicine and biology*. Annual Review of Biomedical Engineering, 2000. **2**(1): p. 9-29.
  72. Slaughter, B.V., et al., *Hydrogels in regenerative medicine*. Advanced Materials, 2009. **21**(32-33): p. 3307-3329.
  73. Van Tomme, S.R., G. Storm, and W.E. Hennink, *In situ gelling hydrogels for pharmaceutical and biomedical applications*. International Journal of Pharmaceutics, 2008. **355**(1): p. 1-18.
  74. Yan, C. and D.J. Pochan, *Rheological properties of peptide-based hydrogels for biomedical and other applications*. Chemical Society Reviews, 2010. **39**(9): p. 3528-3540.
  75. Hersel, U., C. Dahmen, and H. Kessler, *RGD modified polymers: biomaterials for stimulated cell adhesion and beyond*. Biomaterials, 2003. **24**(24): p. 4385-4415.
  76. He, W., et al., *Biodegradable polymer nanofiber mesh to maintain functions of endothelial cells*. Tissue engineering, 2006. **12**(9): p. 2457-2466.
  77. Zhang, H. and S. Hollister, *Comparison of bone marrow stromal cell behaviors on poly (caprolactone) with or without surface modification: studies on cell adhesion, survival and proliferation*. Journal of Biomaterials Science, Polymer Edition, 2009. **20**(14): p. 1975-1993.
  78. van Hest, J.C.M. and D.A. Tirrell, *Protein-based materials, toward a new level of structural control*. Chemical Communications, 2001(19): p. 1897-1904.
  79. Langer, R. and D.A. Tirrell, *Designing materials for biology and medicine*. Nature, 2004. **428**(6982): p. 487-492.
  80. Lee, J., C.W. Macosko, and D.W. Urry, *Mechanical properties of cross-linked synthetic elastomeric polypentapeptides*. Macromolecules, 2001. **34**(17): p. 5968-5974.
  81. Meyer, D.E. and A. Chilkoti, *Quantification of the effects of chain length and concentration on the thermal behavior of elastin-like polypeptides*. Biomacromolecules, 2004. **5**(3): p. 846-851.
  82. Nagapudi, K., et al., *Photomediated solid-state cross-linking of an elastin-mimetic recombinant protein polymer*. Macromolecules, 2002. **35**(5): p. 1730-1737.
  83. McMillan, R.A. and V.P. Conticello, *Synthesis and characterization of elastin-mimetic protein gels derived from a well-defined polypeptide precursor*. Macromolecules, 2000. **33**(13): p. 4809-4821.
  84. Huang, L., et al., *Generation of synthetic elastin-mimetic small diameter fibers and fiber networks*. Macromolecules, 2000. **33**(8): p. 2989-2997.
  85. Humphries, M.J., et al., *Identification of an alternatively spliced site in human plasma fibronectin that mediates cell type-specific adhesion*. The Journal of cell biology, 1986. **103**(6): p. 2637-2647.

86. Nicol, A., et al., *Cell adhesive properties of bioelastic materials containing cell attachment sequences*, in *Biotechnology and Bioactive Polymers* 1994, Springer. p. 95-113.
87. Panitch, A., et al., *Design and biosynthesis of elastin-like artificial extracellular matrix proteins containing periodically spaced fibronectin CS5 domains*. *Macromolecules*, 1999. **32**(5): p. 1701-1703.
88. Bessa, P.C., et al., *Thermoresponsive self-assembled elastin-based nanoparticles for delivery of BMPs*. *Journal of Controlled Release*, 2010. **142**(3): p. 312-318.
89. Boccafoschi, F., et al., *Preparation and Characterization of a Scaffold for Vascular Tissue Engineering by Direct-Assembling of Collagen and Cells in a Cylindrical Geometry*. *Macromolecular Bioscience*, 2007. **7**(5): p. 719-726.
90. Yeo, I.-S., et al., *Collagen-based biomimetic nanofibrous scaffolds: preparation and characterization of collagen/silk fibroin bicomponent nanofibrous structures*. *Biomacromolecules*, 2008. **9**(4): p. 1106-1116.
91. Rubin, J.P., et al., *Collagenous microbeads as a scaffold for tissue engineering with adipose-derived stem cells*. *Plastic and reconstructive surgery*, 2007. **120**(2): p. 414-424.
92. Al-Munajjed, A.A. and F.J. O'Brien, *Influence of a novel calcium-phosphate coating on the mechanical properties of highly porous collagen scaffolds for bone repair*. *Journal of the mechanical behavior of biomedical materials*, 2009. **2**(2): p. 138-146.
93. Shi, S., et al., *RhBMP-2 microspheres-loaded chitosan/collagen scaffold enhanced osseointegration: an experiment in dog*. *Journal of biomaterials applications*, 2009. **23**(4): p. 331-346.
94. Zhang, Y., et al., *The synergetic bone-forming effects of combinations of growth factors expressed by adenovirus vectors on chitosan/collagen scaffolds*. *Journal of Controlled Release*, 2009. **136**(3): p. 172-178.
95. Niu, X., et al., *Porous nano-HA/collagen/PLLA scaffold containing chitosan microspheres for controlled delivery of synthetic peptide derived from BMP-2*. *Journal of Controlled Release*, 2009. **134**(2): p. 111-117.
96. Burke, J.F., et al., *Successful Use of a Physiologically Acceptable Artificial Skin in the Treatment of Extensive Burn Injury*. *Annals of surgery*, 1981. **194**(4): p. 413-428.
97. Vepari, C. and D.L. Kaplan, *Silk as a biomaterial*. *Progress in polymer science*, 2007. **32**(8): p. 991-1007.
98. Scheller, J.r., et al., *Purification of spider silk-elastin from transgenic plants and application for human chondrocyte proliferation*. *Transgenic research*, 2004. **13**(1): p. 51-57.
99. Qiu, W., et al., *Complete recombinant silk-elastinlike protein-based tissue scaffold*. *Biomacromolecules*, 2010. **11**(12): p. 3219-3227.
100. Urry, D.W., et al., *Elastic protein-based polymers in soft tissue augmentation and generation*. *Journal of Biomaterials Science, Polymer Edition*, 1998. **9**(10): p. 1015-1048.

101. Mie, M., Y. Mizushima, and E. Kobatake, *Novel extracellular matrix for cell sheet recovery using genetically engineered elastin-like protein*. Journal of Biomedical Materials Research Part B: Applied Biomaterials, 2008. **86**(1): p. 283-290.
102. Kinikoglu, B., et al., *A smart bilayer scaffold of elastin-like recombinamer and collagen for soft tissue engineering*. Journal of Materials Science: Materials in Medicine, 2011. **22**(6): p. 1541-1554.
103. Martens, A.A., et al., *Triblock Protein Copolymers Forming Supramolecular Nanotapes and pH-Responsive Gels*. Macromolecules, 2009. **42**(4): p. 1002-1009.
104. Martens, A.A., et al., *Dilute gels with exceptional rigidity from self-assembling silk-collagen-like block copolymers*. Soft Matter, 2009. **5**(21): p. 4191-4197.
105. Li, F., et al., *Formation of nanotapes by co-assembly of triblock peptide copolymers and polythiophenes in aqueous solution*. Soft Matter, 2009. **5**(8): p. 1668-1673.
106. Beun, L.H., et al., *Self-Assembly of Silk-Collagen-like Triblock Copolymers Resembles a Supramolecular Living Polymerization*. ACS Nano, 2011. **6**(1): p. 133-140.
107. Smeenk, J.M., et al., *Controlled Assembly of Macromolecular  $\beta$ -Sheet Fibrils*. Angewandte Chemie International Edition, 2005. **44**(13): p. 1968-1971.
108. Topilina, N.I., et al., *Bilayer Fibril Formation by Genetically Engineered Polypeptides: Preparation and Characterization*. Biomacromolecules, 2006. **7**(4): p. 1104-1111.
109. Golinska, M.D., et al., *Fibril Formation by pH and Temperature Responsive Silk-Elastin Block Copolymers*. Biomacromolecules, 2013. **14**(1): p. 48-55.
110. Wertén, M.W.T., et al., *Precision Gels from Collagen-Inspired Triblock Copolymers*. Biomacromolecules, 2009. **10**(5): p. 1106-1113.
111. Skrzyszewska, P.J., et al., *Physical gels of telechelic triblock copolymers with precisely defined junction multiplicity*. Soft Matter, 2009. **5**(10): p. 2057-2062.
112. Ruoslahti, E., *RGD and other recognition sequences for integrins*. Annual Review of Cell and Developmental Biology, 1996. **12**(1): p. 697-715.
113. Wong, J.Y., et al., *Identification and validation of a novel cell-recognition site (KNEED) on the 8th type III domain of fibronectin*. Biomaterials, 2002. **23**(18): p. 3865-3870.

---

## Summary

---



A key part of the growing field of biomedical sciences deals with the development of new, controlled and biocompatible biomaterials. In this thesis we present results on the design, production, purification and characterization of stimuli responsive protein polymers that could ultimately be used in that field. Protein-polymers are composed of two or three blocks that are able to self- and co-assemble. An important theme in the thesis is to highlight the specific advantages of our new protein polymers for future biomedical applications.

We have used recombinant DNA techniques and expression in methylotrophic yeast *Pichia pastoris* for protein production. DNAs encoding various polypeptide blocks were designed, produced using general molecular biology techniques and combined into synthetic genes for protein polymers. Synthetic genes were cloned into *P. pastoris* expression vector pPIC9 that integrates into the yeast genome. Yields were high, typically reaching gram-per-liter (of medium).

In **Chapter 2** we study dual-stimuli (pH, temperature) responsive silk-elastin-like protein polymers (SELPs). These polymers were designed to self- and co-assembly, controlled by both pH and temperature. The first protein is a diblock  $S_{24}E_{40}$  composed of 24 silk-like (*S*) repeats and 40 elastin-like (*E*) repeats. The other protein is a triblock  $S_{12}C_4E_{40}$ , in which the *S* and *E* blocks are separated by a random coil block ( $C_4$ ) that serves as an inert 'spacer'.

A  $C_2S^H C_2$  protein polymer, which consists of a pH responsive, positively charged silk-like middle block  $S^H$ , flanked by two random coil collagen-like blocks  $C_2$  was studied in **Chapter 3**. For this protein we have studied fibril formation and gelling properties at pH values close to neutral, that are crucial for biomedical applications. We find that at physiological pH, these proteins form self-healing physical gels that fulfill many requirements for use in biomedical applications.

In **Chapter 4** we test the influence of enzymatic cross-linking on elasticity and mechanical properties of hydrogels that include collagen-like domains, using microbial transglutaminase (mTGase) as an enzymatic crosslinker that catalyzes the coupling of

glutamines to lysines. We show that even though the collagen-like blocks are not particularly good substrates for the mTGase, the few cross-links that are made have a strong effect on the physical properties of the protein-polymer hydrogels. For silk-collagen fiber gels, the elastic moduli can be increased by a factor of five, and for thermosensitive collagen hydrogels, the enzymatic cross-linking induces qualitatively new behavior, namely shape-memory of hydrogels.

Finally, we study the co-assembly of very asymmetric diblock copolymers with oppositely charged sodium poly(acrylic acid) (NaPAA) with a range of molar masses (**Chapter 5**). This asymmetric diblock consists of a cationic block of 12 lysines connected to a long (400 amino acid) collagen-like block with a net charge that is nearly zero. For shorter Na-PAA chains, spherical complex coacervates micelles are formed, as have been studied before in our lab. But, for long Na-PAA chains a new self-assembled structure is found: a single (Na-PAA) chain pearl-necklace of complex-coacervate micelles.

The general discussion of the thesis in **Chapter 6**, focuses on recombinant and natural hydrogels as biomaterials. We point out the specific advantages of recombinant proteins and also indicate where these still need to be improved in order to be used in biomedical applications. Finally, we make some suggestions for further research in this area.

---

## Samenvatting

---



Een belangrijk onderdeel van het groeiende onderzoeksgebied van de biomedische wetenschappen houdt zich bezig met de ontwikkeling van nieuwe, gecontroleerde en biocompatibele biomaterialen. In dit proefschrift presenteren we de resultaten van het ontwerp, de productie, de opzuivering en de karakterisering van stimuli responsieve eiwitpolymeren die uiteindelijk gebruikt kunnen worden op dat gebied. Eiwitpolymeren bestaan uit twee of drie blokken die kunnen zelf- en co-assembleren. Een belangrijk thema in het proefschrift is om de specifieke voordelen van ons nieuwe eiwitpolymeer voor toekomstige biomedische toepassingen te bespreken.

We hebben recombinant DNA-technieken en expressie in de methylotrufe gist *Pichia pastoris* voor eiwitproductie gebruikt. Stukken DNA die voor verschillende polypeptideblokken coderen, zijn ontworpen, geproduceerd met algemene moleculaire biologische technieken en gecombineerd tot synthetische genen voor eiwitpolymeren. Synthetische genen zijn gekloneerd in *P. pastoris* expressievector pPIC9 dat integreert in het genoom van gist. De opbrengsten waren hoog, met concentraties in orde van grootte van enkele grammen per liter medium.

In **hoofdstuk 2** hebben we zijde-elastine-achtige eiwitpolymeren (SELPs) bestudeerd. Deze polymeren zijn ontworpen om zelf- en co-assemblage, gecontroleerd door zowel pH en temperatuur, te vertonen. Het eerste eiwit is een diblok  $S_{24}E_{40}$  samengesteld uit 24 zijde-achtige (S) herhalingen en 40 elastine-achtige (E) herhalingen. Het andere eiwit is een triblok  $S_{12}C_4E_{40}$ , waarbij de S en E blokken worden gescheiden door het blok  $C_4$ , dat een wanordelijke (statistische) kluwen vormt en dient als een inerte "spacer".

Een  $C_2S^H C_2$  eiwitpolymeer, bestaande uit een pH-responsief, positief geladen zijdeachtige middenblok  $S^H$ , geflankeerd door twee wanordelijke collageenachtige blokken  $C_2$ , wordt besproken in **Hoofdstuk 3**. Van dit eiwit is de fibrilvorming en geleereigenschappen bij pH-waarden dicht bij neutrale pH, die cruciaal is voor biomedische toepassingen, bestudeerd. We vinden dat deze eiwitten bij fysiologische pH zelfherstellende reversibele gels vormen, en voldoen aan veel eisen voor gebruik in biomedische toepassingen.

In **hoofdstuk 4** hebben we de invloed van extra covalente bindingen op elasticiteit en mechanische eigenschappen van hydrogelen die collageen-achtige domeinen hebben, getest. De covalente bindingen zijn gemaakt met microbieel transglutaminase (mTGase) als enzym dat de koppeling van glutamines aan lysines katalyseert. We laten zien dat, hoewel de collageenachtige blokken niet bijzonder goede substraten zijn voor de mTGase, de weinige bindingen die gemaakt worden een grote invloed hebben op de fysische eigenschappen van de eiwitpolymeerhydrogel. Voor zijde-collageenfibergels kan de elastische moduli worden verhoogd met een factor vijf, en in temperatuurgevoelige collageenhydrogels induceren de nieuwe, enzymatisch gekatalyseerde covalente bindingen kwalitatief nieuw gedrag, namelijk geheugenhydrogels, die na vervorming weer naar de originele geometrie kunnen keren.

Tenslotte bestuderen we de co-assemblage van zeer asymmetrische diblokcopolymeren met tegengesteld geladen natriumpoly(acrylzuur) (Na-PAA) met verschillende molaire massa's (**hoofdstuk 5**). Het asymmetrische diblok bestaat uit een kationische blok van 12 lysinen aangesloten op een lange (400 aminozuren) collageen-achtig blok met een netto lading van bijna nul. Met kortere Na-PAA-ketens worden bolvormige complex coacervaatmicellen gevormd, zoals zijn al eerder onderzocht in ons lab. Voor lange Na-PAA-ketens werd een nieuw zelf-geassembleerde structuur gevonden: een enkele (Na-PAA) keten vormt een parelketting van complex-coacervaatmicellen.

De algemene bespreking van het proefschrift in **hoofdstuk 6**, richt zich op recombinante en natuurlijke hydrogels als biomaterialen. Wij wijzen op de specifieke voordelen van recombinante eiwitten en waar deze nog verbeterd moeten worden om te kunnen worden gebruikt in biomedische toepassingen. Tot slot doen we een aantal suggesties voor verder onderzoek op dit gebied.

---

## Streszczenie

---



Kluczową kwestią w dziedzinie nauk biomedycznych jest rozwój i udoskonalenie nowych, bio-zgodnych i kontrolowanych biomateriałów. Pod pojęciem biomateriału, rozumiemy materiał biologiczny który znajduje się w bezpośrednim kontakcie z tkankami organizmu. Do biomateriałów należą między innymi implanty (np. protezy), ale mogą one również służyć do pokrywania powierzchni urządzeń wszczepianych do wnętrza organizmu (np. rozruszników serca, czy sztucznych zastawek serca). Biomateriały są zazwyczaj przeznaczone do długotrwałego kontaktu z organizmem i muszą spełniać odpowiednie kryteria.

W niniejszej pracy przedstawiono wyniki w zakresie projektowania, produkcji, oczyszczania i charakteryzacji (reagujących na bodźce) polimerów białkowych, które mogą być ostatecznie użyte w biomedycynie. Polimery białkowe składają się z dwóch lub trzech bloków, które mogą ulegać samoorganizacji (spontanicznemu uporządkowaniu) lub współorganizacji (uporządkowaniu w obecności dodatkowych czynników). Ważnym aspektem w niniejszej pracy jest zwrócenie uwagi na szczególne zalety nowych polimerów białkowych przy zastosowaniu ich w biomedycynie.

Przy produkcji polimerów białkowych, użyliśmy technik rekombinacji DNA i ekspresji w genetycznie zmodyfikowanych, metylotroficznym drożdżach *Pichia pastoris*. DNA zostało tak zaprojektowane, aby kodowało różne bloki polipeptydów, wytwarzany przy użyciu ogólnych technik biologii molekularnej. Ostatecznie, zaprojektowane bloki zostały połączone tworząc syntetyczne geny polimerów białkowych. W dużym uproszczeniu, te syntetyczne geny zostały sklonowane do wektora ekspresyjnego *P. pastoris* (pPIC9), który integruje się do genomu drożdży. Ekspresja białek była przeprowadzona w bioreaktorze przy stosunkowo wysokiej wydajności, zwykle osiągającej gram na liter pożywki hodowlanej.

W **rozdziale 2** badamy duet - bodźców (pH i temperaturę) reagujących na polimery białkowe jedwabiu-elastyny (*ang.* silk-elastin like polymers, SELPs). Polimery zostały zaprojektowane tak, aby mogły ulegać samo- i współ-organizacji, sterowanej przez bodźce

zewnątrzne (jedwab pod wpływem pH tworzy długie nici, a elastyna ulega odwracalnej agregacji pod wpływem wysokiej temperatury). Pierwsze białko, dwublok  $S_{24}E_{40}$  składa się z 24 powtórzeń inspirowanych jedwabiem (*S*, *ang.* silk) i 40 powtórzeń inspirowanych elastyną (*E*, *ang.* elastin). W drugim białku, trójbloku  $S_{12}C_4E_{40}$ , bloki *S* i *E* zostały rozdzielone dużym obojętnym blokiem inspirowanym kolagenem ( $C_4$ , *ang.* collagen), który ma za zadanie oddzielić, reagujące na bodźce, bloki jedwabiu i elastyny.

W **rozdziale 3**, badano polimer białkowy  $C_2S^H S^H C_2$ , składający się z dodatnio naładowanego środkowego bloku inspirowanego jedwabiem  $S^H$ , który reaguje na zmiany pH. Bloki boczne są inspirowane kolagenem  $C_2$  i obojętne na czynniki zewnętrzne. Białko  $C_2S^H S^H C_2$  tworzy długie włókna, których powstawanie, długość i właściwości są zależne od wartości pH. Dla neutralnego odczynu pH (które jest kluczowe dla zastosowań biomedycznych) sprawdzaliśmy właściwości reologiczne hydrożeli formowanych przez polimer  $C_2S^H S^H C_2$ . Okazuje się, że w fizjologicznym pH, białka tworzą fizyczne, samo-regenerujące się żele, które spełniają większość wymagań dla zastosowań biomedycznych.

W **rozdziale 4** badamy wpływ jakie mają wiązania chemiczne i fizyczne na elastyczność i właściwości mechaniczne hydrożeli zawierających domeny inspirowane kolagenem, przy użyciu transglutaminazy drobnoustrojowej (*ang.* microbial transglutaminase, mTGase) jako środka sieciującego. Transglutaminaza katalizuje reakcję połączenia reszt glutaminowych z aminami pierwszorzędowymi. Z otrzymanych wyników, możemy zaobserwować, że nawet jeśli bloki inspirowane kolagenem nie są szczególnie dobrymi substratami dla transglutaminazy i jedynie nieliczne wiązania są wprowadzone, ma ona silny wpływ na właściwości fizyczne hydrożeli utworzonych z polimerów białkowych. W przypadku hydrożeli utworzonych z  $C_2S^H S^H C_2$ , elastyczne moduły ( $G'$ ) mogą zostać zwiększone nawet pięciokrotnie przy użyciu bardzo niskiej koncentracji enzymu. Dla termoczułych hydrożeli kolagenowych, utworzona sieć enzymatyczna tworzy nowy rodzaj zachowania, a mianowicie tzw. efekt pamięci kształtu (*ang.* shape memory).

**Rozdział 5** jest poświęcony badaniom, interakcji pomiędzy asymetrycznym polimerem białkowym a przeciwnie naładowanymi polimerami kwasu akrylowego (poliakrylanami sodu, Na-PAA<sub>n</sub>). Asymetryczny polimer białkowy ( $C_4K_{12}$ ) składa się z bloku kationowego ( $K_{12}$ ) w którego skład wchodzi 12 lizyn związanych z długim blokiem (400 amino kwasów) inspirowanym kolagenem (którego ładunek jest bliski zeru). Gdy krótsze łańcuchy Na-PAA reagują z asymetrycznym  $C_4K_{12}$ , tworzone są kuliste koacerwaty miceli. W przypadku długich łańcuchów Na-PAA, samoorganizujące się struktury przyjmują kształty tak zwanego łańcucha perłowego (*ang.* pearl-necklace) kompleksów koacerwatów, przy czym “łańcuch” jest tworzony z pojedynczego polimeru kwasu akrylowego, a “perły” z polimeru białkowego  $C_4K_{12}$ . Otrzymana struktura łańcucha perłowego jest pierwszym przypadkiem zaobserwowanym eksperymentalnie dla tego typu polimerów.

Ogólne podsumowanie pracy w **rozdziale 6**, koncentruje się na naturalnych i rekombinowanych hydrożelach jako biomateriałach. Zwracamy uwagę na szczególne zalety rekombinowanych białek, a także wskazujemy, gdzie pewne ulepszenia mogą być poczynione, aby mogły być one użyte w biomedycynie. Ostatecznie, dajemy wskazówki dotyczące dalszych badań w dziedzinie biomateriałów.



---

## Acknowledgements

---



## Acknowledgements

---

First of all, I would like to thank my promotor, Martien Cohen Stuart, and co-promotor, Frits de Wolf, for offering me this PhD position despite my limited knowledge of physical chemistry. I am very grateful for the chance that you have given to me, your support and guidance.

Very special thanks to my second co-promotor Renko de Vries. Without you I would not have been able to finish this thesis. Our relatively short collaboration was, in the end, very efficient. I really enjoyed our meeting and discussions. Thank you for your scientific input, advices and enthusiasm. Thank you for a constant support, without you, I doubt if I would have been able to reach the end.

Special thanks to my daily advisor at FBR, Marc Werten. Marc, thank you for helping me with molecular biology, fermentation and downstream process. Your support made everything much easier. I knew that in any moment I could ask you for advice and you were always there to help me.

To all FBR group, in particular to the people from the lab 3.10 and 3.11: Jan, Emil, Matthe, Twan and Patrick for their help, technical support and also for such a nice atmosphere in the lab. To my officemates over the first two years of my PhD: Sela, Floor, Catarina and David, thank you for all the fun we have had, your friendship and constant support. To other PhDs: Helena, Ischa, Tijs, Wouter, Dianika, Paul and Maarten with whom we were sharing our frustrations and happy moments. And of course to Roelof, from my intership supervisor, you have become my friend. Thank you for your help in the lab, your valuable advices and trust. And to my 'lunch colleagues': Elinor, and Gerda, with whom I was sharing a lot of cooking experience. And finally, I thank to the MSc student Vincent for his contribution in my research. Thank you all!!

When moved to Fysco after the second year of my PhD, I started to discover the facinating world of physical chemistry. For that, I would like to thank Remco for his patience when explaining me light scattering, for sure I would have not had a good start without your help. Frans, thank you for checking my propositions and for your valuable comments, I

## Acknowledgements

---

knew that I could knock to your door asking for your advice or opinion in any time. Jasper, thank you for introducing me into the rheology and for answering my never-ending questions. Josie, our 'Fysko-mother' I knew that I could turn to you sharing cheerful, sad, frustrating moments or just chat and laugh, thank you for being there. Mara, thank you for arranging small and very important stuff whenever I needed it. Ronald thank you for fixing my computer so many times. I also thank Anita and Bert for all the paper work, Hanne and Anton for the technical help, Marleen and Mieke for scientific and non-scientific chats and Hans for amazing stories and such positive attitude.

To my roommates at Fysco: Paulina, Cecilia, Gosia B., Juan and Hande. Girls you are awesome! I could not have wished for better company over these years. I could always turn to you with my sad and cheerful moments and you were always there to listen, give advice or just laugh. Special thanks to Gosia and Juan for being my paranymphs, it is great to have you by my side in the end of this long journey.

I would like to thank all my Fysco colleagues, whom I have met during these years: Marc, Evan, Junyou, Kathelijne, Wiebe, Saskia, Dmitry, Yuan, Cecilia, Marat, Bas, Paulina, Agata, Kamuran, Gosia W., Kasia, Huanhuan, Liykat, Nadia, Helene, Jacob, Sabine (thanks so much for translating the summary), Johan, Yunus, Christian, Maria, Jeroen, Maarten, Rui, Inge, Soumi, Harke, Surender, Lennart, Natalia, Armando, Wolf, Emilia, Pascal and Thao. Thank you for a great company, our trips, movie nights, parties, coffee/lunch breaks and dinners. Thank you for bringing me happiness and so many unforgettable moments. I could not have found better colleagues.

To my crazy team: Helen, Ivush, Anka, Gabri, Waeil, Gosia P., Gui, Maria T., Abdulino, Dasha, Monia, Maria João. Each of you taught me something, show different perspective and you were there even in the toughest moments. Guys you are like family to me! Thanks to your support, I managed to finish this book. You were always there believing in me and giving me so much positive energy. I know this friendship will last forever. You are very close to my heart, even though (some of you) are so far away now. And Gabriiiii, sorry but I have to write it....I have managed to finish my PhD before you ☺

## Acknowledgements

---

I would like to thank my BFF, Anaïs, for such amazing time that we have spent together. You have always supported and encouraged me. I am missing our every-day-chats, sporty days, relaxing dinners, music festivals and of course adventurous trips.

To Stefan, *dzięki za nasze niedzielne wypady 'za miasto' i niezapomniane podróże do naszego kochanego kraju. Ty zawsze potrafisz mnie rozweselić nawet w pochmurne dni!*

I would like to thank my girl-power group: Julia, Zsizi, Alex, Amrei, Laura, Florene and Anastasia for all the funny girlish dinners and talks! Girls you are a huge part of my life. Thank you, thank you, thank you!

To my international friends from Wageningen and Maasticht: Mathieu, Barae, Petrush, Sophie, Francois, Takis, Francesco, Xena, Agata, Julio, Madzia J., Nelleke, Aurel, Saskia, Kitty, Iza, Yansen, Aaron, Lidia, Sidney, Morteza, Yves, Filip and Belen. Thank you for the great dinners and parties. It was such an incredible time in my life and I could not wish for better companions!

To my 'Delftian' friends: Olalla, Carlos, Camilo, Caro, Olga, Barbara and Adam. You have appeared in my life so unexpectedly, and I have never thought that we would become such good friends. I am really happy to have met you and share so many nice moments.

Thank you to my friends from Poland for their unconditional friendship: Kamelia, Jerzu, Kwiecień, Magda, Basia and Bartek. *Kochani, nawet po prawie siedmiu latach spędzonych w Holandii, wy nadal jesteście w moim życiu. Dziękuję za waszą przyjaźń która przetrwała próbę czasu.*

Last but not the least, I would like to thank my family and especially to my parents for their love, constant support, faith and encouragement. *Mamusiu i tatusiu, dziękuję za wasze wsparcie i wiarę. W końcu udało mi się dotrzeć do końca tej długiej drogi, bez was byłoby to niemożliwe. Kocham was podnad wszystko!*

## Acknowledgements

---

And to my grandmas: *Kochane babcie, dziękuję za wasze wsparcie i bezgraniczna miłość którą mnie obdarzacie! Pomimo że nie będziecie mogły dzielić tego dnia ze mną, zawsze jesteście, i będziecie w moim serduchu.*

The last paragraph is to the most important person in my life. I even do not know how to express with words how I feel. Dieguito, you are my love, my best friend, my soulmate. Thank you for your patience, support and help, I feel so lucky to have you by my side. You have given me so much and make my life meaningful.

*Thank you all!*

*Dziękuję wszystkim!*

*Dank jullie wel allemaal!*

*Gracias a todos!*

*Monika*

---

## About the author

---



## About the author

Monika Dominika Golińska was born on July 10, 1984 in Łódź, Poland. She completed with honors her secondary education from XXXI General Liceum in Łódź. In 2003 she started her studies in Biotechnology at the Technical University of Łódź, Faculty of Biotechnology and Food Sciences. During her study she was active member of BEST (Board of European Students of Technology), where she was responsible for organizing (academic/non-academic) courses and Academic Fair for students, cooperation with companies and PR.

In 2006 she spent 6 months at Wageningen University (The Netherlands) as part of Erasmus exchange program, where she completed her BSc thesis entitled “Chromatin remodelling genes in plant growth and development” in the Department of Molecular Biology. In September 2006, she decided to continue her studies at Wageningen University and follow the Biotechnology program. In 2008 she did her internship at Wageningen UR Food & Biobased Research. The project was focused on recombinant proteins and concern design, production and purification of elastin-like protein polymers (ELPs). She graduated from Wageningen University in September 2008.

From November 2008 she continued her scientific education as a PhD student at Wageningen University in the Laboratory of Physical Chemistry and Colloid Science in collaboration with Wageningen UR Food & Biobased Research, under the supervision of prof. dr. M.A. Cohen Stuart, dr. F.A de Wolf and dr. R. de Vries. The research was focused on production and characterization of a new recombinant protein composed of silk-, elastin- and collagen-like protein polymers. The results of that research are presented in this thesis.

In September 2013 she started to work as an Analytical Scientist at Merck Sharp & Dohm (MSD) in the department Method Development & Process Support, located in Oss.



## List of Publications

**M.D. Golinska**, T.T.H. Pham, M.W.T. Werten, F.A. de Wolf, M.A. Cohen Stuart, J. van der Gucht; "Fibril Formation by pH and Temperature Responsive Silk-Elastin Block Copolymers", *Biomacromolecules*, **2013**, 14 (1), pp 48–55

**M.D. Golinska**, F.A. de Wolf, M.A. Cohen Stuart, A. Hernandez-Garcia, R. de Vries; "Pearl-necklace complexes of flexible polyanions with neutral-cationic diblock copolymers", *Soft Matter*, **2013**, 9 (28), pp 6406–6411

**M.D. Golinska**, M.K. Włodarczyk-Biegun, M.W.T. Werten, M.A. Cohen Stuart, F.A. de Wolf, R. de Vries; "Hydrogel and fibril formation of silk-collagen like polymers for biomedical application", *Biomacromolecules*, *Accepted for publication*

**M.D. Golinska**, F.A. de Wolf, M.A. Cohen Stuart, J. van der Gucht and R. de Vries; "Modulation of mechanical properties of hydrogels composed of protein-based polymers using cross-linking enzymes", *Submitted for publication*

C.I.F. Silva, P.J. Skrzyszewska, **M.D. Golinska**, M.W.T. Werten, G. Eggink, F.A. de Wolf; "Tuning of Collagen Triple-Helix Stability in Recombinant Telechelic Polymers", *Biomacromolecules*, **2012**, 13 (5), pp 1250–1258



## Overview of completed training activities

### Courses

2 <sup>nd</sup> Food Hydrocolloids	Wageningen	2009
12 <sup>th</sup> European School of Rheology	Leuven (Belgium)	2009
Research Methods Biomolecules and Interfaces	Wageningen	2012
Advance Soft Matter	Wageningen	2010
Han-sur-Lesse Winterschool	Han-sur-Lesse (Belgium)	2012
Writing and presenting scientific paper	Wageningen	2010
Career Assessment	Wageningen	2013

### Conferences

Physics @ FOM †	Veldhoven	2012
ECIS (European Colloid and Interface Society) †	Prague (Czech Republic)	2010
Dutch Soft Matter Meeting *	Wageningen	2010-2012
Dutch Polymer Days †	Lunteren	2012

### Other meetings and activities

PhD trip*	Switzerland/France	2009
PhD trip*	Singapore/Malaysia/Vietnam	2011
PCC Lab group Meeting & Colloquia	Wageningen	2008-2013
Protein Group meetings	Wageningen	2008-2013
FBR Group meetings	Wageningen	2008-2010

† poster presentation

\* oral presentation

This research was financially supported by the Netherlands Organization for Scientific Research (NWO).

Cover: design and made by Aleksandra Kwiecień

Printing: GildenPrint, Enschede